

Utah State University

DigitalCommons@USU

All U.S. Government Documents (Utah Regional
Depository)

U.S. Government Documents (Utah Regional
Depository)

12-1985

Kinematics of Great Basin Intraplate Extension from Earthquake, Geodetic and Geologic Information

Paul Kendall Eddington

Follow this and additional works at: <https://digitalcommons.usu.edu/govdocs>



Part of the [Geology Commons](#)

Recommended Citation

Eddington, Paul Kendall, "Kinematics of Great Basin Intraplate Extension from Earthquake, Geodetic and Geologic Information" (1985). *All U.S. Government Documents (Utah Regional Depository)*. Paper 528. <https://digitalcommons.usu.edu/govdocs/528>

This Report is brought to you for free and open access by the U.S. Government Documents (Utah Regional Depository) at DigitalCommons@USU. It has been accepted for inclusion in All U.S. Government Documents (Utah Regional Depository) by an authorized administrator of DigitalCommons@USU. For more information, please contact digitalcommons@usu.edu.



KINEMATICS OF GREAT BASIN INTRAPLATE EXTENSION
FROM EARTHQUAKE, GEODETIC AND
GEOLOGIC INFORMATION

by
Paul Kendall Eddington

A thesis submitted to the faculty of
The University of Utah
in partial fulfillment of the requirements for the degree of

Master of Science
in
Geophysics

Department of Geology and Geophysics
University of Utah
December 1985

ABSTRACT

Strain rates assessed from brittle fracture, associated with earthquakes, and total brittle-ductile deformation measured from geodetic data have been compared to paleostrain from Quaternary geology for the intraplate Great Basin of the western United States. These data provide an assessment of the kinematics and mode of lithospheric extension that the western U. S. Cordillera has experienced in the last 5-10 million years. Strain and deformation rates were determined by the seismic moment tensor method using historic seismicity and fault plane solutions. By subdividing the Great Basin into areas of homogeneous strain it was possible to examine regional variations in the strain field. Contemporary deformation of the Great Basin occurs principally along the active seismic zones: the southern Intermountain Seismic Belt - 4.7 mm/a maximum deformation rate, along most of the western boundary, the Sierra Nevada front - 28.0 mm/a maximum deformation rate, and along the west central Nevada seismic belt - 7.5 mm/a maximum deformation rate. The earthquake related strain shows that the Great Basin is characterized by regional E-W extension at 8.4 mm/a in the north that diminishes to NW-SE extension of 3.5 mm/a in the south. These results show 7-10 mm/a deformation associated with earthquakes that compares to 9 mm/a determined from satellite geodesy and tectonic plate models, implying that modern strain is generally reliant on earthquakes. Zones of maximum extension correspond to belts of shallow crust, high heat flow, and Quaternary basaltic volcanism, suggesting that these parameters are related through an effect such as a stress relaxation allowing buoyant uplift and ascension of magmas.

Contemporary strain and deformation rates have also been determined from geodetic measurements yielding maximum deformation of 11.2 mm/a in the Hebgen Lake por-

t/a of the ISB, 3.6 mm/a in the Excelsior area of Nevada, and 2.5 mm/a in the Owens Valley area of the Sierra Nevada front. Paleostrain and deformation rates were determined yielding deformation rate high of 7.4 mm/a along the southern ISB. Geodetically determined strain and deformation rates compare well with rates determined from seismic moments in many areas while paleostrain and deformation rates are 10 times smaller than contemporary rates except in parts of central and southern California, Wyoming, parts of Utah, and along the Idaho-Wyoming border.

PRECEDING PAGE BLANK NOT FILMED

III, IV

TABLE OF CONTENTS

ABSTRACT	iv
LIST OF TABLES	viii
LIST OF FIGURES	ix
ACKNOWLEDGEMENTS	x
INTRODUCTION	1
REGIONAL GEOLOGY AND GEOPHYSICS	6
Cenozoic History	6
Earthquake History of The Great Basin	8
History of Strain Study	12
STRAIN DETERMINATION FROM EARTHQUAKE DATA	15
Brittle Fracture and Crustal Structure	15
Strain Rate Calculations From The Seismic Moment Tensor	17
Homogeneous Seismic Areas	25
Limits and Accuracy	25
EARTHQUAKE DATA	32
Earthquake Catalog	32
Cordilleran Seismicity	33
Fault Plane Solutions	35
STRAIN RATES FROM SEISMICITY	38
Regional Strain Pattern	38
Great Basin Deformation and Strain Rates	42
COMPARISONS OF CONTEMPORARY AND PALEO STRAIN RATES	47
Paleostrain Rate Calculations	47
From Geologic Data	47
Contemporary Strain Rate	52
Summary of Strain Rates	57
Comparisons of Great Basin Extension Rate	59

SUMMARY AND INTERPRETATIONS	62
---------------------------------------	----

APPENDICES

A. Strain Rate Determination Test Case (Preliminary)	64
B. Computer Programs	116
C. Earthquake Source Citations and Fault Plane Solution Table	149
D. Strain Rate Results	155
E. Earthquake Recurrence Rates	243
F. Lithosphere Deformation Model	251

REFERENCES	262
----------------------	-----

LIST OF TABLES

Table	Page
1. Great Basin $M_L 6+$ earthquakes	205
2. Nucleation depths of large Great Basin earthquakes	11
3. Great Basin extension estimates from other workers	13
4. Seismic moments for large earthquakes from published studies	30
5. Effect on moment of study area earthquakes above different minimum magnitudes	34
6. Number of earthquakes, maximum magnitude (M_{max}), principal moment tensor component (M_1), horizontal deformation rates, and maximum horizontal strain rates for homogeneous areas of the Great Basin	39
7. Maximum horizontal Great Basin strain rate, deformation rate, and total extension from this and other studies	45
8. Strain and deformation rates measured using geologic, seismic, and geodetic data	53
9. Geodetically measured strain and deformation rates	56

10

LIST OF FIGURES

Figure	Page
1. Homogeneous seismic study area locations	2
2. Earthquake epicenter maps from data compiled for this study	4-5
3. Great Basin crustal composition and mechanical property profiles	16
4. Unit volume brittle flow diagram	18
5. Fault geometry conventions diagram	22
6. $\log(M_s)$ versus magnitude graph	28
7. Tension axes from fault plane solutions	36
8. Great Basin seismically determined strain/deformation rates	40
9. Seismically determined maximum horizontal extension directions	43
10. Great Basin regional extension	44
11. Western U. S. fault map	49
12. Locations of study area fault centers	50
13. Great Basin paleo-strain and deformation rates from geologic data	51
14. Maximum magnitude capabilities of the western U. S.	54
15. Western U. S. geodetically determined extensional deformation and strain rates	55
16. Western U. S. volcanism and seismically determined deformation rates	62

Handwritten notes:
 - "List All" written vertically in the upper right.
 - "Geologic" written vertically in the middle.
 - "Data" written vertically in the lower middle.
 - A diagonal line is drawn through items 6, 7, and 8.

ACKNOWLEDGEMENTS

I give my thanks to my committee chairman, Dr. Robert B. Smith, for his help and encouragement. The work reported here is part of R. B. Smith's NASA-funded research (NASA contract NAG 5-164) on the relationship between the Great Basin and the San Andreas fault, and builds upon work and results developed by him and his students since 1982. Discussions with P. Lowman, Goddard Space Flight Center; and J. Crowell and B. Crippen, University of California at Santa Barbara, regarding the objective and geologic data were appreciated. Thanks are also due to the other members of my committee, Dr. James Pechmann and Dr. William Nash, for review of the manuscript.

C. Renggli wrote the original strain calculation programs and explained their use to me. G. Randall helped with the initial compilation of earthquake data. I particularly thank R. Cockerham, USGS Menlo Park, California; Dr. H. Kanamori, California Institute of Technology; Dr. A. Ryall, University of Nevada; Dr. B. A. Bolt, University of California - Berkeley; Dr. S. T. Algermissen, B. Askew, and Dr. A. Rogers of the USGS, Golden, Colorado; and the University of Utah Seismograph Stations for regional earthquake data. M. Bauer, D. Gallagher and S. Willett helped compile much of the geologic and geophysical information in the early stages of this project.

Special appreciation must go to my wife, Julie, and my daughter, Brooke, for their patience and support.

A Shell Graduate Fellowship, and a Society of Exploration Geophysicists scholarship supported my training at the University of Utah. Part of this research was done while the author was a visiting graduate fellow at the Lunar and Planetary Institute which is operated by the Universities Research Association under contract NASW3389.

INTRODUCTION

The Great Basin subprovince of the Basin - Range province, western U. S., is an area of active E-W lithospheric extension (Figure 1). The regime has been well documented [Smith and Sbar, 1974; Eaton et al. 1978; Zoback et al. 1981]; however, quantitative measurements of contemporary deformation and magnitudes of extension rates have been difficult to obtain. Various authors have made estimates of local and regional extension using studies of fault plane geometries, intraplate tectonic models, and geodetic measurements [Proffett, 1977; Minster and Jordan, 1984; Savage, 1983].

Brittle strain release in the lithosphere is primarily expressed by earthquakes that can be used to assess regional strain [see for example Doser and Smith, 1982; Hyndman and Weichert, 1983; and Wesnousky et al. 1982a]. Earthquake magnitudes with stress orientations derived from fault plane solutions can also be used to determine seismic moment tensors, that can be used to calculate strain rate tensors [Kostrov, 1974]. These data can then be used to determine horizontal strain and deformation rates. Earthquake data recorded on modern regional networks were used, along with historic data for large events, in these calculations.

The area of this study includes the Great Basin and surrounding areas of extension in southwestern Montana, western Wyoming, southern Idaho, eastern California, and southeastern Oregon (Figure 1). Figure 1 shows areas of assumed homogeneous seismicity and stress orientation used in this study. Great Basin topography is dominated by north-trending, normal-fault bounded ranges separated at ~25 km intervals by alluvium-filled basins. The region has a generally high elevation of about 1-1.5 km and is characterized by high heat flow exceeding 90 mW/m^2 [Lachenbruch and Sass, 1978], low Bouguer gravity

ORIGINAL PAGE IS
OF POOR QUALITY

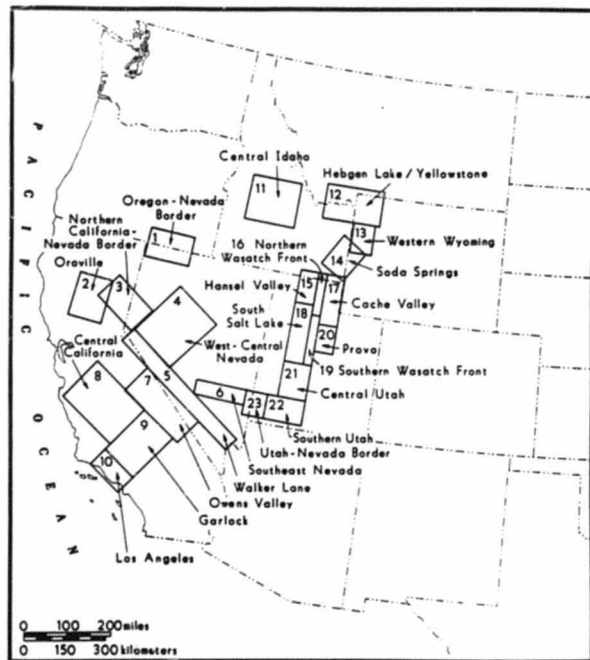


Fig. 1. Homogeneous seismic study area locations

[Eaton et al. 1978], a thin crust, 24-30 km, and low P_n velocities [Smith, 1978]. The seismicity occurs along diffuse N-S bands up to 200 km wide with shallow focal depths (80% of the events were shallower than about 10 km) around the Great Basin's margins [Smith and Sbar, 1974; Wright, 1976; Wallace, 1984] (Figure 2).

Determining contemporary strain rates in the Great Basin using earthquake data fulfilled two objectives; 1) it served as a measure of contemporary brittle strain rates, supplementing fault plane geometry studies and geodetic studies. This is important since fault plane geometry studies determine only paleostrain rates, and geodetic surveys, when available, are limited to small areas; 2) comparing strain rates from earthquake data with strain rates measured using other methods allows an estimation of the relative amount of brittle fracture versus aseismic creep.

In summary, the objectives of the study were: 1) to assess the compiled historical earthquake data set, 2) to determine the contemporary strain and deformation rates both within homogeneous portions of the Great Basin and in surrounding areas using the seismic moment tensor method, and 3) to compare the contemporary strain rates with geologic and geodetic determinations of strain rates.

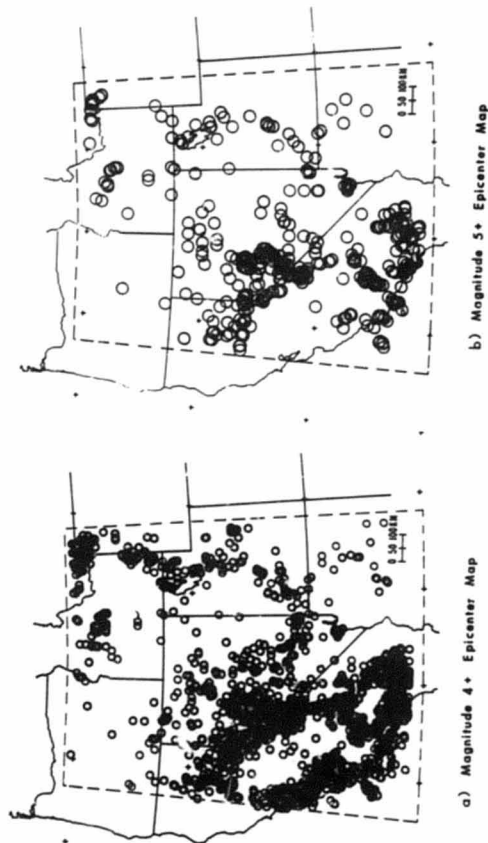
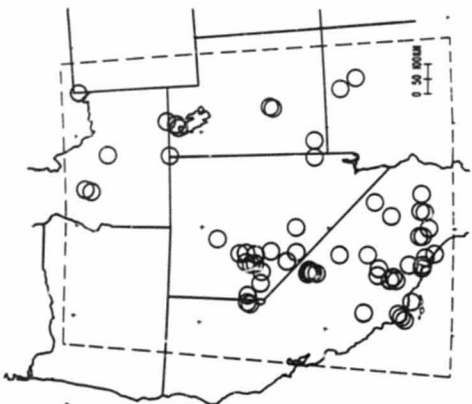


Fig. 2. Earthquake epicenter maps from data compiled for this study. Data covered the period from 1900-1981 including 1983 Borah Peak. Idaho events; a) $M_L > 4$, b) $M_L > 5$, c) $M_L > 6$, d) $M_L > 7$.



d) Magnitude 7+ Epicenter Map



c) Magnitude 6+ Epicenter Map

REGIONAL GEOLOGY AND GEOPHYSICS

Cenozoic History

Extension of the Great Basin began with the cessation of subduction along the west coast of North America about 30 ma. Before this extension regime, Mesozoic volcanism was associated with subduction that produced a calc-alkaline volcanic arc represented by the Sierra Nevada batholith. East of this arc, a foreland belt of folding and thrusting identified as the Sevier - Laramide thrust produced crustal compression and lithospheric shortening.

During the Miocene, about 30-40 ma, subduction was nearing its conclusion and WSW-ENE extension began in the Great Basin region, possibly as a result of back-arc spreading and stress relaxation of the lithosphere (Scholz et al. 1971; Zoback et al. 1981).

A second period of extension followed in the Great Basin region about 10-13 ma (Zoback et al. 1981), initially in the southern Basin - Range of Arizona and northern Mexico (Thompson and Burke, 1974). Marking the beginning of this extensional episode, the direction of extension rotated counterclockwise $\sim 45^\circ$ to a WNW-ESE direction (Zoback et al. 1981). Evidence from palinspastic reconstruction of profiles supports the theory of two separate periods of extension (Von Tish et al. 1985).

The upper crustal structure that developed during the latter period of crustal extension has largely overprinted evidence for the earlier periods of extension and compression (Eaton et al. 1978). However, in some areas, contemporary strain has been accommodated by movement on preexisting faults developed during the early periods of deformation.

[Zoback and Zoback, 1980; Smith and Bruhn, 1984].

The Great Basin is still undergoing E-W extension as evidenced by the regional seismicity and fault plane solution patterns [Smith, 1978; Smith and Lindh, 1978]. Some possible causes of Great Basin lithospheric extension have been suggested, such as lateral crustal loading, active magmatic intrusion, or a combination of these [Lachenbruch and Sass, 1978]. It appears that some mantle upwelling must accompany Great Basin extension to produce the widespread, late Tertiary basaltic volcanism [Best and Hamblin, 1978], high heat flow [Lachenbruch and Sass, 1978], and the high, E-W symmetric elevation of the province [Eaton et al. 1978].

Thompson and Burke [1974] concluded that passive magma intrusion may have occurred because of an onshore extension of the East Pacific rise. Eaton et al. [1978], on the other hand, rejected this passive model in favor of active mantle upwelling and divergence as a driving force for extension. Best and Hamblin [1978] and Stewart [1978] argued that upward movement of mantle material may have occurred to replace the old subducted plate that once existed under the Great Basin province. Smith [1978] coupled the rising mantle idea with the theory of four separate subplates of the the North American plate - namely the Great Basin, Northern Rocky Mountains, and the Sierra Nevada subplates moving away from the Colorado Plateaus subplate.

Atwater [1970] proposed that other factors motivating Great Basin extension were secondary to the region's role as a "soft" boundary of the North American Plate where it intersects the Pacific plate. However, many workers have noted that this model does not account for Great Basin symmetry, nor for the "soft" characteristics of the boundary itself [see for example Eaton et al. 1978; Best and Hamblin, 1978]. From the evidence compiled, it appears that both upward movement of mantle material and proximity of the western Great Basin to the San Andreas fault system have influenced deformation that has occurred in this region.

Earthquake History of The Great Basin

Seismicity within the Great Basin (Figure 2) has been concentrated along the eastern province margin associated with the southern Intermountain Seismic Belt (ISB), along the western province margin, associated with the Sierra Nevada front, and also in central Nevada [Smith, 1978] (Figure 2). Large magnitude earthquakes, $M \geq 6.5$, of the Great Basin have occurred principally in central Nevada, in Owens Valley, California, and at locations of pronounced changes in direction of the trend of the southern ISB (Table 1 and Figure 2c). Not surprisingly, many $M \geq 6$ earthquakes have also occurred along strike-slip faults associated with the San Andreas system in California. Most faulting associated with the San Andreas was not considered in this study and was removed from the data when possible (Figure 2).

Great Basin seismicity is characterized primarily by dip-slip and oblique-slip events throughout most of the region including $M \geq 7$ normal faulting events that produced scarps [Smith, 1978; Smith, 1985; Smith and Lindh, 1978]. Strike-slip and oblique-slip earthquakes have occurred along the region's southern and southwestern borders. According to Greensfelder et al. [1980], the shear zones marked by strike slip earthquakes found in the Walker Lane, the Garlock, and the extreme southern Nevada regions serve to separate zones of contrasting extension rate.

Most earthquakes in the Great Basin occur at depths less than 20 km and 80% are generally less than 10 km [Smith and Bruhn, 1984; Smith and Sbar, 1974]. Hypocenters of the largest earthquakes, $M \geq 7$, however, were located at greater depths, e.g. 15 km [Smith and Richards, 1984; Sibson, 1984] near the hypothesized brittle-ductile transition. Smith and Bruhn [1984] and Sibson [1984] have theorized that large earthquakes nucleate near the brittle-ductile transition where overburden loading can produce large shear stresses and where rocks are still strong enough to support those stresses. For example, three of the largest Great Basin earthquakes and their focal depths (all 15 km) are shown in Table 2. The large magnitude, $M \geq 7$, earthquakes can be clearly correlated with surface-breaking

Table 1. Great Basin $M_L \geq 6+$ earthquakes

yr	date	orig time	lat-n	long-w	depth	M_L	no	gap	dmn	rms
1857	109	1600 0.	34-48.60	119- 1.20	0.	7.9	0	0	0	0.
1872	326	1030 0.	36-36.60	118- 4.80	0.	7.9	0	0	0	0.
1901	1114	439 0.	38-46.15	112- 5.02	0.	6.3	0	0	0	0.
1902	728	657 0.	34-30.00	120-30.00	0.	6.3	0	0	0	0.
1902	801	330 0.	34-36.00	120-24.00	0.	6.3	0	0	0	0.
1902	1117	1950 0.	37-23.58	113-31.20	0.	6.3	0	0	0	0.
1907	920	154 0.	34- 6.00	117-18.00	0.	6.0	0	0	0	0.
1909	1006	250 0.	41-46.00	112-40.00	0.	6.4	0	0	0	0.
1910	924	405 0.	36- 0.	111- 6.00	0.	6.4	0	0	0	0.
1910	1121	2323 0.	38- 0.	117- 0.	0.	6.3	0	0	0	0.
1910	1121	2323 0.	38- 0.	118- 0.	0.	6.0	0	0	0	0.
1912	818	2112 0.	36-30.00	111-30.00	0.	6.4	0	0	0	0.
1914	218	1817 0.	39-30.00	119-48.00	0.	6.0	0	0	0	0.
1914	424	834 0.	39-30.00	119-48.00	0.	6.4	0	0	0	0.
1915	112	431 0.	34-42.00	120-18.00	0.	6.3	0	0	0	0.
1915	112	431 0.	34-30.00	120-30.00	0.	6.3	0	0	0	0.
1915	1003	149 0.	40-30.00	117-30.00	0.	6.0	0	0	0	0.
1915	1003	653 0.	40-30.00	117-30.00	0.	7.8	0	0	0	0.
1916	1023	244 0.	34-54.00	118-54.00	0.	6.0	0	0	0	0.
1916	1110	911 0.	35-30.00	116- 0.	0.	6.1	0	0	0	0.
1918	421	2232 25.00	33-48.00	117- 0.	0.	6.8	0	0	0	0.
1920	622	248 0.	34- 0.	118-30.00	0.	6.3	0	0	0	0.
1920	622	249 45.00	34- 0.	118-24.00	0.	6.3	0	0	0	0.
1921	929	1412 0.	38-40.97	112- 8.98	0.	6.3	0	0	0	0.
1921	930	230 0.	38-40.97	112- 8.98	0.	6.4	0	0	0	0.
1921	1001	1532 0.	38-40.97	112- 8.98	0.	6.3	0	0	0	0.
1922	310	1121 20.00	35-48.00	120-18.00	0.	6.9	0	0	0	0.
1923	723	730 26.00	34- 0.	117-18.00	0.	6.3	0	0	0	0.
1925	629	1442 16.00	34-18.00	119-48.00	0.	7.6	0	0	0	0.
1927	918	207 7.00	37-30.00	118-48.00	0.	6.0	0	0	0	0.
1929	708	1646 6.70	33-54.00	118- 6.00	0.	6.3	0	0	0	0.
1932	1221	610 4.00	38-48.00	117-58.79	0.	6.9	0	0	0	0.
1933	311	154 7.80	33-36.95	117-57.95	16.0	6.3	0	0	0	0.
1933	625	2045 0.	39- 6.00	119-18.00	0.	6.0	0	0	0	0.
1934	130	2016 35.00	38-16.79	118-22.20	0.	6.0	0	0	0	0.
1934	312	1505 48.00	41-42.00	112-48.00	0.	6.6	0	0	0	0.
1934	312	1820 0.	42- 0.	114- 0.	0.	6.1	0	0	0	0.
1934	312	1820 12.00	41-42.00	112-48.00	0.	6.1	0	0	0	0.
1934	608	447 0.	35-48.00	120-19.79	0.	6.0	0	0	0	0.

Table 1. cont.

yr	date	orig time	lat-n	long-w	depth	M_L	no	gap	dmn	rms
1940	518	721 32.70	34- 3.96	116-19.97	16.0	7.0	0	0	0	0.
1941	914	1643 31.80	37-33.95	118-43.97	16.0	6.0	0	0	0	0.
1941	914	1839 11.90	37-33.95	118-43.97	16.0	6.0	0	0	0	0.
1944	712	1930 23.00	44-30.00	115-30.00	0.	6.1	0	0	0	0.
1945	214	301 15.00	44-42.00	115-24.00	0.	6.0	0	0	0	0.
1946	315	1349 35.90	35-42.95	118- 3.00	22.0	6.0	0	0	0	0.
1947	410	1558 6.00	34-58.97	116-33.00	0.	6.2	0	0	0	0.
1948	1204	2343 17.00	33-55.97	116-22.97	0.	6.5	0	0	0	0.
1948	1229	1253 27.00	39-30.00	120- 6.00	0.	6.0	0	0	0	0.
1949	502	1125 47.00	34- 1.10	115-40.97	-	6.1	0	0	0	0.
1952	721	1152 14.00	35- 0.	119- 0.95	16.0	7.7	0	0	0	0.
1952	721	1205 31.00	35- 0.	119- 0.	16.0	6.0	0	0	0	0.
1952	723	38 32.00	35-21.95	118-34.97	16.0	6.0	0	0	0	0.
1952	729	703 47.00	35-22.97	118-51.00	16.0	6.0	0	0	0	0.
1954	706	1113 20.00	39-25.20	118-31.79	0.	6.0	0	0	0	0.
1954	706	2207 41.00	39-18.00	118-30.00	0.	6.0	0	0	0	0.
1954	824	551 32.50	39-34.79	118-27.00	0.	6.0	0	0	0	0.
1954	1216	1107 11.00	39-16.79	118- 7.19	0.	6.9	0	0	0	0.
1954	1216	1111 34.00	39-48.00	118- 6.00	0.	6.0	0	0	0	0.
1959	323	710 20.00	39-36.00	118- 4.19	0.	6.0	0	0	0	0.
1959	623	1435 2.00	39- 4.80	113-49.20	0.	6.3	0	0	0	0.
1959	818	637 15.00	44-49.97	111- 4.98	0.	7.6	0	0	0	0.
1966	816	1802 36.60	37-24.00	114-12.00	33.0	6.0	0	0	0	0.
1966	912	1641 1.10	39-25.20	120- 9.00	0.	6.0	0	0	0	0.
1968	426	1500 0.10	37-18.00	116-30.00	0.	6.3	0	0	0	0.
1971	209	1400 41.80	34-24.65	118-24.50	0.	6.4	0	0	0	0.
1973	606	1300 0.10	37-14.69	116-20.76	0.	6.1	0	0	0	0.
1975	328	231 5.99	42- 3.77	112-31.48	5.0	6.2	0	0	0	0.
1975	603	1420 0.20	37-20.39	116-31.37	0.	6.0	0	0	0	0.
1975	626	1230 0.20	37-16.73	116-22.13	0.	6.1	0	0	0	0.
1975	1028	1430 0.20	37-17.39	116-24.71	0.	6.3	0	0	0	0.
1975	1120	1500 0.10	37-13.50	116-22.70	0.	6.0	0	0	0	0.
1976	103	1915 5.20	37-17.91	116-19.97	0.	6.2	0	0	0	0.
1976	212	1445 0.20	37-16.26	116-29.28	0.	6.3	0	0	0	0.
1976	314	1230 0.20	37-18.36	116-28.26	0.	6.2	0	0	0	0.
1980	525	1633 44.80	37-36.47	118-49.27	3.7	6.4	0	0	0	0.
1980	525	1944 48.10	37-19.86	118-49.79	0.	6.1	0	0	0	0.
1980	525	1944 52.15	37-33.37	118-47.43	6.4	6.5	0	0	0	0.
1980	527	1450 57.12	37-27.82	118-49.40	2.4	6.3	0	0	0	0.
1980	527	1451 56.70	37-26.87	118-47.90	0.	6.2	0	0	0	0.
1983	1028	1406 6.79	43-58.07	115-53.94	16.0	7.3	19	106	70	0.32

Table 2. Nucleation depths of large Great Basin earthquakes

Date	Location	Magnitude	Depth (Km)
1954	Dixie Valley, Nevada	6.9	15
1959	Hebgen Lake, Montana	7.5	15± 3
1983	Borah Peak, Idaho	7.3	16± 4

Adapted from Smith and Richins [1984]

faults. However, for smaller earthquakes, generally less than M 6.5, there is a lack of surface faulting [Smith, 1982].

History of Strain Study

Quantifying deformation in the Great Basin has been a natural culmination of studies of Great Basin Cenozoic history. The amount and rate of extension in the Great Basin have been estimated by many workers with disparate results (percentage of extension ranging from 10-300 %). Some of the estimates (Table 3) are as follows: Thompson and Burke [1974] have estimated extension of 100 km or 10% based on fault geometries, amounts of slip on Quaternary faults, and Pleistocene Lake shorelines in Dixie Valley, Nevada. Strain rates derived from seismicity in the paper by Greensfelder et al. [1980] agreed with this 10% extension rate in this area. Jordan et al. [1985] calculated a deformation rate of less than 9 mm/a (or less than 10-15% extension) based on the theory that the relative velocity of the Pacific and North American plates, up to 55 mm/a, was not totally accounted for by motion along the San Andreas fault. Thus a deficit must be made up in Great Basin and offshore California deformation.

Lachenbruch and Sass [1978] used thermal properties and reduced heat flow to estimate a total Great Basin extension rate of 10-20%. This estimate is equivalent to a deformation rate of 5-10 mm/a.

Other fault geometry/slip-rate studies have suggested higher estimates of crustal extension, depending largely on inferred fault dip at depth. There is evidence that some Great Basin faults become listric at depth [Smith, 1977; Smith and Bruhn, 1984] and the resulting shallower dips may yield higher extension estimates.

Zoback et al. [1981] have estimated Great Basin total extension in the last 10 ma to be 15-30%. Wright [1976] has subdivided the region by primary faulting style into northern and southern parts (normal faults to the North and strike-slip and oblique-slip faults to the south) and calculated 10% extension for the northern section and 50% extension in the

Table 3. Great Basin extension estimates from other workers

Author	Percent Extension	Method
Thompson and Burke [1974]	10	fault geometries/ slip rates
Greensfelder [1980]	10	seismicity
Jordan et al. [1985]	10-15	tectonic plate interaction
Zoback et al. [1981]	15-30	fault geometries/ slip rates
Wright [1976]	10 northern region	fault geometries/ slip rates
	50 southern region	fault geometries/ slip rates
Proffett [1977]	10-15 central region	fault geometries/ slip rates
	50-100 east and west margins	fault geometries/ slip rates
	30-35 entire Great Basin	fault geometries/ slip rates
Lachenbruch and Sass [1978]	10-20	heat flow
Hamilton and Meyers [1966]	100-300	palinspastic reconstruction
Von Tish et al. [1985]	~60 for Sevier Desert, Utah	palinspastic reconstruction/ reflection seismology

south. Proffett [1977] studied the highly faulted Yerrington, Nevada district and used his results to infer 10-15% extension in the central Great Basin where faults are less dense and appear to dip more steeply. Along the east and west boundaries where faulting is more pervasive and fault planes appear to have shallow dips at depth, Proffett estimated crustal extension to be from 50-100%. His study concluded a total Great Basin extension of 30-35% and included extension back to 17-18 ma.

Palinspastic reconstructions have been carried out assuming extension back to the Mesozoic by Hamilton and Meyers [1966, as reported by Zoback et al. 1981] resulting in total extension of 100-300%. Zoback et al. [1981] postulated that some of the variation in total crustal deformation results stems from a failure to recognize and differentiate between the two different extensional episodes discussed above. Von Tish et al. [1985] have recently shown from reflection profiles in the eastern Great Basin that these two episodes have produced up to 60% local extension. Consequently, workers who failed to recognize the different extension episodes would have averaged over both phases and calculated higher total extension for the Great Basin.

STRAIN DETERMINATION FROM EARTHQUAKE DATA

Brittle Fracture and Crustal Structure

Earthquakes result from strain released through brittle fracture in the lithosphere. The lithosphere's mechanical properties change with depth according to rock composition, temperature, and strain rate [Sibson, 1984; Smith and Bruhn, 1984; Caristan and Brace, 1980]. The uppermost crust experiences brittle deformation under stress while deeper crustal rocks of the same composition deform more ductilely as temperature increases. Based on Byerly's brittle behavior law and power law for creep, Smith and Bruhn [1984] concluded that the Great Basin can be modeled with an upper brittle layer (about 8 km thick) underlain by a quasi-plastic layer, a second brittle layer (approximately 2 km thick) at a depth of about 15 km, and a third brittle layer, also about 2 km thick at 25 km depth (Figure 3). Changes in rock composition with depth account for the three different brittle layers.

The maximum depth of brittle behavior controls the depth at which earthquakes nucleate. Stresses in the crust increase with depth in the brittle layers because of overburden loading, and then decrease at still greater depths as the rocks become increasingly ductile, primarily from increased temperature. The greater the degree of quasi-plasticity in rocks, the more they deform aseasonally instead of supporting high deviatoric stresses. The result is that high deviatoric stresses needed to generate large earthquakes develop in the deepest of the brittle layers. Historically, large earthquakes in the Great Basin have nucleated at depths of about 15-20 km while smaller earthquakes typically nucleate at shallower depths [Smith et al. 1984b; Smith and Richins, 1984; Smith, 1985]. The brittle strain release that causes these earthquakes can be calculated using the method described below.

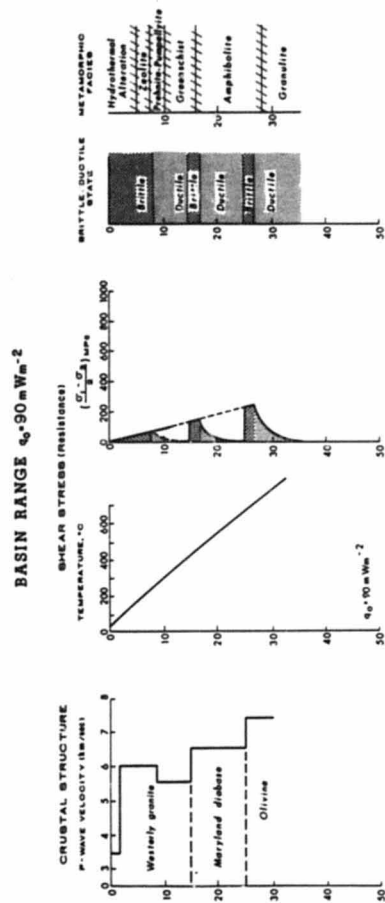


Fig. 3. Great Basin crustal composition and mechanical property profiles. Profiles are from Smith and Bruhn [1984].

Strain Rate Calculations From The Seismic Moment Tensor

The seismic moment method described here was used to calculate stress, strain and seismic moment information from earthquake magnitudes and fault plane solutions following the work of Kostrov [1974], Anderson [1979], Molnar [1979], and Doser and Smith [1982]. The process involves the following steps. First, earthquake magnitudes for given areas of homogeneous strain were converted to scalar moments, and average stress orientations were determined from fault plane solutions. Second, moment tensors were calculated for each earthquake and then summed; then the eigenvalues and eigenvectors of the summed moment tensor were determined. A synthetic fault-plane solution was then calculated for the summed events in each area. Finally, strain rates and deformation rates were determined from the summed moment tensors using Kostrov's [1974] formula:

$$\dot{\epsilon}_{ij} = \frac{\sum m_{ij}}{(2\mu\Delta V\Delta t)} \quad (1)$$

where $\dot{\epsilon}_{ij}$ are the strain rate tensor components, m_{ij} are the components of the moment tensor. The summation represents the component summation of moments mentioned above, ΔV is the volume of the block we are considering, Δt is the time difference between first and last events, and μ is the shear modulus taken to be 3.3×10^{11} dynes/cm² [Molnar, 1979]. The moment tensor is defined by the equation:

$$m_{ij} = M_s(b_j n_i + b_i n_j) \quad (2)$$

where \bar{b} is the unit vector in the displacement direction and \bar{n} is the unit vector perpendicular to the fault plane [Gilbert, 1970].

Kostrov [1974] assumed that deformation occurs on many separate dislocations (Figure 4). Consequently, it is not necessary to study individual fault geometries if stress orientations can be established by other means.

Let us examine each of the major steps mentioned above (hereafter A, B, and

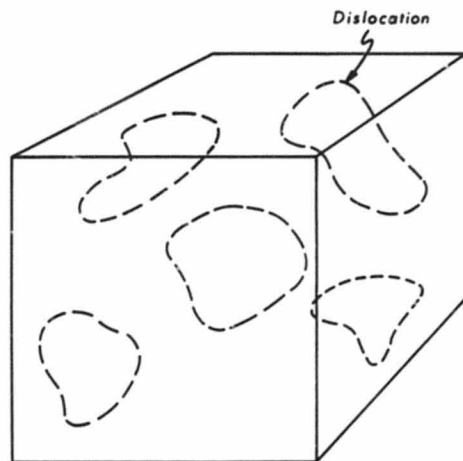


Fig. 4. Unit volume brittle flow diagram. Closed dotted lines represent dislocations [Kostrov, 1974].

C) in more detail using a sample case to illustrate. The program 'nstrain' which incorporates most of the following calculations is included in Appendix B along with other programs used in this study. Also, Files 1-5, input and output files associated with a test case in the Oregon-Nevada border area (area 1) of this study are included in Appendix A. The Oregon-Nevada area files are considered because that area experienced only 71 earthquakes of $M_L > 2.5$ during the study period and so the files are small enough to be conveniently included in the text. The programs are marked with the capital letters that correspond to the part of this text that explains them. All computer programs referred to in this text will be denoted with single quotes ('example').

A) *Conversion of magnitudes to seismic moments* - The seismic moment and seismic moment rates of a single fault are given by:

$$M_s = \mu A u \quad (3a)$$

$$\dot{M}_s = \mu A \dot{u} \quad (3b)$$

where u = slip, A = fault plane area, μ = shear modulus, and \dot{u} and \dot{M}_s = slip rate and moment rate respectively [after Aki, 1966].

When possible, seismic moments for large ($M_L > 7$) earthquakes were taken from the results of other workers [e.g., Hanks et al. 1975; Sieh, 1977; Doser, 1985]. Seismic moments for smaller events were estimated using empirical moment-magnitude relations. Some examples of moment-magnitude relations for indicated areas and types of deformation are:

$$\log(M_0) = 1.1M_L + 18.4, \quad 3.7 \leq M_L \leq 6.6; \quad (4a)$$

Utah (extension) [Doser and Smith, 1982]

$$\log(M_0) = 1.2M_L + 18.0, \quad 3.7 \leq M_L \leq 6.6; \quad (4b)$$

Utah (extension) [Doser and Smith, 1982]

$$\log(M_0) = 1.09M_L + 17.46, \quad 3.0 \leq M_L \leq 6.3; \quad (4c)$$

Mammoth Lakes, California (extension) [Archuleta et al. 1977]

$$\log(M_0) = 1.5M_L + 16.0, \quad 2.0 \leq M_L \leq 6.8; \quad (4d)$$

California (compressive strike-slip) [Thatcher and Hanks, 1973].

Equation (4a) was applied to the Great Basin extensional events and equation (4d) was used for California oblique-slip and strike-slip events. The magnitudes were converted to the local magnitudes (Richter magnitude), M_L , scale in this study.

The next step is to associate a regional stress field orientation with each region of homogeneous strain (defined later in this chapter, see Figure 1). The stress orientations from observed fault plane solutions for a given area were weighted and averaged providing the resulting average stress orientation. This direction was assumed for all earthquakes in a given area. This "average" stress orientation was found by calculating an average synthetic fault plane solution using the moment tensors of those earthquakes with known fault plane solutions.

For example, File 1 is the earthquake summary file for area 1. File 2 lists the three focal mechanisms available for that area taken from Smith and Lindh [1978], and C. F. Kienle and R. W. Couch (unpublished data, 1977). 'Nstrain' was used to process these three earthquakes resulting in the synthetic fault plane solution listed in File 3. This 'synthetic fault plane solution' gives the average stress orientation mentioned above. The last two lines of File 3 list the two strikes and dips of the synthetic fault plane solution nodal planes. The rest of the file gives the positions of the principal stress axes for plotting. Rakes for the two nodal planes were determined, then strikes, dips and rakes were applied to each earthquake in the 'nstrain' input file (File 4) in lieu of the unavailable fault plane solutions.

Also included in this input file (File 4) were the name of the synthetic fault plane solution output file (called 'fmain' for area 1), the region name ('Nevada - Oregon

border" in this example) and the number of events to be considered (71 here). These three sources of information constitute the first three lines of the input file. The last four lines contain the coefficient of friction to be used in constructing the synthetic fault plane solution, the area dimensions, the time period considered and the rotation of the area box with respect to North. This information completed the 'nstrain' input file. The remaining steps of the analysis, steps B) and C) were carried out with 'nstrain'.

B) Calculate, sum and diagonalize moment tensors - The strike, dip and rake of the assumed fault plane of each earthquake were used to find its moment tensor. The conventions and symbols from Aki and Richards [p. 106, 1980] used for these values are

ϕ - strike - measured clockwise from north

δ - dip - measured in a plane perpendicular to both the horizontal and the nodal planes, from horizontal down to the nodal plane

λ - rake - measured in the nodal plane down from the horizontal to the slip vector

See Figure 5 for an illustration of these conventions.

The data for the auxiliary plane were used only to determine the slip vector on the fault plane for printout using these equations:

$$\text{slip vector trend, } \phi_{s1} = \phi_{s2} - 90^\circ \quad (5a)$$

$$\text{slip vector plunge, } \delta_{s1} = 90^\circ - \delta_{s2} \quad (5b).$$

The data for the fault plane, along with the scalar moment, M_0 , are used to find the moment tensor according to Aki and Richards' [p. 117, 1980] equations:

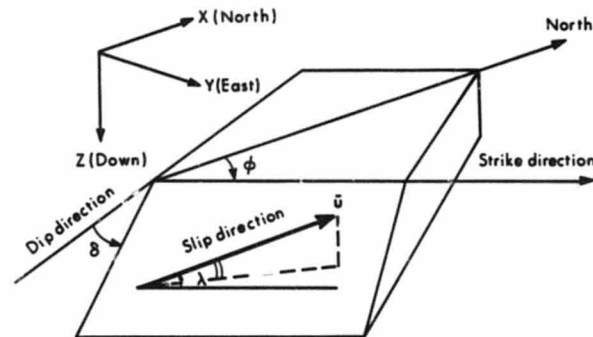


Fig. 5. Fault geometry conventions diagram. Conventions are from Aki and Richards [1980].

$$m_{xx} = -Mo(\sin \delta \cos \lambda \sin 2\phi + \sin 2\delta \sin \lambda \sin^2 \phi) \quad (6a)$$

$$m_{xy} = m_{yx} = Mo(\sin \delta \cos \lambda \cos 2\phi + (1/2) \sin 2\delta \sin \lambda \sin 2\phi) \quad (6b)$$

$$m_{zz} = m_{nn} = -Mo(\cos \delta \cos \lambda \cos \phi + \cos 2\delta \sin \lambda \sin \phi) \quad (6c)$$

$$m_{yy} = Mo(\sin \delta \cos \lambda \sin 2\phi - \sin 2\delta \sin \lambda \cos^2 \phi) \quad (6d)$$

$$m_{yz} = m_{zy} = -Mo(\cos \delta \cos \lambda \sin \phi - \cos 2\delta \sin \lambda \cos \phi) \quad (6e)$$

$$m_{nn} = Mo(\sin 2\delta \sin \lambda). \quad (6f)$$

Next, the eigenvalues and the eigenvectors of the moment tensor, m_{ij} , are calculated using a math library subroutine 'eign' which uses a solution algorithm for cubic equations [Forsythe, Malcolm and Moler, p. 49, 1977]. We arrive at the cubic equation via the following system of equations

$$\begin{bmatrix} m_{xx} & m_{xy} & m_{xz} \\ m_{yx} & m_{yy} & m_{yz} \\ m_{zx} & m_{zy} & m_{zz} \end{bmatrix} \begin{bmatrix} l \\ m \\ n \end{bmatrix} = \Gamma \begin{bmatrix} l \\ m \\ n \end{bmatrix} \quad (7)$$

that reduce to

$$\det \begin{bmatrix} m_{xx} - \Gamma & m_{xy} & m_{xz} \\ m_{yx} & m_{yy} - \Gamma & m_{yz} \\ m_{zx} & m_{zy} & m_{zz} - \Gamma \end{bmatrix} = 0 \quad (8)$$

where l , m , and n are the direction cosines of the principal axis associated with each principal value, Γ_i .

Equation (8) can be reduced to a cubic equation in Γ , and then solved by 'eign'. The resulting three eigenvalues, Γ_i , and their associated eigenvectors are not only the principal moment values and axes, but are also the primary stress values and axes [Kostrov,

1974; Aki and Richards, p. 117, 1980].

From this point, the moment tensors of individual events can be summed by component and the resulting regional moment tensor can be diagonalized as above.

Referring to File 5/ which contains the Oregon-Nevada Border area 'nstrain' results as an example, note that the bulk of the output from 'nstrain' consists of the echoed input information, moment tensor, eigenvalues and eigenvectors for each event. After these are listed, the regional moment tensor is presented along with its eigenvalues and eigenvectors.

C) *Strain and deformation rates* - Assuming linear elasticity, the moment tensor can be converted to the strain rate tensor using Kostrov's [1974] equations:

$$\dot{\epsilon}_{ij} = \frac{\Sigma m_{ij}}{(2\mu \Delta V \Delta t)} \quad (1)$$

To find the maximum strain rates in the horizontal plane, the two-by-two strain rate matrix (9) was then diagonalized.

$$\begin{bmatrix} \dot{\epsilon}_{xx} & \dot{\epsilon}_{xy} \\ \dot{\epsilon}_{yx} & \dot{\epsilon}_{yy} \end{bmatrix} \quad (9)$$

From this point, finding the deformation rate in the direction of the maximum horizontal strain rate is a simple matter of trigonometrically calculating the distance, L , across the study area in that direction and then multiplying that distance, L , by the strain-rate as in

$$\text{deformation rate (mm/s)} = (\dot{\epsilon}_{max}) \times L \quad (10).$$

The strain and deformation rates for the Oregon-Nevada border area are listed in the last section of File 5/ entitled "Determination of the Strain Rate." The area dimensions as well as the time span considered are also listed there.

Homogeneous Seismic Areas

One goal of this study was to determine detailed local as well as more regionalized strain rates. To determine local strain rates, Kostrov's method was applied to the smaller areas of more homogeneous strain release shown in Figure 1.

The boundaries of the areas in Utah were established previously by C. Renggli and R. B. Smith (unpublished data, 1983) based on area seismicity and geology. The choice of other area boundaries was similarly based on: 1) fault types and orientations shown in the paper by Greensfelder et al. [1980]; 2) similarities derived from fault plane solutions' P and T axes (maximum and minimum principal stress axes); and 3) similarities in Quaternary geology. The three criteria were usually compatible, although an occasional fault plane solution would display P and T axes inconsistent with area surface geology and other area fault plane solutions.

Limits and Accuracy

The accuracy of the method described above is limited primarily by discretization, approximations, by incompleteness and vagueness in the earthquake catalogs and fault plane solution data, and by incorrect magnitude-moment conversions.

First, recall that to find strain, Kostrov's equation (1) requires a reference volume, V . The discrete area subdivisions described above, with an assumed brittle zone depth of 15km, define this volume term. Although the area boundaries were chosen to enclose geologically and geophysically homogeneous regions, it is obvious that no real strain field is completely homogeneous in discrete blocks, nor will it change magnitude and orientation discontinuously at block boundaries. Consequently, the area boundaries shown in Figure 1 could be misplaced 10-20 km. (For example, see the discussion of the Central Utah area in the "STRAIN RATES FROM SEISMICITY" section). This introduces an error of $\pm 5\%$ in strain magnitude and $\pm 15^\circ$ in strain direction.

Completeness of the earthquake data, particularly the percentage of events for

which fault plane solutions have been determined, is a second limitation. The seismic moment tensor method requires both a magnitude and a fault plane solution for each earthquake. Unfortunately, less than 1% of the earthquakes used were accompanied by fault plane solutions; however, most events of $M \geq 6$ in each area had solutions.

Averaging the stress orientations of the available fault plane solutions and applying the resulting "average fault plane solution" to each earthquake alleviated the lack of fault plane solutions for each event, but required an assumption of uniform strain release for all magnitude earthquakes. I know that, in many areas of the Great Basin, $M < 4$ events produce a variety of fault plane orientations, sometimes not the same as the larger, $M \geq 6$, events. Since fault plane solutions for larger magnitude events were usually available and since larger events account for most of the moment in any area (an increase of 1 in magnitude is approximately equal to multiplying the moment by 10), the effect of this assumption on the accuracy of the strain rates is less than 5%.

Another limitation arises from variations in type of magnitude used M_L , m_b , or M_s . The earthquake data in some catalogs did not specify which magnitude scale was used. The main earthquake data file was a combination of several independently compiled catalogs. Simply treating all the magnitudes the same would introduce significant error when magnitudes were converted to moments. For example, if one were to assume that all the earthquakes in an 'nstrain' input file were given in M_s , but all were really in m_b , (the worst case) the resulting error in strain and deformation rates could be as great as 25 - 30%.

Fortunately, there were several independent sources available which gave magnitude scales for many of these events. The U.S. Geological Survey Great Basin Study provided a carefully prepared earthquake file that covered the period from 1900 to 1977 [Askew and Algermissen, 1983]. Using the magnitude data of the University of Utah Seismograph Stations, and correlating with the USGS file and with published data on specific events (for example the work by Hanks et al. [1975] on California earthquakes), helped minimize the

error caused by incorrect magnitude scale assumptions to 10%.

Error can also be introduced in the magnitude-moment conversion even if proper magnitude scales are assumed. Hanks and Boore [1984] suggested that different magnitude scales established for different parts of California are not really characteristic of different areas, but are dependent on the range of the earthquake magnitudes used to create them. Their assertion is that $\log(\text{moment})$ vs. magnitude is not a linear relationship, but that the magnitude of the slope of the curve increases with increasing earthquake magnitude (Figure 6). Thus, if only large magnitude earthquakes were used to establish a linear moment-magnitude relation, the slope of that line would be too steep and moments for small earthquakes would be underestimated. Conversely, if only smaller magnitude events were used, the slope would be too small and the moments for larger earthquakes would be underestimated.

The primary moment-magnitude relation used in this study, equation (4a), by Doser and Smith [1982] was based on spectral analyses of extensional earthquakes in Utah with magnitudes in the range M_L 3.7-6.6. Thus, the moments of $3.7 < M_L < 6.6$ events would be accurately predicted by equation (4a). An earthquake magnitude outside this range might be converted inaccurately to a seismic moment. However, since smaller earthquakes have orders of magnitude less impact on the total moment than larger events and since moments for most $M_L > 7$ earthquakes were taken from independently determined results in the literature, possible nonlinearity of the moment-magnitude relation contributed less than 5% underestimation of moment in any given area.

Relation (4d) of Thatcher and Hanks [1973] used to determine the moments of California strike-slip events was based on 138 events with magnitudes between M_L 2.0 - 6.8, almost all being M_L 3+ and most M_L 4+. Thus, the argument supporting equation (4a) applies almost exactly to equation (4d) (which was used to determine moments in the Central California, Garlock, and Los Angeles areas).

Another important limitation in moment-magnitude conversions is the variation

in published seismic moment determinations for earthquakes. For example, Hanks et al. [1975] determined a moment for the 1952 Fort Tejon, California earthquake of 9.0×10^{17} dyne-cm while Sieh [1977] gave a moment range of 5.0×10^{17} - 8.7×10^{17} dyne-cm for the same event. Variation in recorded seismic moments can vary by a factor of three. This corresponds to possible error of $\pm 300\%$ in strain rate results.

Seismic moments were taken from the results of other workers for 12 earthquakes ranging in magnitude from M_L 6.1 to M 7.9 (M is moment magnitude, Hanks and Kanamori [1979]) (Table 4). However, independent moments were not found for the large central Nevada earthquakes. The error in seismic moment determinations for large earthquakes using moment-magnitude relations is also a factor of three because of scatter in moment-magnitude curves. Hence, a $\pm 300\%$ error is possible whether the moment came from the literature or from a moment-magnitude relation.

Wesnousky et al. [1982b] also suggested that earthquake frequency distributions for single faults are not characterized exactly by equation

$$\log(N) = a - bM \quad (11)$$

but instead aftershocks and foreshocks follow such a pattern while the main shocks achieve anomalously high magnitudes. That is, on a $\log(N)$ vs. M plot, as $\log(N)$ approaches zero, a main shock will have a magnitude 1-1.5 units higher than equation (11) predicts.

Hyndman and Weichert [1983], Schwartz and Coppersmith [1984], Anderson and Luco [1983], and Wesnousky et al. [1982b] have also theorized that $\log(N)$ versus M is not linear. They have shown that the number of earthquakes falls off from the linear rate at high magnitudes. Schwartz and Coppersmith argued that an impulse in the number of $M = m$ earthquakes then occurs. Hyndman and Weichert [1983] used nonlinear recurrence relations to estimate seismic moment rates and strain rates in the Pacific Northwest. In this study, empirical moment-magnitude relations were applied only to real events, not to events predicted by recurrence relations. Hence, nonlinear recurrence relations did not affect strain

Table 4. Seismic moments for large earthquakes from published studies.

Earthquake	M_L	Moment dyne-cm	Reference
California	Jan 9, 1857	M_s 8.3	$5.3-8.7 \times 10^{27}$ Sieh [1977]
			9.0×10^{27} Hanks et al. [1975]
	March 26, 1872	M_s 8.3	5.0×10^{26} Hanks et al. [1975]
	March 15, 1946	6.0	1.0×10^{25} Hanks et al. [1975]
	July 21, 1952	7.7	2.0×10^{27} Hanks et al. [1975]
	July 21, 1952	6.0	3.0×10^{25} Hanks et al. [1975]
	July 29, 1952	6.0	3.0×10^{25} Hanks et al. [1975]
Feb 9, 1971	6.4	1.0×10^{26} Hanks et al. [1975]	
Utah	1934	6.6	7.7×10^{25} Doser and Smith [1982]
Hobgen Lake	1959	7.6	1.0×10^{27} Doser [1985]
Idaho	1975	6.2	1.5×10^{25} Doser [1985]
Yellowstone	1975	6.1	7.5×10^{24} Doser [1985]
Borah Peak	1983	7.3	3.3×10^{26} Doser [1985]

rate calculations.

The fact that smaller earthquakes, with magnitudes $M < 4$, have not been included from earlier periods of recording also adds to moment underestimation. However, because the large magnitude earthquakes contribute most of the moment, underestimation from both incorrect magnitude-moment conversions and incomplete small earthquake listings was less than 5%.

A more fundamental limitation of determining strain rates from earthquake data is the assumption of an idealized, brittle medium. There is evidence that at some time around 10-20 Ma, the Great Basin stress field rotated $\sim 45^\circ$ in the horizontal plane from WSW-ESE to WNW-ESE [Zoback et al. 1981]. Reactivation of preexisting faults by the present stress field could have introduced error into the results of this study. However, Kostrov's [1974] method, equation (1), assumes statistical distributions and orientations of dislocations in the deforming material. Hence, fault plane orientations of all events were not necessary for the calculations.

The total error in strain and deformation rate calculations because of these limitations is $\pm 325\%$ in magnitude and $\pm 15\%$ in direction. The error in strain magnitude is almost entirely from uncertainty in seismic moment determination for large earthquakes which overshadows all other sources of error.

EARTHQUAKE DATA

Earthquake Catalog

The primary earthquake data used in this study were from a compilation by R. B. Smith and co-workers of data principally from the University of Utah, University of Nevada, National Earthquake Information Service (NEIS), United States Geological Survey (USGS), California Institute of Technology, University of California at Berkeley, and other sources. A complete listing of the earthquake summary files used in this study is given in Appendix C.

The earthquake catalog produced for this study contains a listing of the felt and instrumentally recorded earthquakes from the western U. S. Cordillera during the 19th and 20th centuries up to and including most of 1981. Before 1967, earthquake recording was hampered by a lack of seismograph network coverage. Consequently, only earthquakes recorded after 1900 were considered accurate enough and the files sufficiently complete for use in this study. Because of their large size and impact on the calculations, the 1857 Ms 8.3 Fort Tejon, California and the 1872 Ms 8.3 Owens Valley, California earthquakes were included in this study. All events within the Nevada Test Site were removed from the catalogs studied. No attempt was made to distinguish between manmade and natural events.

The record of M4+ earthquakes was considered to be reasonably complete post 1900 since the number of events of M4+ recorded in this century varies little from year to year. The M4+ earthquakes, shown in Figure 2a, contributed most of the moment and corresponded to the areas of maximum deformation.

For example, in the Walker-Lane, Nevada area (area # 5 in Figure 1) the

maximum horizontal deformation rate including all the events totaled 2.9 mm/a. The same area with only M4+ earthquakes included yielded a 2.7 mm/a deformation rate. Earthquakes with magnitudes less than M4 were responsible for only about 6% of the brittle deformation during this century in that area, so some incompleteness for small magnitude events was not critical to the interpretation.

Table 5 shows the total scalar moment produced by M4+, M5+, M6+, and M7+ Great Basin and southern California earthquakes. These data show that the 3630 earthquakes with magnitudes $4 \leq M < 7$ accounted for only 18% of the seismic moment released in all M4+ earthquakes; whereas the seven M7+ earthquakes produced 82% of the moment.

In addition to the University of Utah main file discussed above, two additional sources of earthquake summary listings were used. First, a newer USGS earthquake file for the Great Basin area including earthquakes from 1803 - 1977 [Askew and Algermissen, 1983] was used to correlate and correct the magnitudes of all M4+ earthquakes common to the main file and the new USGS file (most of the earthquakes found in the main file that were recorded before 1977 are included in the new USGS file). About 20 earthquakes listed only in the new USGS file were added to the primary file. Second, the University of Utah file of the 1983 Borah Peak, Idaho earthquake and its aftershocks [Richins et al. 1985] was added to the Central Idaho area listing.

Cordilleran Seismicity

The data used in this study included ~50,000 earthquakes out of the ~120,000 events summarized in the various catalogs. The area covered by the main earthquake file extended from longitude 100° - 130° W and from latitude 30° - 50° N; Figure 2 shows the seismicity confined primarily to the study area (longitude 109°30' - 125° West and latitude 33°30' - 46°).

The areas of most active seismicity occurred at or near changes in direction of

Table 5. Effect on moment of study area earthquakes above different minimum magnitudes

M_{min}	No. of Earthquakes	Moment (dyne-cm)
4	3637	2.2×10^{28}
5	572	2.1×10^{28}
6	80	2.6×10^{28}
7	7	1.8×10^{28}

the ISB; along the Great Basin's western border; in Central Nevada; and along the San Andreas fault and its associated system. Almost half of the earthquakes studied were located in the San Andreas, Garlock, and White Wolf fault zones (areas 8, 9 and 10 in central and southern California). Figure 2d shows that, of the seven $M7+$ earthquakes that occurred in the study area, three were located in the Los Angeles, and Garlock areas; one $M7+$ event each occurred in the Owens Valley, California, West Central Nevada, Hebgen Lake/ Yellowstone Park, and Central Idaho areas.

Fault Plane Solutions

The fault plane solution data used in this study were compiled by C. Renggli and R. B. Smith (unpublished data, 1983) primarily from the data of Smith and Lindh's (1978) Table 5-1. These were augmented by fault plane solutions for the 1959 Hebgen Lake, Montana earthquakes [Doser, 1984], for the 1983 Borah Peak earthquake sequence [Doser, 1985], and by focal mechanisms for Great Basin earthquakes based on surface wave analyses by Patton [1984].

Information taken from fault plane solutions include the strike, dip, and rake of each nodal plane (following the Aki and Richards' conventions (Figure 5)). Typically, rakes would be missing (with only the two nodal plane strikes and dips given) or incorrect, so rakes were calculated from the strikes and dips of the two nodal planes. The updated tabulation of all focal mechanisms is summarized in Appendix C and 'T' axes are presented in Figure 7. These axes show that extension across the Great Basin is generally N-S in Idaho, Montana and Wyoming, and E-W throughout the rest of the Great Basin.

Next the USGS file of Askew and Algermissen [1983] was sorted into the homogeneous areas mentioned earlier, and then sorted according to magnitude scale. Since many of the events in the Askew and Algermissen USGS file had magnitudes listed in more than one scale, the order of preference for scale used was M_L first, then M_s , and finally m_b , if a given event was listed under neither of the other scales. Next, the primary file for each area

ORIGINAL PAGE IS
OF POOR QUALITY

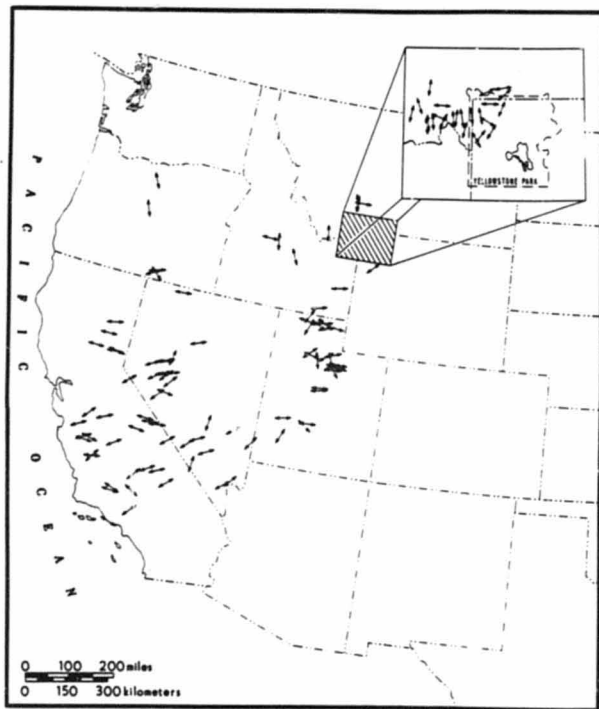


Fig. 7. Tension axes from fault plane solutions. Those used in this study were from Smith and Lindh [1978], Doser [1984], Kienle and Couch (unpublished data, 1977), and Patton [1984].

was compared to each of the three newly created USGS files for that area. USGS magnitudes were assumed in case of contradiction and all m_s and M_s magnitudes were converted to M_L using Gutenberg and Richter's [1956] equations:

$$M_L = 1.4m_s - 2.4 \quad (12a)$$

$$M_L = 0.76M_s + 1.6 \quad (12b)$$

so that equation (4a), or (4d) could be used for magnitude-moment conversions. If the primary file contained duplicates of an event found in a USGS file, the event which most closely matched the USGS version was retained.

After the primary area file was brought into conformity with the USGS file, it was sorted into chronological order (occasionally events were out of sequence) and all detectable duplicates not already eliminated were deleted according to the criteria that any two events that occurred within 10 seconds and 15km of each other were considered to be the same event. The original primary file contained about 1% duplicates. Finally magnitudes were converted to moments in an input file for 'nstrain' so that strain and deformation rates could be calculated.

STRAIN RATES FROM SEISMICITY

Regional Strain Pattern

Strain and deformation rates calculated from the earthquake data are given in detail in Appendix D. Note that results for the Northern Utah areas were calculated previously by Sroch et al. [1984a]. A summary of the results for each area is presented in Table 6 and in Figure 8. Time periods for given areas vary according to the data available but were generally from 1900 to 1981. Figure 8 also includes for comparison some of Anderson's [1979] results for southern California and Hyndman and Weichert's [1983] results for the Pacific Northwest.

The general results show a principal east - west direction of extension for the seismically active parts of the Great Basin. E-W extension was especially prevalent on the west edge of the Great Basin; in Idaho, Montana, and Wyoming, extension was more N-S; and in Utah, extension trended more NW-SE. Some exceptions were in central Utah and along the Utah-Nevada border (areas 18, 20, 21 and 23) where the principal horizontal strain corresponded to compression rather than extension.

The central Wasatch front region (area 18) has had little earthquake activity in historic time and so has a low deformation rate of only 0.001 mm/a - too small to be reliable.

The Colorado Plateaus-Great Basin transition zone (area 20) may be influenced by the neighboring N-S compression. The central Utah area would seem geographically to be more closely associated with the Great Basin; however, here, the stress orientation of the area was determined primarily from a single event with a near-vertical nodal plane on the extreme eastern edge of the area. The stress orientation for the Utah-Nevada border area

Table 6. Number of earthquakes, maximum magnitude (M_{max}), principal moment tensor component (M_1), horizontal deformation rates, and maximum horizontal strain rates for homogeneous areas of the Great Basin

area no.	area name	number of earthquakes	M_{max}	M_1 (dyne-cm/a)	horizontal deformation (mm/a)	strain rate (sec ⁻¹)
1	Oregon-Nevada Border	71	5.0 M _s	2.3x10 ²³	0.2	2.4x10 ⁻¹⁷ N65°W
2	Oroville	590	6.0 M _s	7.6x10 ²³	0.5	8.6x10 ⁻¹⁷ N87°W
3	Northern California - Nevada Border	1429	6.4 M _L	1.7x10 ²⁴	1.6	2.1x10 ⁻¹⁶ N90°W
4	West-Central Nevada	2533	7.8 M _L	1.9x10 ²⁵	7.5	1.0x10 ⁻¹⁵ N69°W
5	Walker Lane	2237	6.0 M _L	1.8x10 ²⁴	2.9	1.3x10 ⁻¹⁶ N46°W
6	Southeast Nevada	118	6.0 m _b	5.5x10 ²³	0.22	9.6x10 ⁻¹⁷ N22°W
7	Owens Valley	3809	8.3 M _b	4.9x10 ²⁵	28.0	3.7x10 ⁻¹⁵ N83°E
8	Central California	20827	6.9 M _L	3.3x10 ²⁴	1.1	-1.8x10 ⁻¹⁶ N19°E
9	Garlock	5647	8.3 M _L	8.9x10 ²⁵	59.	-6.8x10 ⁻¹⁵ N13°W
10	Los Angeles	4175	6.3 M _L	2.4x10 ²⁴	1.2	-1.8x10 ⁻¹⁶ N27°W
11	Central Idaho	918	7.3 M _L	4.5x10 ²⁴	2.0	3.3x10 ⁻¹⁵ N29°E
12	Hogden Lake Yellowstone Park	1332	7.6 M _L	1.3x10 ²⁵	4.7	1.1x10 ⁻¹⁷ N41°W
13	Western Wyoming	1159	4.5 M _L	6.7x10 ²²	0.07	2.7x10 ⁻¹⁷ N81°W
14	Soda Springs	242	5.0 M _L	1.9x10 ²⁴	0.12	6.3x10 ⁻¹⁷ N67°E
15	Hamsel Valley	1944	6.8 M _L	1.8x10 ²⁴	1.5	3.8x10 ⁻¹⁶ N78°E
16	Northern Wasatch Front	166	5.7 M _L	7.9x10 ²³	0.04	1.3x10 ⁻¹⁶ N79°E
17	Cache Valley	789	5.9 M _L	41.0x10 ²³	0.29	-4.1x10 ⁻¹⁶ N66°W
18	South Salt Lake	141	5.4 M _L	3.7x10 ²³	0.001	1.3x10 ⁻¹⁶ N76°E
19	Southern Wasatch Front	520	5.7 M _L	1.7x10 ²³	0.13	-1.5x10 ⁻¹⁷ N33°W
20	Provo	249	5.7 M _L	3.2x10 ²²	0.06	-2.6x10 ⁻¹⁶ N35°W
21	Central Utah	962	6.9 M _L	2.2x10 ²⁴	1.5	4.5x10 ⁻¹⁷ N59°E
22	Southern Utah	234	5.5 M _L	1.5x10 ²³	0.23	-4.5x10 ⁻¹⁶ N64°E
23	Utah - Nevada Border	94	6.3 M _L	5.8x10 ²³	1.0	-4.5x10 ⁻¹⁶ N64°E

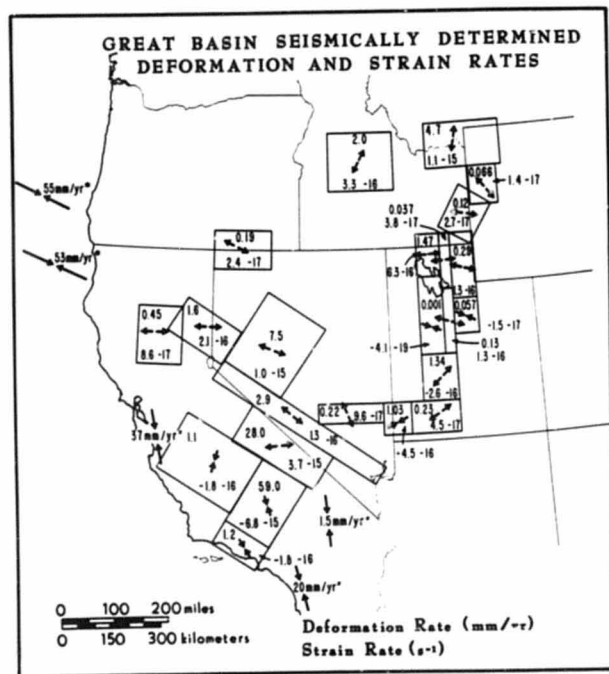


Fig. 8. Great Basin seismically determined strain/deformation rates. In each area, top value is deformation rate in mm/a, bottom value is strain rate in s^{-1} ; (second number is power of 10); * from Hyndman and Weichert [1983], # from Anderson [1979].

was determined from a single large strike-slip event, M6.1, 1966. This solution is anomalous, hence the stress orientation was not adequately accounted for. However, this strike-slip earthquake is the first of many that extend westward across southern Nevada.

The largest deformation rates were associated with the western margins of the Great Basin along the northern California-Nevada border (1.6 mm/a), in West-Central Nevada (7.5 mm/a), along the Walker Lane (2.9 mm/a), and in the Owens Valley (28.0 mm/a), areas 3, 4, 5 and 7. Deformation in the Owens Valley area was exceptionally high because of the 1872 *M*_s 8.3 Owens Valley earthquake.

Another region of high strain occurred along the Great Basin's eastern border. Deformation rates of 1.0 to 4.7 mm/a were found in areas where the trend of the ISB changes: for example at the Hebgen Lake/ Yellowstone Park; Hansel Valley, northern Utah; Central Utah; and Utah-Nevada border areas (areas 12, 15, 21 and 23).

The deformation in the Central Idaho area was due principally to the 1983, M7.3, Borah Peak, Idaho sequence and does not fit either of the two trends mentioned above. The central Idaho area is associated with a northwest extension of the Great Basin eastern margin.

Note that Askew and Algermissen [1983] assigned some large earthquakes in central Nevada lower magnitudes than usually found in the literature. The Dixie Valley and Fairview Peak, Nevada earthquakes were given magnitudes of M 7.1 and M 6.8 by Tocher [1957]. Askew and Algermissen [1983], however, listed values of *M*_L 6.9 and *M*_L 6.0. As stated earlier, Askew and Algermissen's catalog was considered the standard. When the larger magnitudes were considered, the West-Central Nevada area yielded a deformation rate of 9.1 mm/a and a strain rate of $1.2 \times 10^{-15}/\text{sec}$.

Except for the Owens Valley area, deformation rates in these rapidly deforming areas ranged from 1 to 9 mm/a - about 10 times greater than in other areas of the Great Basin. However, they were 10 times less than the ~60 mm/a deformation rate found in the Garlock area (note that most of the Garlock area moment came from the 1857 *M*_s 8.3 Fort

Tejon earthquakes produced by fracture on the San Andreas fault along the south edge of the Garlock area).

In addition to spatial variations in strain and deformation magnitudes, it is also interesting to note spatial variations in the orientation of the maximum horizontal strain and deformation rates. Figure 9 shows just the maximum horizontal extension vectors associated with each area. The dotted arrows represent the minimum horizontal strain rate axes in areas that displayed compressive maximum strain rates. The south Salt Lake and Provo areas (areas 18 and 20) were not included in Figure 9 since the south Salt Lake area displays insignificant strain rates and the Provo area is associated with Colorado Plateaus stresses. Figure 9 shows that in the extreme northern Great Basin, across central Idaho and the Yellowstone Park area, the maximum extension direction was NNE-SSW. In the southern study area, principally across southern Utah and southern Nevada, the direction of maximum extension was NNW-SSE. Throughout the central Great Basin, comprised of Nevada, Utah, and northwestern California, extension is oriented almost exclusively E-W.

Great Basin Deformation And Strain Rates

Deformation and strain rates were also calculated across the entire Great Basin to estimate intraplate-wide deformation rates (along profiles B-B', B-B'' and C-C', Figure 10). The components of the deformation rates along each profile were summed to give the overall values.

Profile B-B', a line across northern California, Nevada, and northern Utah had a 10.0 mm/a deformation rate. Profile B-B'' is an east-west line with an 8.4 mm/a rate. The southern profile, C-C', is an east-west line across southeastern California, southern Nevada, and southern Utah. Here, the deformation rate was 3.5 mm/a; however, if Owens Valley deformation is projected up to C-C', the deformation rate increases to 29.2 mm/a. (The extension rates found along these profiles are listed in Table 7 and are shown in Figure 10). The deformation and strain rates along line B-B'' are considered the most

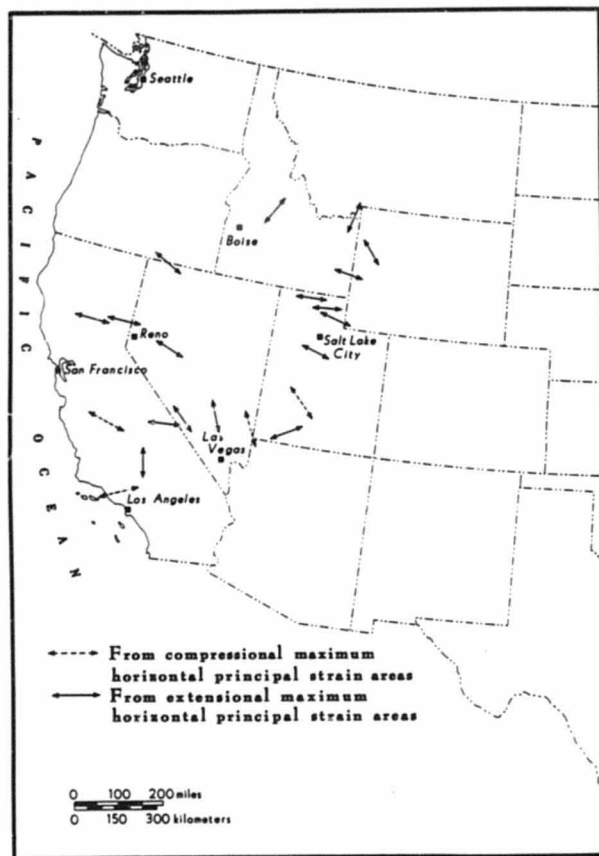


Fig. 9. Seismically determined maximum horizontal extension directions. Dotted arrows indicate compressive maximum horizontal strain.

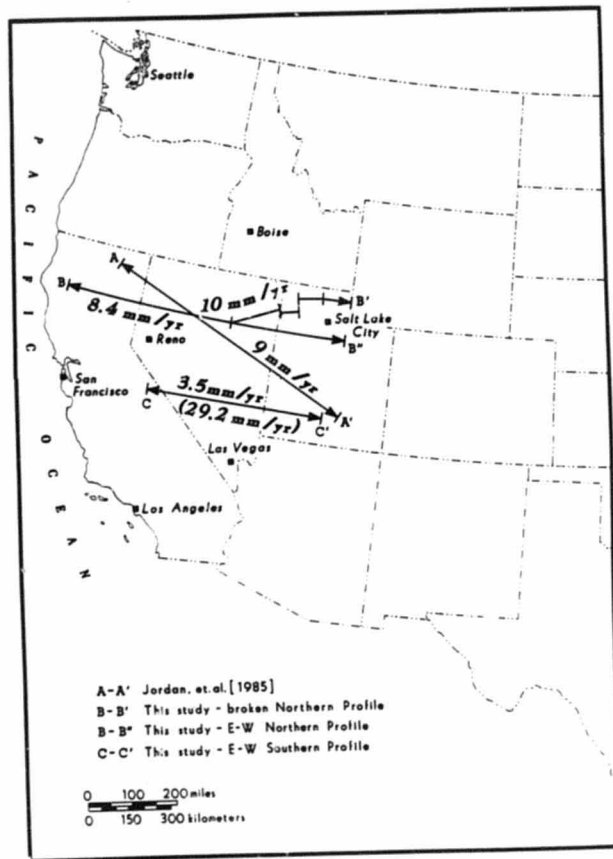


Fig. 10. Great Basin regional extension. A-A' is from Jordan et al. [1985]; B-B', B-B'', and C-C' from this study. Value in parentheses below C-C' includes deformation from Owens Valley, California.

Table 7. Maximum horizontal Great Basin strain rate, deformation rate, and total extension from this and other studies

Reference - Method	Strain Rate (sec^{-1})	Deformation Rate (mm/yr)	Total Extension %
Seismic Results			
B-B'	2.6×10^{-16}	10.0	~10
B-B''	2.2×10^{-16}	8.4	~10
C-C'	1.3×10^{-16}	3.5	~10
Jordan et al. [1985] - satellite geodesy			
A-A'		< 9	
Wright [1976] - geology			
north		5.8-7.5	~10
south		3.7-10.1	10-50
Proffett [1977] - geology		200	30-35
Thompson and Burke [1974] - geology	3.2×10^{-16}	8	10
Eston et al. [1978] - geology	3.2×10^{-16}	8	10
Zoback et al. [1981] - summary			15-39
Minster and Jordan [1984] - summary			
Geology ¹		3-20	
heat flow ²		3-12	
paleoseismicity ³		1-12	
seismicity ⁴		5-22	

¹ Hamilton and Meyers [1966], Stewart [1978], Davis [1980], Proffett [1977]

² Lachenbruch [1979]

³ Wallace [1978], Thompson and Burke [1974], Greensfelder et al. [1980]

⁴ Greensfelder et al. [1980], Anderson [1979]

representative for the Great Basin because of its central location and since the absence of line bends makes its strain and deformation rate calculations the most straightforward. A-A' results are from Jordan et al. [1985] for later comparison.

Note that the deformation rate is more than twice as high in the northern Great Basin than it is in the southern Great Basin if the Owens Valley area is not considered. When strain rates were considered, it was found that B-B' experienced 2.7×10^{-16} /sec, B-B'' yielded 2.2×10^{-16} /sec and C-C' yielded 1.4×10^{-16} /sec; the northern profiles displayed almost twice the strain rate of the southern profile, consistent with deformation rate results.

COMPARISON OF CONTEMPORARY AND PALEOSTRAIN RATES

To clarify the role of the seismically determined strain rates discussed previously, comparisons with strain rates found with other methods are useful. Two methods to be addressed here are geologic and geodetic determinations of strain rates. These, with Great Basin extension rates calculated by other workers, give insight into contemporary versus paleostrain rates in this region.

Paleostrain Rate Calculations From Geologic Data

Strain rates from geologic data (slip rates on faults) were determined using a conversion of fault slip rates to seismic moment. Mapped slip rates and fault plane geometries were used to determine only the scalar moment following the equation:

$$M_s = \mu Au. \quad (3a)$$

From this seismic moment and the s_{gs} of the fault displacement, strain rate can be found using:

$$\dot{\epsilon} = \frac{M_s k}{2 \mu l_1 l_2 l_3} \quad \text{[Anderson, 1979]} \quad (13)$$

where l_1 , l_2 and l_3 = volume

$$k = 0.75 \quad (0.75 \leq k \leq 0.96)$$

$\dot{\epsilon}$ = scalar strain rate.

\dot{M}_s = scalar moment rate.

Moments for faults in the western U. S. were calculated previously by R. B. Smith et al. (unpublished data, 1984) assuming average fault dip of 60° on some of the western U. S. faults shown in Figure 11. Smith also made these calculations assuming 40° fault dips that gave increased horizontal extension rates by a factor of 1.5. The 60° dip assumption was used in this study. Ages of the faulting ranged from 10,000 a to 10 ma. Moments and strain rates for the Wasatch front were determined from fault segmentation and slip rates by Schwartz and Coppersmith [1984]. Paleodeformation rates calculated for some areas in southern California by Anderson [1979] were also included in Figure 4. Geologic results for the Borah Peak, Idaho area are from Scott et al. [1984].

The faults were grouped for this study into the same areas as used in the seismic strain rate determination where possible. Figure 12 shows the centers of some of the faults from Figure 11 on a map of the western U. S. The seismic moment rates were determined using equation (3a) and then summed. The direction of extension was assessed to be east-west for most of the Great Basin. North-south compression was assumed for areas associated with the San Andreas fault system (the Central California and Los Angeles areas) and in Idaho and Montana.

The primary drawbacks of the geologic data lie in their interpretation and lack of completeness. First, in order for the results to be complete, all major faults must be included and assigned accurate slips, areas, and displacement ages. While there are numerous references to Holocene and Quaternary faults throughout the region, less than 30% had slip rates. Fault dips at depth must also be accurately estimated since low-angle normal fault dips yield higher horizontal extension rate estimates. Second, even if surface exposures of faults are adequate and all major faults have been studied in an area, only large earthquakes, $M6.5+$, will have produced any surface displacement in the first place. Consequently, underestimation of paleostrain in a given area is almost certain.

Paleodeformation rates yield the highest values in two regions (Figure 13 and

ORIGINAL PAGE IS
OF POOR QUALITY

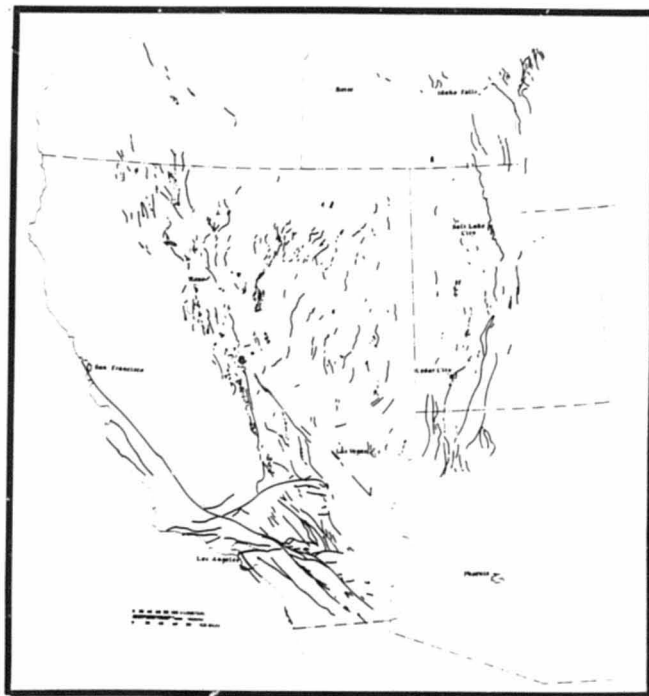


Fig. 11. Western U. S. fault map. Data from Smith et al. (unpublished data, 1982)

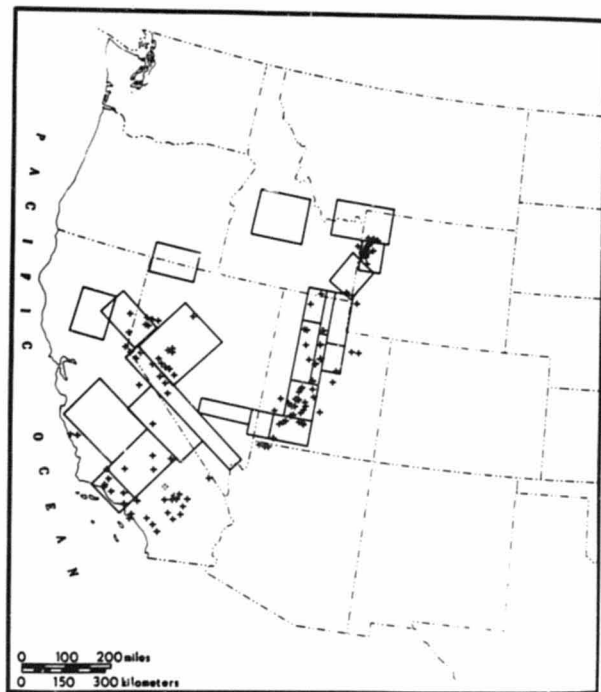


Fig. 12. Locations of study area fault centers. Study areas are superimposed.

ORIGINAL PAGE IS
OF POOR QUALITY

GEOLOGICALLY DETERMINED DEFORMATION AND STRAIN RATES

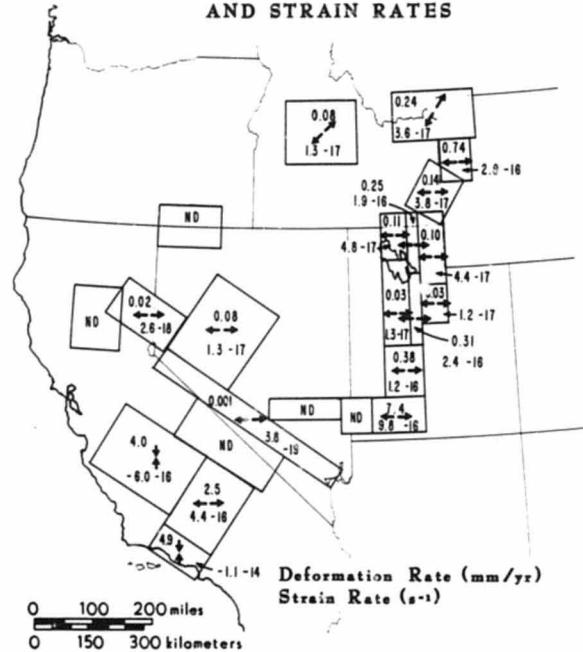


Fig. 13. Great Basin paleostrain and deformation rates from geologic data. Top value is deformation rate in mm/a, bottom value is strain rate in s^{-1} (second number is power of 10).

Table 8). High deformation rates were determined for Hebgen Lake/ Yellowstone Park, 0.24 mm/a; and in Wyoming, 0.74 mm/a. Here, the ISB changes from a N-S trend in Utah to a NNE-SSW trend in southeast Idaho and western Wyoming. High deformation rates were also calculated for the Central and southern Utah areas (0.38 and 7.4 mm/a) where the ISB changes trend from N-S in most of Utah to E-W in southeast Nevada. Concentration of deformation in these regions is much less pronounced in paleostrain results than it is in seismically determined results.

Data for the west side of the Great Basin were considered incomplete resulting in either unavailable or low deformation rates. Figure 14 shows that both the east and west margins of the Great Basin have experienced $M > 7$ earthquakes that produce high deformation. This map was determined using geologic data [Thenhaus and Wentworth, 1982; R. B. Smith et al. unpublished data, 1983], so incomplete fault study was the problem, not inadequate fault exposures.

Contemporary Strain Rate

Geodetic trilateration and triangulation networks have been used by several workers to determine strain rates - primarily J. Savage (USGS) and R. Snay (NGS) and co-workers. For purposes of comparison, Savage's [1983] summary of strain rates of different USGS trilateration networks was used along with modifications and additions taken from Savage et al. [preprint, 1985] and Snay et al. [1984].

Some problems associated with geodetic determinations are inaccurate measurements because of inconsistent location of measurement stations and inconsistent measuring technique. Also a factor in the usefulness of geodetic measurements is the sparseness of measurements throughout the western U. S. with the exception of California. The available geodetic data are presented in Figure 15 and Tables 8 and 9.

Geodetic strain rates are only available in about half of the areas considered in the seismic strain rate determination. In many areas where geodetic strain measurements

Table 8. Strain and deformation rates measured using geologic, seismic, and geodetic data

Area	Geologic		Seismic		Geodetic	
	Def. Rate (mm/a)	Strain Rate (sec^{-1})	Def. Rate (mm/a)	Strain Rate (sec^{-1})	Def. Rate (mm/a)	Strain Rate (sec^{-1})
Oregon - Nevada Border			0.19	2.4×10^{-17}		
Oroville			0.5	8.6×10^{-17}		
Northern California - Nevada Border	0.02	2.6×10^{-18}	1.6	2.1×10^{-16}		
West-central Nevada	0.08	1.3×10^{-17}	7.5	1.0×10^{-15}	2.0	1.6×10^{-15}
Walker Lane	0.001	3.8×10^{-19}	2.9	1.3×10^{-16}	3.6	1.9×10^{-15}
Southeast Nevada			0.22	9.6×10^{-17}		
Owens Valley			28.0	3.7×10^{-15}	2.5	2.5×10^{-15}
Central California	4.0	-1.9×10^{-16}	1.1	-1.8×10^{-16}	1.8	-2.9×10^{-15}
Gardlock	2.5	4.4×10^{-16}	59.0	-6.8×10^{-15}	11.2	-5.1×10^{-15}
Los Angeles	49.3	-1.1×10^{-14}	1.2	-1.8×10^{-16}	13.5	-4.8×10^{-15}
Central Idaho*	0.08	1.3×10^{-17}	2.0	3.3×10^{-16}		
Hebgen Lake/ Yellowstone Park	0.24	3.5×10^{-17}	4.7	1.1×10^{-15}	11.2	8.9×10^{-15}
Western Wyoming	0.74	2.9×10^{-16}	0.07	1.4×10^{-17}		
Soda Springs	0.14	3.8×10^{-17}	0.12	2.7×10^{-17}		
Hansel Valley	0.11	4.8×10^{-17}	1.5	6.3×10^{-16}		
Northern Wasatch Front	0.25	1.9×10^{-16}	0.04	3.8×10^{-17}	0.6	3.2×10^{-16}
Cache Valley	0.10	4.4×10^{-17}	0.29	1.3×10^{-16}		
South Salt Lake	0.03	1.3×10^{-17}	0.001	-4.1×10^{-19}		
Southern Wasatch Front	0.31	2.4×10^{-16}	0.13	1.3×10^{-16}		
Provo	0.03	1.2×10^{-17}	0.06	-1.5×10^{-16}		
Central Utah	0.38	1.2×10^{-16}	1.3	-2.6×10^{-16}		
Southern Utah	7.4	9.8×10^{-16}	0.23	4.5×10^{-17}		
Utah - Nevada Border			1.0	-4.5×10^{-16}		

* from Scott et al. [1984].

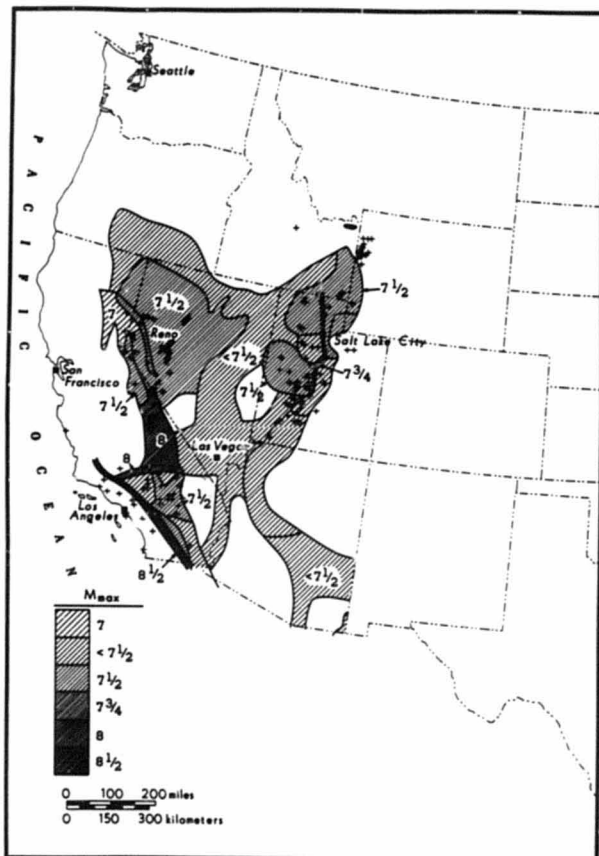


Fig. 14. Maximum magnitude capabilities of the western U. S. Data from Smith (unpublished data, 1982), and Thenhaus and Wentworth [1982]. Crosses, +, indicate centers of mapped faults.

ORIGINAL PAGE IS
OF POOR QUALITY

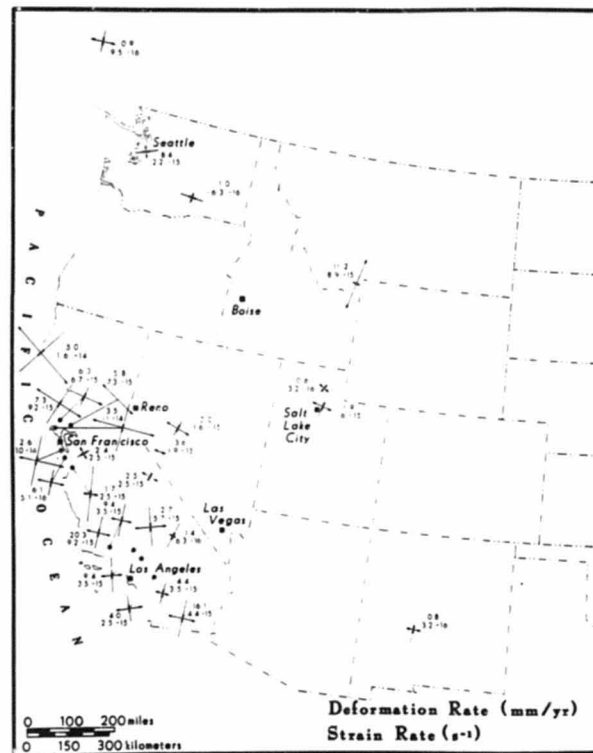


Fig. 15. Western U. S. geodetically determined extensional deformation and strain rates. The top number is deformation rate (mm/a) and the bottom is strain rate (s^{-1}). The second number is power of 10 from Savage [1983], Savage et al. [1984], and Snay et al. [1984].

Table 9. Geodetically measured strain and deformation rates

Network	Period (yr)	Principal Extension direction	ϵ_1		ϵ_2		Reference
			Def. Rate (mm/a)	Strain Rate (sec ⁻¹)	Def. Rate (mm/a)	Strain Rate (sec ⁻¹)	
Johnstone	1914-66	N87°E± 15°	0.9	9.5x10 ⁻¹⁶	1.2	-9.5x10 ⁻¹⁶	1
Seattle	1972-79	N20°W± 6°	8.4	2.2x10 ⁻¹⁵	7.7	-3.8x10 ⁻¹⁵	1
Hanford	1972-81	N5°E± 14°	1.0	-6.3x10 ⁻¹⁶	1.6	-1.3x10 ⁻¹⁵	1
Hebgen	1973-84	N14°E± 1°	11.2	8.9x10 ⁻¹⁵	2.6	-1.6x10 ⁻¹⁵	2
Ogden	1972-84	N57°W± 13°	0.6	3.2x10 ⁻¹⁶	1.1	-6.3x10 ⁻¹⁶	2
Shelter Cove	1930-76	N58°W°	5.0	1.6x10 ⁻¹⁴	5.0	-1.6x10 ⁻¹⁴	1
Geysir	1972-79	N74°W± 2°	7.3	9.2x10 ⁻¹⁵	2.8	-8.9x10 ⁻¹⁵	1
Santa Rosa	1972-81	N81°W± 2°	6.3	6.7x10 ⁻¹⁵	2.2	-3.5x10 ⁻¹⁵	1
Napa	1976-80	N63°W± 8°	5.8	7.3x10 ⁻¹⁵	0.3	3.2x10 ⁻¹⁶	1
Point Reyes	1972-80	N88°W± 3°	3.5	1.1x10 ⁻¹⁴	2.0	-8.9x10 ⁻¹⁵	1
Fairview	1973-79	N74°W± 11°	2.0	1.6x10 ⁻¹⁵	13.2	-3.8x10 ⁻¹⁵	1
Peninsula	1970-80	N88°W± 7°	2.6	1.0x10 ⁻¹⁴	1.4	-8.9x10 ⁻¹⁵	1
Mocho	1973-81	N43°W± 4°	2.4	2.5x10 ⁻¹⁵	2.0	-2.5x10 ⁻¹⁵	1
Excelsior	1972-79	N81°W± 7°	3.6	1.9x10 ⁻¹⁵	0.	0.	1
Loma Prieta	1972-80	N87°W± 4°	6.1	5.1x10 ⁻¹⁵	3.0	-4.8x10 ⁻¹⁵	1
Pajaro	1973-81	N98°W± 2°	1.7	2.5x10 ⁻¹⁵	4.8	-1.0x10 ⁻¹⁴	1
Carrizo	1977-81	N89°W± 4°	20.3	9.2x10 ⁻¹⁵	1.8	-2.9x10 ⁻¹⁵	1
Los Padres	1973.8-81.4	N89°E	9.4	3.5x10 ⁻¹⁵	13.5	-4.8x10 ⁻¹⁵	1
Palmdale	1971.6-80.9	N76°E	2.7	5.7x10 ⁻¹⁵	3.8	-6.0x10 ⁻¹⁵	1
Garlock	1973.2-80.9	N74°E	1.4	6.3x10 ⁻¹⁶	11.2	-5.1x10 ⁻¹⁵	1
Tehachapi	1973.7-80.9	N77°E	9.4	3.5x10 ⁻¹⁵	10.8	-3.8x10 ⁻¹⁵	1
Cajon	1974.3-81.3	N80°E	4.	3.5x10 ⁻¹⁵	6.4	-5.1x10 ⁻¹⁵	1
Anza	1974.0-81.2	N87°W	4.0	2.5x10 ⁻¹⁵	6.6	-3.3x10 ⁻¹⁵	1
Salton	1972.9-81.1	N89°E	16.1	4.4x10 ⁻¹⁵	24.2	-7.0x10 ⁻¹⁵	1
Socorro	1972-84	N84°E± 15°	0.8	3.2x10 ⁻¹⁶	0.8	-6.3x10 ⁻¹⁶	2
Owens Valley	1975-79	N69°W± 11°	2.5	2.5x10 ⁻¹⁵	2.1	-2.2x10 ⁻¹⁵	1
Salt Lake City	1962-74	N76°W± 15°	1.9	1.6x10 ⁻¹⁵	4.0	2.5x10 ⁻¹⁵	3

References: 1) Savage [1983], 2) Savage et al. [preprint, 1985], 3) Snay et al. [1984]

were available, these values were close to the values measured seismically; however, sometimes the geodetic rates were 10-20 times larger (Table 8).

Geodetically determined strain rates were probably higher than seismically determined counterparts owing to spatial sampling differences. Geodetic networks were usually three to five times smaller than the areas used in this study and focussed on the most actively deforming regions. Consequently, higher strain rates would be expected for geodetic network results.

The Walker Lane area (area 5) was an apparent example of different areal coverage with different contemporary strain rates. The seismically and geodetically determined strain rates for this area differ by almost an order of magnitude (1.3×10^{-14} /sec and 1.9×10^{-15} /sec respectively). However, the seismic and geodetic deformation rate results for the area were 2.9 mm/a - from earthquake data and 3.6 mm/a measured geodetically [Savage, 1983]. The Excelsior fault was probably the source of most deformation in this area and was sampled in both methods. Thus, when area size discrepancies are eliminated, the resulting deformations are almost identical.

Summary of Strain Rates

Table 8 shows that paleostrain rates are generally one to two orders of magnitude lower than contemporary strain rates. The exceptions to this pattern were: 1) the Los Angeles, Wyoming, south Salt Lake, southern Utah, and northern Wasatch front areas where the paleodeformation rates of 49.3, 0.74, 0.03, 7.4, and 0.25 mm/a were significantly larger than seismically determined rates of 1.2, 0.07, 0.001, 0.23, 0.04, and 0.13 mm/a; and 2) in the Idaho-Wyoming, 0.14 versus 0.12 mm/a; central California, 4.0 versus 1.1; Cache Valley, Utah, 0.1 versus 0.3 mm/a; and the southern Wasatch front, 0.31 versus 0.13 mm/a areas where paleo- versus seismically determined deformation rates were within a factor of four. These results suggest that historic seismicity and deformation in the areas named above have been lower than average levels, since the seismic values are no larger than the

underestimated paleodeformation values. It is also possible that these areas have more complete geologic data than other areas.

Paleostrain rates in Figure 13 also show that deformation along the ISB, up to 7.4 mm/a in the Southern Utah area, was greater than along the western margins of the Great Basin with up to 0.08 mm/a in the West-Central Nevada area). This result is the opposite of the results determined using earthquake data where deformation rates along the ISB were as high as 2.8 mm/a, in the Hebgen Lake/Yellowstone area, and deformation rates in the western half of the Great Basin were as high as 7.5 mm/a in the West-Central Nevada area. This difference is probably the result of lack of geologic data and temporal variation in seismic activity.

Anderson [1979] calculated values of 2.0 mm/a deformation rate in the Los Angeles area compared to 1.2 mm/a from the earthquake contribution. Likewise, he estimated deformation rates of 8.0 and 1.5 mm/a in the Garlock and Owens Valley areas where seismicity rates were 59.0 mm/a in the Garlock area and 28.0 mm/a in Owens Valley.

Contemporary and paleodeformation comparisons also support the existence of an anomalous Wasatch front seismic gap. The northern Wasatch Front area (area 16) contains the Wasatch fault - the primary surface breaking fault of the eastern Great Basin. Area 16 is also bordered on the east and west by seismically active areas (the Cache Valley and Hansel Valley areas). In contrast, the northern Wasatch front area has been quiet. Less than 200 earthquakes have been recorded there in the last 78 years. The maximum magnitude earthquake to be recorded in the area during this time period was M_L 5.7.

Smith [1978] suggested that this "seismic gap" along the northern Wasatch fault is temporary and might be seismically filled on a longer time scale. The deformation rate from seismicity for the northern Wasatch front was 0.04 mm/a and for the southern Wasatch front was 0.13 mm/a. In contrast, the geologic rates were 0.25 mm/a and 0.31 mm/a north and south. The higher paleodeformation values suggest that contemporary seismic quiescence is indeed anomalous.

Comparisons of Great Basin Extension Rate

Earthquake induced deformation rates of 10.0 mm/a on B-B' and 8.4 mm/a on B-B'' determined along the two northern profiles in Figure 10 compare well with deformation rates determined from other studies. For example, Lachenbruch and Sass [1978] determined 5-10 mm/a extension for the Great Basin using heat flow constraints and thermal models of extension (Table 7). Also, Jordan et al. [1985] estimated a deformation rate across the Great Basin of less than 9 mm/a from North American-Pacific intraplate tectonic models, while the seismically determined deformation rate along line B-B'' was 8.4 mm/a (Table 7) - close for two different methods. This implies that the North American/Pacific plate interaction modeled by Jordan et al. [1985] may contribute a component to Great Basin extension. This comparison also leads to the conclusion that most of the extension in the Great Basin is expressed as earthquake generated brittle fracture.

The strain rates found along the profiles mentioned above can also be compared to results from other workers (Table 7). For example, Thompson and Burke [1974] arrived at a deformation rate estimate of 8 mm/a from geologic data. Wright [1976] used geologic data to determine a deformation rate across the northern Great Basin of 5.8 - 7.8 mm/a. Also, Minster and Jordan's [1984] Table 3 (included in Table 7) listed deformation rates in the range 1-22 mm/a derived from various workers' results. All these deformation rates are compatible with the 8.4 mm/a results obtained in this study for profile B-B''. Also, Wright's [1976] southern area results were 3.7-10.1 mm/a - comparable with the deformation rate of 3.5 mm/a found in this study for profile C-C' across the southern Great Basin.

These comparisons suggest that since geologically inferred and contemporary strain rates are similar, the mechanism that facilitates Great Basin extension today probably operated throughout Quaternary times as well. Had the mechanism changed, we would expect to see greater differences in deformation rates between contemporary and paleo-estimations.

Also, contemporary versus paleostrain rate comparisons in the Great Basin

suggest that the seismic record, though perhaps experiencing short-term, local variability, is probably a reasonable indicator of future seismicity on a regional scale. This conclusion is analogous to the findings of Wesnousky et al. (1982a) for Japanese seismicity. In their study, contemporary variations in seismic activity were determined to be short-term effects that disappeared over periods of many hundreds of years.

SUMMARY AND INTERPRETATIONS

This study has shown that, on a regional scale, contemporary strain rates from seismicity are comparable with strain rates determined from modern, geodetic measurements, and with paleostrain rates determined from geologic data.

Regionally, an E-W Great Basin extension rate of 8.4 mm/a was determined from earthquake data. Locally, contemporary strain was concentrated at changes in direction of the Intermountain Seismic Belt that marks the Great Basin eastern boundary; along the western margin of the Great Basin; in central Nevada; and in some other scattered areas primarily on the region boundaries. Great Basin contemporary deformation rates in the range 1-28 mm/a were found in this study, where rates of 20-50 mm/a were determined for active interplate subduction and transform faulting in the Pacific Northwest determined from seismicity by Hyndman and Weichert (1983) showing that Great Basin deformation rates from seismicity were, on average, from 2 to 10 times lower than plate convergence rates.

Patterns of high seismicity and deformation rate along the margins of the Great Basin show that most, and probably the deepest, brittle fracture occurs along these margins. The stress release and opening of fractures represented by this seismicity have probably allowed magma to intrude the lithosphere, and in some cases reach the surface. Figure 16, a map of surface volcanism for the last 5 ma [Smith and Luedke, 1984] and of high, seismically determined deformation rates, suggests that brittle fracture and subsequent magma intrusion has persisted along the edges of the Great Basin for at least the last few million years.

The local and regional deformation rate results, summarized above, suggest that

ORIGINAL PAGE IS
OF POOR QUALITY

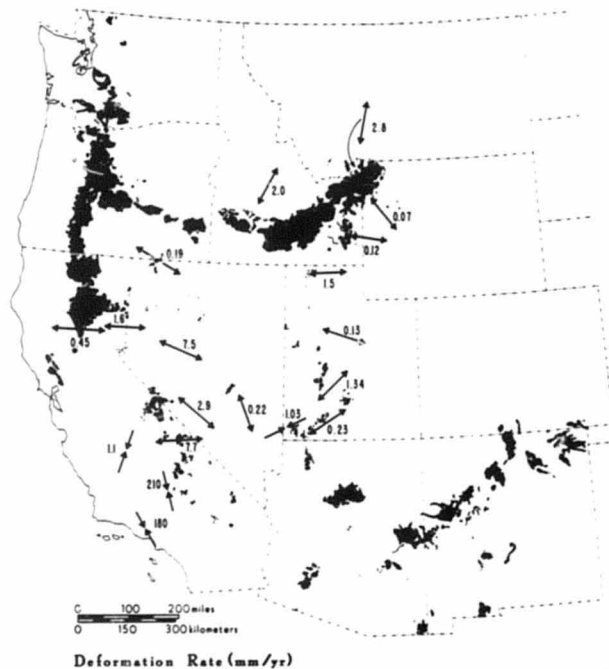


Fig. 16. Western U. S. volcanism and seismicity determined deformation rates. Volcanism is from Smith and Luedke (1984) and deformation rates are in mm/a.

brittle fracture has been produced as the principal strain release, although it may ultimately be produced by creep and flow at depth through coupling in the upper-crust. It follows that most extension in the Great Basin has been expressed as brittle fracture in the upper 10 km of the crust. Thus creep in the whole of the lithosphere cannot exceed the brittle strain.

The observation that regional brittle strain release is comparable to other estimates of strain suggests that extension has been expressed consistently at depths less than 20 km. This is true on a regional level even over short time periods. Thus, contemporary mechanisms for strain release in the Great Basin must have been operating throughout the Quaternary. It follows that regional seismicity is a good indicator of future seismic activity. However, on a local scale, such as the Wasatch front, seismic quiescence reflects gaps in the seismicity that should fill in within the period of an earthquake cycle.

STRAIN DETERMINATION TEST CASE

APPENDIX A

File 1. Oregon-Nevada Border area earthquake summary catalog

yr	date	orig time	lat-n	long-w	depth	mag	no gap	dan	res		
37	525	536	0.	41 30.00	119 48.00	0.	5.39	0	0	0.	0.
53	708	301	15.00	42 24.00	119 6.00	0.	3.50	0	0	0.	0.
56	110	837	24.00	41 30.00	119 6.00	0.	4.63	0	0	0.	0.
58	312	1209	16.00	42 24.00	120 0.	0.	4.63	0	0	0.	0.
58	312	1209	19.00	42 0.	119 30.00	0.	4.50	0	0	0.	0.
58	929	853	37.00	42 18.00	118 6.00	0.	4.63	0	0	0.	0.
59	1014	1434	49.00	42 12.00	118 24.00	0.	3.90	0	0	0.	0.
62	830	1335	29.00	41 48.00	118 48.00	0.	5.80	0	0	0.	0.
66	128	1800	9.10	41 36.00	118 12.00	20.00	3.20	0	0	0.	0.
68	527	553	34.00	42 12.23	119 44.93	0.	3.80	0	0	0.	0.
68	528	8	49.00	42 15.72	119 48.59	0.	3.20	0	0	0.	0.
68	528	51	3.00	42 15.35	119 46.80	0.	3.20	0	0	0.	0.
68	528	1255	44.70	42 11.88	119 48.72	0.	3.20	0	0	0.	0.
68	530	35	59.80	42 18.00	119 48.00	0.	4.60	0	0	0.	0.
68	531	306	38.00	42 5.46	119 46.79	0.	3.20	0	0	0.	0.
68	603	1327	39.70	42 12.00	119 48.00	0.	4.60	0	0	0.	0.
68	604	233	0.	42 14.64	119 46.50	0.	3.70	0	0	0.	0.
68	604	234	15.70	42 18.00	119 54.00	0.	3.20	0	0	0.	0.
68	604	238	27.00	42 18.89	119 47.15	0.	3.20	0	0	0.	0.
68	604	335	49.80	42 19.70	119 45.29	0.	3.20	0	0	0.	0.
68	604	552	32.00	42 17.28	119 49.20	0.	3.20	0	0	0.	0.
68	604	622	19.00	42 12.30	119 50.81	0.	3.20	0	0	0.	0.
68	604	1058	22.80	42 17.81	119 54.00	0.	3.20	0	0	0.	0.
68	605	451	56.80	42 18.29	119 56.81	0.	3.20	0	0	0.	0.
68	605	512	36.00	42 14.64	119 54.36	0.	3.20	0	0	0.	0.
68	605	737	45.00	42 15.60	119 54.59	0.	3.20	0	0	0.	0.
68	605	804	40.00	42 16.92	119 48.60	0.	3.30	0	0	0.	0.
8	605	820	38.00	42 17.45	119 49.91	0.	3.20	0	0	0.	0.
68	605	1408	40.00	42 18.12	119 51.59	0.	3.80	0	0	0.	0.

yr	date	orig time	lat-n	long-w	depth	mag	no gap	dan	rms
68	612	120 56.00	42 6.00	120 0.	0.	3.40	0	0	0. 0.
68	612	146 22.40	42 6.17	119 53.22	0.	3.20	0	0	0. 0.
68	621	2033 28.00	42 12.84	119 39.11	0.	3.20	0	0	0. 0.
68	622	9.39 53.50	42 11.57	119 49.43	0.	3.20	0	0	0. 0.
68	624	1103 17.30	42 17.21	119 50.34	0.	3.20	0	0	0. 0.
70	102	2052 11.10	41 57.60	118 41.90	0.	3.10	0	0	0. 0.
70	103	801 56.50	42 4.61	118 55.25	0.	3.60	0	0	0. 0.
72	113	357 33.10	41 35.58	118 38.27	0.	2.90	0	0	0. 0.
73	225	1133 57.00	41 48.59	118 28.79	0.	3.00	0	0	0. 0.
73	225	1419 45.00	41 48.59	118 28.79	0.	3.40	0	0	0. 0.
73	227	152 22.00	41 48.59	118 28.79	0.	3.70	0	0	0. 0.
73	227	418 21.00	41 48.59	118 28.79	0.	3.80	0	0	0. 0.
73	227	952 0.	41 48.59	118 28.79	0.	3.30	0	0	0. 0.
73	227	1235 38.00	41 48.59	118 28.79	0.	3.30	0	0	0. 0.
73	302	1128 42.30	41 49.86	118 32.75	5.00	3.20	0	0	0. 0.
73	302	1206 13.00	41 48.59	118 28.79	0.	3.30	0	0	0. 0.
73	302	1217 20.00	41 48.59	118 28.79	0.	3.20	0	0	0. 0.
73	302	1414 6.00	41 48.59	118 28.79	0.	4.10	0	0	0. 0.
73	303	300 3.30	41 48.59	118 27.42	5.00	3.20	0	0	0. 0.
73	303	334 51.00	41 49.20	118 40.25	5.00	3.20	0	0	0. 0.
73	303	335 51.00	41 48.59	118 28.79	0.	4.70	0	0	0. 0.
73	303	345 12.00	41 48.59	118 28.79	0.	3.60	0	0	0. 0.
73	303	807 24.00	41 48.59	118 28.79	0.	3.40	0	0	0. 0.
73	303	1004 31.00	41 48.59	118 28.79	0.	3.40	0	0	0. 0.
73	303	1852 4.30	41 50.63	118 25.13	5.00	3.20	0	0	0. 0.
73	306	1049 50.00	41 48.59	118 28.79	0.	3.00	0	0	0. 0.
73	309	330 57.00	41 48.59	118 28.79	0.	3.00	0	0	0. 0.
74	103	258 32.90	41 45.00	119 18.00	0.	3.00	0	0	0. 0.
74	426	2303 23.10	42 6.11	118 17.87	0.	2.50	0	0	0. 0.
74	724	1559 54.30	41 30.78	118 44.70	0.	2.90	0	0	0. 0.
74	1216	2141 40.70	42 9.60	119 22.68	0.	2.90	0	0	0. 0.
75	902	1448 28.60	41 58.86	118 57.47	0.	4.00	0	0	0. 0.

66

yr	date	orig time	lat-n	long-w	depth	mag	no gap	dan	rms
78	516	2004 55.90	41 46.61	118 41.88	0.	3.10	0	0	0. 0.
80	411	642 49.90	42 12.60	119 36.77	0.	3.30	0	0	0. 0.
80	411	644 11.40	42 13.19	119 36.60	0.	3.10	0	0	0. 0.
80	411	729 47.60	42 16.70	119 34.56	0.	3.20	0	0	0. 0.
80	412	1319 26.60	42 1.62	119 36.29	0.	3.40	0	0	0. 0.
80	427	1354 34.30	41 59.27	118 56.40	0.	4.40	0	0	0. 0.
80	428	1355 34.00	41 51.90	118 54.54	5.00	4.30	0	0	0. 0.
80	428	1707 9.60	41 59.88	118 54.29	0.	4.00	0	0	0. 0.
80	428	1707 10.10	41 50.75	118 55.86	5.00	3.80	0	0	0. 0.
80	503	17 39.30	41 55.61	118 47.58	0.	4.40	0	0	0. 0.

67

File 2. Oregon-Nevada Border area fault plane solutions

event	location	P axis	T axis	Str	dip	rake	str	dip	rate
53 C 73	41.83 118.48	288 48	-67 358 58	-95					
H2 S 608684	42.3 119.77	91 98	171 148 98	8					
58 S 608738	42.17 119.92	865 35 128 13	4 88	-119 268 38	-17				

File 3. Oregon-Nevada Border area synthetic fault plane solution

area1
 T1 181.236938 -8.195988
 P1 -169.227844 67.141898
 N2 -18.759273 34.957188
 N1 -11.319819 22.887987
 B
 238.8 34.8
 8.6 66.3

File 4. Oregon-Nevada Border area 'nstrain' input file

fealin
 nevada oregon border
 71
 370525005
 230, 34, -46
 1, 66, -114
 2.1e+24
 530708003
 230, 34, -46
 1, 66, -114
 1.8e+22
 560110008
 230, 34, -46
 1, 66, -114
 3.1e+23
 580312012
 230, 34, -46
 1, 66, -114
 3.1e+23
 580312012
 230, 34, -46
 1, 66, -114
 2.2e+23
 580929008
 230, 34, -46
 1, 66, -114
 3.1e+23
 591014014
 230, 34, -46
 1, 66, -114
 4.9e+22
 620830013
 230, 34, -46
 1, 66, -114
 6.0e+24
 660128018
 230, 34, -46
 1, 66, -114
 8.3e+21
 680527005
 230, 34, -46
 1, 66, -114
 3.8e+22
 680528000
 230, 34, -46
 1, 66, -114
 8.3e+21
 680528000
 230, 34, -46

730225014
 230, 34, -46
 1, 66, -114
 1.4e+22
 730227001
 230, 34, -46
 1, 66, -114
 3.0e+22
 730227004
 230, 34, -46
 1, 66, -114
 3.8e+22
 730227009
 230, 34, -46
 1, 66, -114
 1.1e+22
 730227012
 230, 34, -46
 1, 66, -114
 1.1e+22
 730302011
 230, 34, -46
 1, 66, -114
 8.3e+21
 730302012
 230, 34, -46
 1, 66, -114
 1.1e+22
 730302012
 230, 34, -46
 1, 66, -114
 8.3e+21
 730302014
 230, 34, -46
 1, 66, -114
 8.1e+22
 730303003
 230, 34, -46
 1, 66, -114
 8.3e+21
 730303003
 230, 34, -46
 1, 66, -114
 8.3e+21
 730303003
 230, 34, -46
 1, 66, -114
 3.7e+23
 730303003
 230, 34, -46
 1, 66, -114
 2.3e+22
 730303008

230, 34, -46
 1, 66, -114
 1.4e+22
 730303010
 230, 34, -46
 1, 66, -114
 1.4e+22
 730303018
 230, 34, -46
 1, 66, -114
 8.3e+21
 730306010
 230, 34, -46
 1, 66, -114
 5.0e+21
 730309003
 230, 34, -46
 1, 66, -114
 5.0e+21
 740103002
 230, 34, -46
 1, 66, -114
 5.0e+21
 740426023
 230, 34, -46
 1, 66, -114
 1.4e+21
 740724015
 230, 34, -46
 1, 66, -114
 3.9e+21
 741216021
 230, 34, -46
 1, 66, -114
 3.9e+21
 750902014
 230, 34, -46
 1, 66, -114
 6.3e+22
 780516020
 230, 34, -46
 1, 66, -114
 6.5e+21
 800411006
 230, 34, -46
 1, 66, -114
 1.1e+22
 800411006
 230, 34, -46
 1, 66, -114
 6.5e+21
 800411007
 230, 34, -46

1, 66, -114
 8.3e+21
 800412013
 230, 34, -46
 1, 66, -114
 1.4e+22
 800427013
 230, 34, -46
 1, 66, -114
 1.7e+23
 800428013
 230, 34, -46
 1, 66, -114
 1.3e+23
 800428017
 230, 34, -46
 1, 66, -114
 6.3e+22
 800428017
 230, 34, -46
 1, 66, -114
 3.8e+22
 800503000
 230, 34, -46
 1, 66, -114
 1.7e+23
 0.8
 111, 1, 222, 2, 15,
 53
 0.

File 5. Oregon-Nevada Border area 'nstrain' output

COMPUTATION OF A SYNTHETIC FAULT PLANE SOLUTION FROM A REGIONAL MOMENT TENSOR

nevada oregon border

370525065

Fault plane solution number 1
 fault plane: strike= 230. dip= 34. slip= -46. degrees
 auxiliary plane: strike= 1. dip= 66. slip=-114. degrees
 Moment Mo= 2.1e+24 dyne-cm
 slipvector=(0.016,-.913,0.407) vecaz= -89.0 vecdip= 24.0
 moment tensor

M11=	1.9e+22	M12=	-8.3e+23	M13=	3.4e+23	
M21=	-8.3e+23	M22=	1.4e+24	M23=	1.3e+24	dyne-cm
M31=	3.4e+23	M32=	1.3e+24	M33=	-1.4e+24	

Eigenvectors: component 1=N, 2=E, 3=??
 eigenvector 1=(-.310,0.902,0.302) vecaz.= 109.0 vecdip= 17.6
 eigenvector 2=(0.904,0.181,0.388) vecaz.= 11.3 vecdip= 22.9
 eigenvector 3=(-.296,-.393,0.871) vecaz.= -126.9 vecdip= 60.5

530708003

Fault plane solution number 2
 fault plane: strike= 230. dip= 34. slip= -46. degrees
 auxiliary plane: strike= 1. dip= 66. slip=-114. degrees
 Moment Mo= 1.8e+22 dyne-cm
 slipvector=(0.016,-.913,0.407) vecaz= -89.0 vecdip= 24.0
 moment tensor

M11=	1.6e+20	M12=	-7.1e+21	M13=	2.9e+21	
M21=	7.1e+21	M22=	1.2e+22	M23=	1.1e+22	dyne-cm
M31=	2.9e+21	M32=	1.1e+22	M33=	-1.2e+22	

Eigenvectors: component 1=N, 2=E, 3=V
 eigenvector 1=(-.310,0.902,0.302) vecaz.= 109.0 vecdip= 17.6
 eigenvector 2=(0.904,0.181,0.388) vecaz.= 11.3 vecdip= 22.9
 eigenvector 3=(-.296,-.393,0.871) vecaz.= -126.9 vecdip= 60.5

560110008

Fault plane solution number 3
 fault plane: strike= 230. dip= 34. slip= -46. degrees
 auxiliary plane: strike= 1. dip= 66. slip=-114. degrees
 Moment Mo= 3.1e+23 dyne-cm
 slipvector=(0.016,-.913,0.407) vecaz.= -89.0 vecdip= 24.0
 moment tensor 3:
 M11= 2.7e+21 M12= -1.2e+23 M13= 5.1e+22
 M21= -1.2e+23 M22= 2.0e+23 M23= 1.9e+23 dyne-cm
 M31= 5.1e+22 M32= 1.9e+23 M33= -2.1e+23

Eigenvectors: component 1=N, 2=E, 3=V
 eigenvector 1=(-.310,0.902,0.302) vecaz.= 109.0 vecdip= 17.6
 eigenvector 2=(0.904,0.181,0.388) vecaz.= 11.3 vecdip= 22.9
 eigenvector 3=(-.296,-.393,0.871) vecaz.= -126.9 vecdip= 60.5

ORIGINAL PAGE IS
OF POOR QUALITY

580312012

Fault plane solution number 4
 fault plane: strike= 230. dip= 34. slip= -46. degrees
 auxiliary plane: strike= 1. dip= 66. slip=-114. degrees
 Moment Mo= 3.1e+23 dyne-cm
 slipvector=(0.016,-.913,0.407) vecaz.= -89.0 vecdip= 24.0
 moment tensor 4:
 M11= 2.7e+21 M12= -1.2e+23 M13= 5.1e+22

76

M21= -1.2e+23 M22= 2.0e+23 M23= 1.9e+23 dyne-cm
 M31= 5.1e+22 M32= 1.9e+23 M33= -2.1e+23

Eigenvectors: component 1=N, 2=E, 3=V
 eigenvector 1=(-.310,0.902,0.302) vecaz.= 109.0 vecdip= 17.6
 eigenvector 2=(0.904,0.181,0.388) vecaz.= 11.3 vecdip= 22.9
 eigenvector 3=(-.296,-.393,0.871) vecaz.= -126.9 vecdip= 60.5

580312012

Fault plane solution number 5
 fault plane: strike= 230. dip= 34. slip= -46. degrees
 auxiliary plane: strike= 1. dip= 66. slip=-114. degrees
 Moment Mo= 2.2e+23 dyne-cm
 slipvector=(0.016,-.913,0.407) vecaz.= -89.0 vecdip= 24.0
 moment tensor 5:
 M11= 1.9e+21 M12= -8.7e+22 M13= 3.6e+22
 M21= -8.7e+22 M22= 1.4e+23 M23= 1.4e+23 dyne-cm
 M31= 3.6e+22 M32= 1.4e+23 M33= -1.5e+23

Eigenvectors: component 1=N, 2=E, 3=V
 eigenvector 1=(-.310,0.902,0.302) vecaz.= 109.0 vecdip= 17.6
 eigenvector 2=(0.904,0.181,0.388) vecaz.= 11.3 vecdip= 22.9
 eigenvector 3=(-.296,-.393,0.871) vecaz.= -126.9 vecdip= 60.5

580929008

Fault plane solution number 6
 fault plane: strike= 230. dip= 34. slip= -46. degrees
 auxiliary plane: strike= 1. dip= 66. slip=-114. degrees
 Moment Mo= 3.1e+23 dyne-cm

ORIGINAL PAGE IS
OF POOR QUALITY

77

slipvector=(0.016,-.913,0.407) vecaz= -89.0 vecdip= 24.0
 moment tensor 6:
 M11= 2.7e+21 M12= -1.2e+23 M13= 5.1e+22
 M21= -1.2e+23 M22= 2.0e+23 M23= 1.9e+23
 M31= 5.1e+22 M32= 1.9e+23 M33= -2.1e+23 dyne-cm

Eigenvectors: component 1=N, 2=E, 3=V
 eigenvector 1=(-.310,0.902,0.302) vecaz.= 109.0 vecdip= 17.6
 eigenvector 2=(0.904,0.181,0.388) vecaz.= 11.3 vecdip= 22.9
 eigenvector 3=(-.296,-.393,0.871) vecaz.= -126.9 vecdip= 60.5

591014014

Fault plane solution number 7
 fault plane: strike= 230. dip= 34. slip= -46. degrees
 auxiliary plane: strike= 1. dip= 66. slip= -114. degrees
 Moment Mo= 4.9e+22 dyne-cm
 slipvector=(0.016,-.913,0.407) vecaz= -89.0 vecdip= 24.0
 moment tensor 7:
 M11= 4.3e+20 M12= -1.9e+22 M13= 8.0e+21
 M21= 1.9e+22 M22= 3.2e+22 M23= 3.0e+22
 M31= 0.0e+21 M32= 3.0e+22 M33= -3.3e+22 dyne-cm

Eigenvectors: component 1=N, 2=E, 3=V
 eigenvector 1=(-.310,0.902,0.302) vecaz.= 109.0 vecdip= 17.6
 eigenvector 2=(0.904,0.181,0.388) vecaz.= 11.3 vecdip= 22.9
 eigenvector 3=(-.296,-.393,0.871) vecaz.= -126.9 vecdip= 60.5

620B30013

Fault plane solution number 8

CRITICAL PAGE IS
OF POOR QUALITY

78

fault plane: strike= 230. dip= 34. slip= -46. degrees
 auxiliary plane: strike= 1. dip= 66. slip= -114. degrees
 Moment Mo= 6.0e+24 dyne-cm
 slipvector=(0.016,-.913,0.407) vecaz= -89.0 vecdip= 24.0
 moment tensor 8:
 M11= 5.3e+22 M12= -2.4e+24 M13= 9.8e+23
 M21= -2.4e+24 M22= 3.9e+24 M23= 3.7e+24
 M31= 9.8e+23 M32= 3.7e+24 M33= -4.0e+24 dyne-cm

Eigenvectors: component 1=N, 2=E, 3=V
 eigenvector 1=(-.310,0.902,0.302) vecaz.= 109.0 vecdip= 17.6
 eigenvector 2=(0.904,0.181,0.388) vecaz.= 11.3 vecdip= 22.9
 eigenvector 3=(-.296,-.393,0.871) vecaz.= -126.9 vecdip= 60.5

660128018

Fault plane solution number 9
 fault plane: strike= 230. dip= 34. slip= -46. degrees
 auxiliary plane: strike= 1. dip= 66. slip= -114. degrees
 Moment Mo= 0.3e+21 dyne-cm
 slipvector=(0.016,-.913,0.407) vecaz= -89.0 vecdip= 24.0
 moment tensor 9:
 M11= 7.3e+19 M12= -3.3e+21 M13= 1.4e+21
 M21= -3.3e+21 M22= 5.5e+21 M23= 5.1e+21
 M31= 1.4e+21 M32= 5.1e+21 M33= -5.5e+21 dyne-cm

Eigenvectors: component 1=N, 2=E, 3=V
 eigenvector 1=(-.310,0.902,0.302) vecaz.= 109.0 vecdip= 17.6
 eigenvector 2=(0.904,0.181,0.388) vecaz.= 11.3 vecdip= 22.9
 eigenvector 3=(-.296,-.393,0.871) vecaz.= 126.9 vecdip= 60.5

CRITICAL PAGE IS
OF POOR QUALITY

79

680527005

Fault plane solution number 10
fault plane: strike= 230. dip= 34. slip= -46. degrees
auxiliary plane: strike= 1. dip= 66. slip=-114. degrees
Moment Mo= 3.8e+22 dyne-cm
slipvector=(0.016,-.913,0.407) vecaz= -89.0 vecdip= 24.0
moment tensor 10:
M11= 3.4e+20 M12= -1.5e+22 M13= 6.2e+21
M21= -1.5e+22 M22= 2.5e+22 M23= 2.3e+22 dyne-cm
M31= 6.2e+21 M32= 2.3e+22 M33= -2.5e+22

Eigenvectors: component 1=N, 2=E, 3=V
eigenvector1=(-.310,0.902,0.302) vecaz.= 109.0 vecdip= 17.6
eigenvector2=(0.904,0.181,0.388) vecaz.= 11.3 vecdip= 22.9
eigenvector3=(-.296,-.393,0.871) vecaz.= -126.9 vecdip= 60.5

680528000

Fault plane solution number 11
fault plane: strike= 230. dip= 34. slip= -46. degrees
auxiliary plane: strike= 1. dip= 66. slip=-114. degrees
Moment Mo= 8.3e+21 dyne-cm
slipvector=(0.016,-.913,0.407) vecaz= -89.0 vecdip= 24.0
moment tensor 11:
M11= 7.3e+19 M12= -3.3e+21 M13= 1.4e+21
M21= -3.3e+21 M22= 5.5e+21 M23= 5.1e+21 dyne-cm
M31= 1.4e+21 M32= 5.1e+21 M33= -5.5e+21

Eigenvectors: component 1=N, 2=E, 3=V
eigenvector1=(-.310,0.902,0.302) vecaz.= 109.0 vecdip= 17.6
eigenvector2=(0.904,0.181,0.388) vecaz.= 11.3 vecdip= 22.9
eigenvector3=(-.296,-.393,0.871) vecaz.= -126.9 vecdip= 60.5

80

680528000

Fault plane solution number 12
fault plane: strike= 230. dip= 34. slip= -46. degrees
auxiliary plane: strike= 1. dip= 66. slip=-114. degrees
Moment Mo= 8.3e+21 dyne-cm
slipvector=(0.016,-.913,0.407) vecaz= -89.0 vecdip= 24.0
moment tensor 12:
M11= 7.3e+19 M12= -3.3e+21 M13= 1.4e+21
M21= -3.3e+21 M22= 5.5e+21 M23= 5.1e+21 dyne-cm
M31= 1.4e+21 M32= 5.1e+21 M33= -5.5e+21

Eigenvectors: component 1=N, 2=E, 3=V
eigenvector1=(-.310,0.902,0.302) vecaz.= 109.0 vecdip= 17.6
eigenvector2=(0.904,0.181,0.388) vecaz.= 11.3 vecdip= 22.9
eigenvector3=(-.296,-.393,0.871) vecaz.= -126.9 vecdip= 60.5

680528012

Fault plane solution number 13
fault plane: strike= 230. dip= 34. slip= -46. degrees
auxiliary plane: strike= 1. dip= 66. slip=-114. degrees
Moment Mo= 8.3e+21 dyne-cm
slipvector=(0.016,-.913,0.407) vecaz= -89.0 vecdip= 24.0
moment tensor 13:
M11= 7.3e+19 M12= -3.3e+21 M13= 1.4e+21
M21= -3.3e+21 M22= 5.5e+21 M23= 5.1e+21 dyne-cm
M31= 1.4e+21 M32= 5.1e+21 M33= -5.5e+21

Eigenvectors: component 1=N, 2=E, 3=V

81

eigenvector 1=(-.310,0.902,0.302) vecaz.= 109.0 vecdip= 17.6
eigenvector 2=(0.904,0.181,0.388) vecaz.= 11.3 vecdip= 22.9
eigenvector 3=(-.296,-.393,0.871) vecaz.= -126.9 vecdip= 60.5

680530000

Fault plane solution number 14
fault plane: strike= 230. dip= 34. slip= -46. degrees
auxiliary plane: strike= 1. dip= 66. slip=-114. degrees
Moment Mo= 2.9e+23 dyne-cm
slipvector=(0.016,-.913,0.407) vecaz= -89.0 vecdip= 24.0
moment tensor 14:
M11= 2.6e+21 M12= -1.1e+23 M13= 4.7e+22
M21= -1.1e+23 M22= 1.9e+23 M23= 1.8e+23 dyne-cm
M31= 4.7e+22 M32= 1.8e+23 M33= -1.9e+23

Eigenvectors: component 1=N, 2=E, 3=V
eigenvector 1=(-.310,0.902,0.302) vecaz.= 109.0 vecdip= 17.6
eigenvector 2=(0.904,0.181,0.388) vecaz.= 11.3 vecdip= 22.9
eigenvector 3=(-.296,-.393,0.871) vecaz.= -126.9 vecdip= 60.5

680531003

Fault plane solution number 15
fault plane: strike= 230. dip= 34. slip= -46. degrees
auxiliary plane: strike= 1. dip= 66. slip=-114. degrees
Moment Mo= 8.3e+21 dyne-cm
slipvector=(0.016,-.913,0.407) vecaz= -89.0 vecdip= 24.0
moment tensor 15:
M11= 7.3e+19 M12= -3.3e+21 M13= 1.4e+21
M21= 3.3e+21 M22= 5.5e+21 M23= 5.1e+21 dyne cm

ORIGINAL PAGE IS
OF POOR QUALITY

82

M31= 1.4e+21 M32= 5.1e+21 M33= -5.5e+21

Eigenvectors: component 1=N, 2=E, 3=V
eigenvector 1=(-.310,0.902,0.302) vecaz.= 109.0 vecdip= 17.6
eigenvector 2=(0.904,0.181,0.388) vecaz.= 11.3 vecdip= 22.9
eigenvector 3=(-.296,-.393,0.871) vecaz.= -126.9 vecdip= 60.5

680603013

Fault plane solution number 16
fault plane: strike= 230. dip= 34. slip= -46. degrees
auxiliary plane: strike= 1. dip= 66. slip=-114. degrees
Moment Mo= 2.9e+23 dyne-cm
slipvector=(0.016,-.913,0.407) vecaz= -89.0 vecdip= 24.0
moment tensor 16:
M11= 2.6e+21 M12= -1.1e+23 M13= 4.7e+22
M21= -1.1e+23 M22= 1.9e+23 M23= 1.8e+23 dyne-cm
M31= 4.7e+22 M32= 1.8e+23 M33= -1.9e+23

Eigenvectors: component 1=N, 2=E, 3=V
eigenvector 1=(-.310,0.902,0.302) vecaz.= 109.0 vecdip= 17.6
eigenvector 2=(0.904,0.181,0.388) vecaz.= 11.3 vecdip= 22.9
eigenvector 3=(-.296,-.393,0.871) vecaz.= -126.9 vecdip= 60.5

680604002

Fault plane solution number 17
fault plane: strike= 230. dip= 34. slip= -46. degrees
auxiliary plane: strike= 1. dip= 66. slip=-114. degrees
Moment Mo= 2.0e+22 dyne-cm
slipvector=(0.016,-.913,0.407) vecaz= -89.0 vecdip= 24.0

83

moment tensor 17:
M11= 2.7e+20 M12= -1.2e+22 M13= 4.9e+21
M21= -1.2e+22 M22= 2.0e+22 M23= 1.8e+22 dyne-cm
M31= 4.9e+21 M32= 1.8e+22 M33= -2.0e+22

Eigenvectors: component 1=N, 2=E, 3=V
eigenvector 1=(-.310,0.902,0.302) vecaz.= 109.0 vecdip= 17.6
eigenvector 2=(0.904,0.181,0.388) vecaz.= 11.3 vecdip= 22.9
eigenvector 3=(-.296,-.393,0.871) vecaz.= -126.9 vecdip= 60.5

680604002

Fault plane solution number 18
fault plane: strike= 230. dip= 34. slip= -46. degrees
auxiliary plane: strike= 1. dip= 66. slip=-114. degrees
Moment Mo= 8.3e+21 dyne-cm
slipvector=(0.016,-.913,0.407) vecaz= -89.0 vecdip= 24.0

moment tensor 18:
M11= 7.3e+19 M12= -3.3e+21 M13= 1.4e+21
M21= -3.3e+21 M22= 5.5e+21 M23= 5.1e+21 dyne-cm
M31= 1.4e+21 M32= 5.1e+21 M33= -5.5e+21

Eigenvectors: component 1=N, 2=E, 3=V
eigenvector 1=(-.310,0.902,0.302) vecaz.= 109.0 vecdip= 17.6
eigenvector 2=(0.904,0.181,0.388) vecaz.= 11.3 vecdip= 22.9
eigenvector 3=(-.296,-.393,0.871) vecaz.= -126.9 vecdip= 60.5

680604002

Fault plane solution number 19
fault plane: strike= 230. dip= 34. slip= -46. degrees

86

auxiliary plane: strike= 1. dip= 66. slip=-114. degrees
Moment Mo= 8.3e+21 dyne-cm
slipvector=(0.016,-.913,0.407) vecaz= -89.0 vecdip= 24.0

moment tensor 19:
M11= 7.3e+19 M12= -3.3e+21 M13= 1.4e+21
M21= -3.3e+21 M22= 5.5e+21 M23= 5.1e+21 dyne-cm
M31= 1.4e+21 M32= 5.1e+21 M33= -5.5e+21

Eigenvectors: component 1=N, 2=E, 3=V
eigenvector 1=(-.310,0.902,0.302) vecaz.= 109.0 vecdip= 17.6
eigenvector 2=(0.904,0.181,0.388) vecaz.= 11.3 vecdip= 22.9
eigenvector 3=(-.296,-.393,0.871) vecaz.= -126.9 vecdip= 60.5

680604003

Fault plane solution number 20
fault plane: strike= 230. dip= 34. slip= -46. degrees
auxiliary plane: strike= 1. dip= 66. slip=-114. degrees
Moment Mo= 8.3e+21 dyne-cm
slipvector=(0.016,-.913,0.407) vecaz= -89.0 vecdip= 24.0

moment tensor 20:
M11= 7.3e+19 M12= -3.3e+21 M13= 1.4e+21
M21= -3.3e+21 M22= 5.5e+21 M23= 5.1e+21 dyne-cm
M31= 1.4e+21 M32= 5.1e+21 M33= -5.5e+21

Eigenvectors: component 1=N, 2=E, 3=V
eigenvector 1=(-.310,0.902,0.302) vecaz.= 109.0 vecdip= 17.6
eigenvector 2=(0.904,0.181,0.388) vecaz.= 11.3 vecdip= 22.9
eigenvector 3=(-.296,-.393,0.871) vecaz.= -126.9 vecdip= 60.5

680604005

85

Fault plane solution number 21
 fault plane: strike= 230. dip= 34. slip= -46. degrees
 auxiliary plane: strike= 1. dip= 66. slip=-114. degrees
 Moment Mo= 8.3e+21 dyne-cm
 slipvector=(0.016,-.913,0.407) vecaz= -89.0 vecdip= 24.0
 moment tensor 21:
 M11= 7.3e+19 M12= -3.3e+21 M13= 1.4e+21
 M21= -3.3e+21 M22= 5.5e+21 M23= 5.1e+21 dyne-cm
 M31= 1.4e+21 M32= 5.1e+21 M33= -5.5e+21

Eigenvectors: component 1=N, 2=E, 3=V
 eigenvector1=(-.310,0.902,0.302) vecaz.= 109.0 vecdip= 17.6
 eigenvector2=(0.904,0.181,0.388) vecaz.= 11.3 vecdip= 22.9
 eigenvector3=(-.296,-.393,0.871) vecaz.= -126.9 vecdip= 60.5

680604006

Fault plane solution number 22
 fault plane: strike= 230. dip= 34. slip= -46. degrees
 auxiliary plane: strike= 1. dip= 66. slip=-114. degrees
 Moment Mo= 8.3e+21 dyne-cm
 slipvector=(0.016,-.913,0.407) vecaz= -89.0 vecdip= 24.0
 moment tensor 22:
 M11= 7.3e+19 M12= -3.3e+21 M13= 1.4e+21
 M21= -3.3e+21 M22= 5.5e+21 M23= 5.1e+21 dyne-cm
 M31= 1.4e+21 M32= 5.1e+21 M33= -5.5e+21

Eigenvectors: component 1=N, 2=E, 3=V
 eigenvector1=(-.310,0.902,0.302) vecaz.= 109.0 vecdip= 17.6
 eigenvector2=(0.904,0.181,0.388) vecaz.= 11.3 vecdip= 22.9
 eigenvector3=(-.296,-.393,0.871) vecaz.= -126.9 vecdip= 60.5

86

680604010

Fault plane solution number 23
 fault plane: strike= 230. dip= 34. slip= -46. degrees
 auxiliary plane: strike= 1. dip= 66. slip=-114. degrees
 Moment Mo= 8.3e+21 dyne-cm
 slipvector=(0.016,-.913,0.407) vecaz= -89.0 vecdip= 24.0
 moment tensor 23:
 M11= 7.3e+19 M12= -3.3e+21 M13= 1.4e+21
 M21= -3.3e+21 M22= 5.5e+21 M23= 5.1e+21 dyne-cm
 M31= 1.4e+21 M32= 5.1e+21 M33= -5.5e+21

Eigenvectors: component 1=N, 2=E, 3=V
 eigenvector1=(-.310,0.902,0.302) vecaz.= 109.0 vecdip= 17.6
 eigenvector2=(0.904,0.181,0.388) vecaz.= 11.3 vecdip= 22.9
 eigenvector3=(-.296,-.393,0.871) vecaz.= -126.9 vecdip= 60.5

680605004

Fault plane solution number 24
 fault plane: strike= 230. dip= 34. slip= -46. degrees
 auxiliary plane: strike= 1. dip= 66. slip=-114. degrees
 Moment Mo= 8.3e+21 dyne-cm
 slipvector=(0.016,-.913,0.407) vecaz= -89.0 vecdip= 24.0
 moment tensor 24:
 M11= 7.3e+19 M12= -3.3e+21 M13= 1.4e+21
 M21= -3.3e+21 M22= 5.5e+21 M23= 5.1e+21 dyne-cm
 M31= 1.4e+21 M32= 5.1e+21 M33= -5.5e+21

Eigenvectors: component 1=N, 2=E, 3=V
 eigenvector1=(-.310,0.902,0.302) vecaz.= 109.0 vecdip= 17.6

87

eigenvector2=(0.904,0.181,0.388) vecaz.= 11.3 vecdip= 22.9
eigenvector3=(-.296,-.393,0.871) vecaz.= -126.9 vecdip= 60.5

680605005

Fault plane solution number 25
fault plane: strike= 230. dip= 34. slip= -46. degrees
auxiliary plane: strike= 1. dip= 66. slip=-114. degrees
Moment Mo= 8.3e+21 dyne-cm
slipvector=(0.016,-.913,0.407) vecaz.= 89.0 vecdip= 24.0
moment tensor 25:
M11= 7.3e+19 M12= -3.3e+21 M13= 1.4e+21
M21= -3.3e+21 M22= 5.5e+21 M23= 5.1e+21 dyne-cm
M31= 1.4e+21 M32= 5.1e+21 M33= -5.5e+21

Eigenvectors: component 1=N, 2=E, 3=V
eigenvector1=(-.310,0.902,0.302) vecaz.= 109.0 vecdip= 17.6
eigenvector2=(0.904,0.181,0.388) vecaz.= 11.3 vecdip= 22.9
eigenvector3=(-.296,-.393,0.871) vecaz.= -126.9 vecdip= 60.5

680605007

Fault plane solution number 26
fault plane: strike= 230. dip= 34. slip= -46. degrees
auxiliary plane: strike= 1. dip= 66. slip=-114. degrees
Moment Mo= 8.3e+21 dyne-cm
slipvector=(0.016,-.913,0.407) vecaz.= -89.0 vecdip= 24.0
moment tensor 26:
M11= 7.3e+19 M12= -3.3e+21 M13= 1.4e+21
M21= 3.3e+21 M22= 5.5e+21 M23= 5.1e+21 dyne-cm
M31= 1.4e+21 M32= 5.1e+21 M33= -5.5e+21

88

Eigenvectors: component 1=N, 2=E, 3=V
eigenvector1=(-.310,0.902,0.302) vecaz.= 109.0 vecdip= 17.6
eigenvector2=(0.904,0.181,0.388) vecaz.= 11.3 vecdip= 22.9
eigenvector3=(-.296,-.393,0.871) vecaz.= -126.9 vecdip= 60.5

680605008

Fault plane solution number 27
fault plane: strike= 230. dip= 34. slip= -46. degrees
auxiliary plane: strike= 1. dip= 66. slip=-114. degrees
Moment Mo= 1.1e+22 dyne-cm
slipvector=(0.016,-.913,0.407) vecaz.= -89.0 vecdip= 24.0
moment tensor 27:
M11= 9.7e+19 M12= -4.4e+21 M13= 1.8e+21
M21= -4.4e+21 M22= 7.2e+21 M23= 6.8e+21 dyne-cm
M31= 1.8e+21 M32= 6.8e+21 M33= -7.3e+21

Eigenvectors: component 1=N, 2=E, 3=V
eigenvector1=(-.310,0.902,0.302) vecaz.= 109.0 vecdip= 17.6
eigenvector2=(0.904,0.181,0.388) vecaz.= 11.3 vecdip= 22.9
eigenvector3=(-.296,-.393,0.871) vecaz.= -126.9 vecdip= 60.5

680605008

Fault plane solution number 28
fault plane: strike= 230. dip= 34. slip= -46. degrees
auxiliary plane: strike= 1. dip= 66. slip=-114. degrees
Moment Mo= 8.3e+21 dyne-cm
slipvector=(0.016,-.913,0.407) vecaz.= -89.0 vecdip= 24.0
moment tensor 28:

88

DETERMINATION OF THE STRAIN RATE:

The specified volume= 137.5x148.8x 15.0km³

The strain rates for the last 79.0 years in the directions
of the principal stresses:

extensional : $9.1e-10/yr = 1.8e-13/sec$
intermediate : $-1.8e-10/yr = -3.6e-13/sec$
compressional: $-9.1e-10/yr = -1.8e-13/sec$

The horizontal and vertical strain rates:

Maximum horizontal: $8.7e-10/yr = 2.7e-17/sec$ Azimuths N81W

Minimum horizontal: $-1.3e-10/yr = -4.1e-18/sec$ Azimuths N 9E

Vertical : $-7.4e-10/yr = -2.3e-17/sec$

ENTER region boundary rotation

-63.2000

razmax

17.5856

The maximum horizontal deformation rate = $1.2e-01$ mm/yr

C-3

COMPUTATION OF A SYNTHETIC FAULT PLANE SOLUTION FROM A REGIONAL MOMENT TENSOR

HANSEL VALLEY REGION

Hansel Valley 1934

Fault plane solution number 1

fault plane: strike= 5. dip= 88. slip= -78. degrees

auxiliary plane: strike= 128. dip= 28. slip=-154. degrees

Moment Mo= 7.7e+25 dyne-cm

slipvector=(.296, .171, .948) vecaz= 38.8 vecdip= 78.8

moment tensor 1:

M11=	-4.3e+24	M12=	2.3e+25	M13=	-1.8e+25		
M21=	2.3e+25	M22=	2.9e+25	M23=	6.7e+25	dyne-cm	
M31=	-1.8e+25	M32=	6.7e+25	M33=	-2.5e+25		

Eigenvectors: component 1=N, 2=E, 3=V

eigenvector1=(.178, .838, .532) vecaz.= 78.4 vecdip= 32.1

eigenvector2=(-.941, -.223, .337) vecaz.= -178.6 vecdip= 19.7

eigenvector3=(.292, -.558, .777) vecaz.= -52.4 vecdip= 51.8

Pocatello Valley 1975

Fault plane solution number 2

fault plane: strike= 225. dip= 39. slip= -53. degrees

auxiliary plane: strike= 1. dip= 68. slip=-116. degrees

Moment Mo= 1.5e+25 dyne-cm

slipvector=(.815, -.866, .588) vecaz= -89.8 vecdip= 38.8

moment tensor 2:

M11=	1.8e+23	M12=	-5.9e+24	M13=	3.2e+24		
M21=	-5.9e+24	M22=	1.2e+25	M23=	6.7e+24	dyne-cm	
M31=	3.2e+24	M32=	6.7e+24	M33=	-1.2e+25		

Eigenvectors: component 1=N, 2=E, 3=V

eigenvector1=(-.324, .926, .194) vecaz.= 189.3 vecdip= 11.2

eigenvector2=(.895, .234, .379) vecaz.= 14.6 vecdip= 22.3

eigenvector3=(-.385, -.297, .985) vecaz.= -135.8 vecdip= 64.8

Hansel Valley composite 1976

Fault plane solution number 3

fault plane: strike= 195. dip= 55. slip= -58. degrees

auxiliary plane: strike= 319. dip= 49. slip=-135. degrees

ORIGINAL PAGE IS
OF POOR QUALITY

Moment Mo= 5.3e+22 dyne-cm
 eigenvector1=(-.495, -.578, .656) vecaz= 229.8 vecdip= 41.8
 moment tensor 3:
 M11= -1.4e+22 M12= 1.7e+22 M13= 2.7e+22
 M21= 5.0e+22 M22= -9.9e+21 M23= -9.9e+21
 M31= 2.7e+22 M32= -9.9e+21 M33= -4.5e+22

Eigenvectors: component 1=N, 2=E, 3=V
 vecaz= -182.7 vecdip= 2.2
 eigenvector1=(-.289, -.977, .838)
 eigenvector2=(-.938, -.158, .878)
 eigenvector3=(-.389, .142, .869) vecaz= 164.4 vecdip= 58.1

PV1c

Fault plane solution number 4
 fault plane: strike=353, dip= 57, slip=-66, degrees
 auxiliary plane: strike=134, dip= 48, slip=-121, degrees
 Moment Mo= 3.7e+23 dyne-cm
 slipvector=(-.462, .447, .766) vecaz= 44.8 vecdip= 58.8
 moment tensor 4:
 M11= 3.5e+22 M12= 1.6e+23 M13= -6.5e+22
 M21= 1.6e+23 M22= 2.7e+23 M23= 1.5e+23
 M31= -6.5e+22 M32= 1.5e+23 M33= -3.1e+23

Eigenvectors: component 1=N, 2=E, 3=V
 vecaz= 66.1 vecdip= 9.8
 eigenvector1=(-.481, .983, .157)
 eigenvector2=(-.888, .331, .341) vecaz= 159.4 vecdip= 19.9
 eigenvector3=(-.256, -.274, .927) vecaz= -47.8 vecdip= 68.8

PV2e

Fault plane solution number 5
 fault plane: strike=122, dip= 56, slip=-75, degrees
 auxiliary plane: strike=182, dip= 55, slip=-168, degrees
 Moment Mo= 1.8e+25 dyne-cm
 slipvector=(-.679, .458, .574) vecaz= 34.8 vecdip= 35.8
 moment tensor 5:
 M11= 5.2e+24 M12= 5.1e+24 M13= -3.7e+24
 M21= 4.4e+24 M22= 4.4e+24 M23= -1.1e+24
 M31= -3.7e+24 M32= -1.1e+24 M33= -9.6e+24

Eigenvectors: component 1=N, 2=E, 3=V
 vecaz= -138.7 vecdip= 9.8
 eigenvector1=(-.748, -.668, .171) vecaz= -138.7 vecdip= 9.8
 eigenvector2=(-.888, .888, .888) vecaz= .8 vecdip= 98.8

eigenvector3=(.229, -.885, .974) vecaz= -1.2 vecdip= 76.8

n1985

Fault plane solution number 6
 fault plane: strike=135, dip= 23, slip=-133, degrees
 auxiliary plane: strike= 1, dip= 73, slip=-73, degrees
 Moment Mo= 1.4e+23 dyne-cm
 slipvector=(-.817, -.956, .292) vecaz= -89.8 vecdip= 17.8
 moment tensor 6:
 M11= -4.6e+28 M12= 3.6e+22 M13= -1.1e+22
 M21= 1.1e+22 M22= 7.1e+22 M23= 1.1e+23
 M31= -1.1e+22 M32= 1.1e+23 M33= -7.1e+22

Eigenvectors: component 1=N, 2=E, 3=V
 vecaz= 77.7 vecdip= 26.7
 eigenvector1=(-.191, .873, .449) vecaz= 77.7 vecdip= 26.7
 eigenvector2=(-.961, .873, .266) vecaz= 175.6 vecdip= 15.5
 eigenvector3=(-.288, -.482, .853) vecaz= -67.5 vecdip= 58.5

n1989

Fault plane solution number 7
 fault plane: strike=135, dip= 23, slip=-133, degrees
 auxiliary plane: strike= 1, dip= 73, slip=-73, degrees
 Moment Mo= 2.1e+25 dyne-cm
 slipvector=(-.917, -.956, .292) vecaz= -89.8 vecdip= 17.8
 moment tensor 7:
 M11= -7.3e+22 M12= 5.6e+24 M13= -1.8e+24
 M21= 5.6e+24 M22= 1.1e+25 M23= 1.7e+25
 M31= -1.8e+24 M32= 1.7e+25 M33= -1.1e+25

Eigenvectors: component 1=N, 2=E, 3=V
 vecaz= 77.7 vecdip= 26.7
 eigenvector1=(-.191, .873, .449) vecaz= 77.7 vecdip= 26.7
 eigenvector2=(-.961, .873, .266) vecaz= 175.6 vecdip= 15.5
 eigenvector3=(-.288, -.482, .853) vecaz= -67.5 vecdip= 58.5

n1934a

Fault plane solution number 8
 fault plane: strike=135, dip= 23, slip=-133, degrees
 auxiliary plane: strike= 1, dip= 73, slip=-73, degrees
 Moment Mo= 1.3e+25 dyne-cm

```

slipvector=(.817,-.956,.292)  vecax=-89.8  vecdip=17.8
moment tensor 8:
M11= -3.4e+22  M12= 3.4e+24  M13= -1.1e+24
M21= 1.8e+25  M22= 1.8e+25  M23= -6.8e+24
M31= -1.1e+24  M32= 1.8e+25  M33= -6.8e+24
Eigenvectors: component 1=N, 2=E, 3=V
eigenvector1=(.191,.873,.449)  vecax.= 77.7  vecdip= 26.7
eigenvector2=(-.961,.873,.266)  vecax.= 175.6  vecdip= 15.5
eigenvector3=(.288,-.482,.853)  vecax.= -67.5  vecdip= 58.5

```

n1934b

```

Fault plane solution number 9
fault plane: strike=135, dip= 23, slip=-133, degrees
auxiliary plane: strike= 73, slip= -73, degrees
Moment Mo=1.6e+24 dyne-cm
slipvector=(.817,-.956,.292)  vecax=-89.8  vecdip= 17.8
moment tensor 9:
M11= -3.5e+21  M12= 2.7e+23  M13= -8.6e+22
M21= 2.7e+23  M22= 5.4e+23  M23= 8.2e+23
M31= -8.6e+22  M32= 8.2e+23  M33= -5.4e+23
Eigenvectors: component 1=N, 2=E, 3=V
eigenvector1=(.191,.873,.449)  vecax.= 77.7  vecdip= 26.7
eigenvector2=(-.961,.873,.266)  vecax.= 175.6  vecdip= 15.5
eigenvector3=(.288,-.482,.853)  vecax.= -67.5  vecdip= 58.5

```

n1934c

```

Fault plane solution number 16
fault plane: strike=135, dip= 23, slip=-133, degrees
auxiliary plane: strike= 73, slip= -73, degrees
Moment Mo=3.6e+23 dyne-cm
slipvector=(.817,-.956,.292)  vecax=-89.8  vecdip= 17.8
moment tensor 16:
M11= -1.6e+21  M12= 1.3e+23  M13= -4.1e+22
M21= 1.3e+23  M22= 3.8e+23  M23= 3.8e+23
M31= -4.1e+22  M32= 3.8e+23  M33= -2.5e+23
Eigenvectors: component 1=N, 2=E, 3=V
eigenvector1=(.191,.873,.449)  vecax.= 77.7  vecdip= 26.7
eigenvector2=(-.961,.873,.266)  vecax.= 175.6  vecdip= 15.5
eigenvector3=(.288,-.482,.853)  vecax.= -67.5  vecdip= 58.5

```

ORIGINAL PAGE IS
OF POOR QUALITY

n1934d

```

Fault plane solution number 11
fault plane: strike=135, dip= 23, slip=-133, degrees
auxiliary plane: strike= 73, slip= -73, degrees
Moment Mo=3.6e+24 dyne-cm
slipvector=(.817,-.956,.292)  vecax=-89.8  vecdip= 17.8
moment tensor 11:
M11= -1.2e+22  M12= 9.5e+23  M13= -2.1e+23
M21= 9.5e+23  M22= 1.9e+24  M23= 2.9e+24
M31= -2.1e+23  M32= 2.9e+24  M33= -1.9e+24
Eigenvectors: component 1=N, 2=E, 3=V
eigenvector1=(.191,.873,.449)  vecax.= 77.7  vecdip= 26.7
eigenvector2=(-.961,.873,.266)  vecax.= 175.6  vecdip= 15.5
eigenvector3=(.288,-.482,.853)  vecax.= -67.5  vecdip= 58.5

```

n1934e

```

Fault plane solution number 12
fault plane: strike=135, dip= 23, slip=-133, degrees
auxiliary plane: strike= 73, slip= -73, degrees
Moment Mo=3.6e+24 dyne-cm
slipvector=(.817,-.956,.292)  vecax=-89.8  vecdip= 17.8
moment tensor 12:
M11= -1.2e+22  M12= 9.5e+23  M13= -2.1e+23
M21= 9.5e+23  M22= 1.9e+24  M23= 2.9e+24
M31= -2.1e+23  M32= 2.9e+24  M33= -1.9e+24
Eigenvectors: component 1=N, 2=E, 3=V
eigenvector1=(.191,.873,.449)  vecax.= 77.7  vecdip= 26.7
eigenvector2=(-.961,.873,.266)  vecax.= 175.6  vecdip= 15.5
eigenvector3=(.288,-.482,.853)  vecax.= -67.5  vecdip= 58.5

```

n1942

```

Fault plane solution number 13
fault plane: strike=135, dip= 23, slip=-133, degrees
auxiliary plane: strike= 73, slip= -73, degrees
Moment Mo=1.4e+23 dyne-cm
slipvector=(.817,-.956,.292)  vecax=-89.8  vecdip= 17.8

```

moment tensor13:
 M11= -4.6e+28 M12= 3.6e+22 M13= -1.1e+22
 M21= 3.0e+22 M22= 7.1e+22 M23= 1.1e+23 dyne-cm
 M31= -1.1e+22 M32= 1.1e+22 M33= -7.1e+22

Eigenvalues: component 1=N, 2=E, 3=V
 eigenvalue1=(-.861, .873, .266) vecax.= 175.6 vecdip= 15.5
 eigenvalue2=(-.288, -.482, .853) vecax.= -67.5 vecdip= 58.5
 eigenvalue3=(.288, -.482, .853)

n1973

Fault plane solution number14

fault plane: strike=135, dip= 23, slip=-133, degrees

auxiliary plane: strike=1, dip= 73, slip=-73, degrees

Moment No. 8.1e+22 dyne-cm

slipvector1(.817, -.956, .292) vecax.= -89.8 vecdip= 17.8

moment tensor14:
 M11= -3.6e+28 M12= 2.8e+22 M13= -8.9e+21
 M21= 2.8e+22 M22= 8.4e+22 M23= 8.4e+22 dyne-cm
 M31= -8.9e+21 M32= 8.4e+22 M33= -5.5e+22

Eigenvalues: component 1=N, 2=E, 3=V

eigenvalue1=(.191, .873, .449) vecax.= 77.7 vecdip= 26.7
 eigenvalue2=(-.961, .873, .266) vecax.= 175.6 vecdip= 15.5
 eigenvalue3=(.288, -.482, .853) vecax.= -67.5 vecdip= 58.5

n1975

Fault plane solution number15

fault plane: strike=135, dip= 23, slip=-133, degrees

auxiliary plane: strike=1, dip= 73, slip=-73, degrees

Moment No. 9.1e+22 dyne-cm

slipvector1(.817, -.956, .292) vecax.= -89.8 vecdip= 17.8

moment tensor15:
 M11= -2.8e+28 M12= 2.1e+22 M13= -6.9e+21
 M21= 2.1e+22 M22= 4.3e+22 M23= 6.5e+22 dyne-cm
 M31= -6.9e+21 M32= 6.5e+22 M33= -4.3e+22

Eigenvalues: component 1=N, 2=E, 3=V

eigenvalue1=(.191, .873, .449) vecax.= 77.7 vecdip= 26.7
 eigenvalue2=(-.961, .873, .266) vecax.= 175.6 vecdip= 15.5
 eigenvalue3=(.288, -.482, .853) vecax.= -67.5 vecdip= 58.5

n1978

Fault plane solution number16

fault plane: strike=135, dip= 23, slip=-133, degrees

auxiliary plane: strike=1, dip= 73, slip=-73, degrees

Moment No. 2.1e+23 dyne-cm

slipvector1(.817, -.956, .292) vecax.= -89.8 vecdip= 17.8

moment tensor16:
 M11= -9.9e+28 M12= 7.6e+22 M13= -2.4e+22 dyne-cm
 M21= 7.6e+22 M22= 1.5e+23 M23= 2.5e+23
 M31= -2.4e+22 M32= 2.5e+23 M33= -1.5e+23

Eigenvalues: component 1=N, 2=E, 3=V

eigenvalue1=(.191, .873, .449) vecax.= 77.7 vecdip= 26.7
 eigenvalue2=(-.961, .873, .266) vecax.= 175.6 vecdip= 15.5
 eigenvalue3=(.288, -.482, .853) vecax.= -67.5 vecdip= 58.5

Regional moment tensor:

M11= 9.4e+23 M12= 2.4e+25 M13= -1.5e+25
 M21= 1.8e+25 M22= 6.9e+25 M23= 1.1e+26 dyne-cm
 M31= -1.5e+25 M32= 1.1e+26 M33= -7.8e+25

Eigenvalues:
 sigma1= 1.3e+26 sigma2= 3.2e+24 sigma3= -1.4e+26

Eigenvalues: component 1=N, 2=E, 3=V

eigenvalue1=(.171, .873, .456) vecax.= 78.5 vecdip= 27.1
 eigenvalue2=(-.961, .853, .273) vecax.= 176.9 vecdip= 15.8
 eigenvalue3=(.214, -.486, .847) vecax.= -66.3 vecdip= 57.3

SYNTHETIC FAULT PLANE SOLUTION:

coefficient of internal friction=.888 ==> alpha= 25.7 degrees

slipvector1(.276, .273, .921) vecax.= 45.0 vecdip= 67.

nodal plane2: strike=135, dip= 23.

T1=(.896, .884, .149) vecax.= 84.0 vecdip= 9.

B=(-.961, .853, .273) vecax.= 177.0 vecdip= 16.

P1=(-.288, -.478, .958) vecax.= -33.0 vecdip= 72.

slipvec2=(-.826, -.961, .277) vecax.= -88.0 vecdip= 16.

nodal plane1: strike=2, dip= 74.

T2=(.230, .662, .718) vecaz= 78. vecdip= 45.
E=(-.961, -.953, -.273) vecaz= 177. vecdip= 16.
P2=(.143, -.747, .649) vecaz= -79. vecdip= 48.

DETERMINATION OF THE STRAIN RATE:

The specified volume= 125.2x 68.3x 18.8km³

The strain rates for the last 74 years in the directions of the principal stress
extensional : 3.2e-08/yr = 5.5e-12/sec
intermediate : 7.7e-10/yr = 1.3e-13/sec
compressional: -3.2e-08/yr = -5.6e-12/sec

The horizontal and vertical strain rates:
Maximum horizontal: 2.8e-08/yr = 6.3e-16/sec Azimuth: N67E
Minimum horizontal: -3.2e-09/yr = -1.8e-16/sec Azimuth: N23W
Vertical : -1.7e-08/yr = -5.3e-16/sec
ENTER region boundary rotation
.80000000e+00
razmax
.672963715e+02

The maximum horizontal deformation rate = 1.4788 mm/yr

COMPUTATION OF A SYNTHETIC FAULT PLANE SOLUTION FROM A REGIONAL MOMENT TENSOR

NORTHERN WASATCH FRONT

Brigham City composite 1976

Fault plane solution number 1
fault plane: strike= 147. dip= 63. slip= 184. degrees
auxiliary plane: strike= 356. dip= 38. slip= -64. degrees
Moment Mo= 1.2e+22 dyne-cm
slipvector=(-.035, -.499, .066) vecaz= 266.8 vecdip= 68.8
moment tensor 1:
M11= 4.4e+20 M12= 3.3e+21 M13= -5.8e+21
M21= 3.3e+21 M22= 9.2e+21 M23= -5.1e+21
M31= -5.8e+21 M32= -5.1e+21 M33= -9.7e+21 dyne-cm

Eigenvectors: component 1=N, 2=E, 3=V
eigenvector1=(-.369, -.883, .298) vecaz.= -112.7 vecdip= 16.9
eigenvector2=(-.874, .436, .216) vecaz.= 153.5 vecdip= 12.4
eigenvector3=(.317, .174, .932) vecaz.= 28.8 vecdip= 68.8

Fielding 1978

Fault plane solution number 2
fault plane: strike= 154. dip= 78. slip= 88. degrees
auxiliary plane: strike= 348. dip= 28. slip= 95. degrees
Moment Mo= 1.3e+22 dyne-cm
slipvector=(-.117, -.321, .948) vecaz= 258.8 vecdip= 78.8
moment tensor 2:
M11= -1.2e+21 M12= -3.8e+21 M13= 4.4e+21
M21= -3.8e+21 M22= -6.5e+21 M23= 8.7e+21
M31= 4.4e+21 M32= 8.7e+21 M33= 8.2e+21 dyne-cm

Eigenvectors: component 1=N, 2=E, 3=V
eigenvector1=(.288, .369, .986) vecaz.= 68.7 vecdip= 64.9
eigenvector2=(-.983, .427, .833) vecaz.= 154.7 vecdip= 1.9
eigenvector3=(-.375, -.825, .422) vecaz.= -114.4 vecdip= 25.8

m1986

Fault plane solution number 3
fault plane: strike= 148. dip= 17. slip= -129. degrees
auxiliary plane: strike= 9. dip= 77. slip= -78. degrees

Moment Mo= 1.4e+23 dyne-cm
 slipvector1=(.152, -.952, .225) vecaz= -81.8 vcdip= 13.8
 moment tensor 3:
 M11= -5.9e+21 M12= 1.5e+22 M13= -2.9e+22
 M21= 1.5e+22 M22= 6.5e+22 M23= -5.9e+22
 M31= -2.3e+22 M32= 1.2e+23 M33= -5.9e+22

Eigenvalues: component 1=N, 2=E, 3=V
 eigenvector1=(.811, .857, .516) vecaz= 89.3 vcdip= 31.8
 eigenvector2=(-.978, -.899, .184) vecaz= -174.2 vcdip= 18.6
 eigenvector3=(.288, -.586, .837) vecaz= -67.6 vcdip= 56.8

m1989

Fault plane solution number 4
 fault plane: strike=148, dip= 17, slip=129, degrees
 auxiliary plane: strike= 9, dip= 77, slip= -78, degrees
 Moment Mo= 1.4e+23 dyne-cm
 slipvector1=(.152, -.952, .225) vecaz= -81.8 vcdip= 13.8
 moment tensor 4:
 M11= -5.9e+21 M12= 1.5e+22 M13= -2.3e+22
 M21= 1.5e+22 M22= 6.5e+22 M23= -5.9e+22
 M31= -2.3e+22 M32= 1.2e+23 M33= -5.9e+22

Eigenvalues: component 1=N, 2=E, 3=V
 eigenvector1=(.811, .857, .516) vecaz= 89.3 vcdip= 31.8
 eigenvector2=(-.978, -.899, .184) vecaz= -174.2 vcdip= 18.6
 eigenvector3=(.288, -.586, .837) vecaz= -67.6 vcdip= 56.8

m1913

Fault plane solution number 5
 fault plane: strike=148, dip= 17, slip=129, degrees
 auxiliary plane: strike= 9, dip= 77, slip= -78, degrees
 Moment Mo= 1.4e+23 dyne-cm
 slipvector1=(.152, -.952, .225) vecaz= -81.8 vcdip= 13.8
 moment tensor 5:
 M11= -5.9e+21 M12= 1.5e+22 M13= -2.2e+22
 M21= 1.5e+22 M22= 6.5e+22 M23= -5.9e+22
 M31= -2.3e+22 M32= 1.2e+23 M33= -5.9e+22

Eigenvalues: component 1=N, 2=E, 3=V
 eigenvector1=(.811, .857, .516) vecaz= 89.3 vcdip= 31.8
 eigenvector2=(-.978, -.899, .184) vecaz= -174.2 vcdip= 18.6

eigenvector3=(.288, -.586, .837) vecaz= -67.6 vcdip= 56.8

m1914a

Fault plane solution number 6
 fault plane: strike=148, dip= 17, slip=129, degrees
 auxiliary plane: strike= 9, dip= 77, slip= -78, degrees
 Moment Mo= 1.4e+23 dyne-cm
 slipvector1=(.152, -.952, .225) vecaz= -81.8 vcdip= 13.8
 moment tensor 6:
 M11= -5.9e+21 M12= 1.5e+22 M13= -2.2e+22
 M21= 1.5e+22 M22= 6.5e+22 M23= -5.9e+22
 M31= -2.3e+22 M32= 1.2e+23 M33= -5.9e+22

Eigenvalues: component 1=N, 2=E, 3=V
 eigenvector1=(.811, .857, .516) vecaz= 89.3 vcdip= 31.8
 eigenvector2=(-.978, -.899, .184) vecaz= -174.2 vcdip= 18.6
 eigenvector3=(.288, -.586, .837) vecaz= -67.6 vcdip= 56.8

m1914b

Fault plane solution number 7
 fault plane: strike=148, dip= 17, slip=129, degrees
 auxiliary plane: strike= 9, dip= 77, slip= -78, degrees
 Moment Mo= 4.7e+24 dyne-cm
 slipvector1=(.152, -.952, .225) vecaz= -81.8 vcdip= 13.8
 moment tensor 7:
 M11= -2.8e+23 M12= 5.4e+23 M13= -7.9e+23
 M21= -2.8e+23 M22= 2.2e+24 M23= 4.8e+24
 M31= -7.9e+23 M32= 4.8e+24 M33= -2.8e+24

Eigenvalues: component 1=N, 2=E, 3=V
 eigenvector1=(.811, .857, .516) vecaz= 89.3 vcdip= 31.8
 eigenvector2=(-.978, -.899, .184) vecaz= -174.2 vcdip= 18.6
 eigenvector3=(.288, -.586, .837) vecaz= -67.6 vcdip= 56.8

m1915

Fault plane solution number 8
 fault plane: strike=148, dip= 17, slip=129, degrees
 auxiliary plane: strike= 9, dip= 77, slip= -78, degrees
 Moment Mo= 1.4e+23 dyne-cm

ORIGINAL PAGE IS
 OF POOR QUALITY

m192#c

Fault plane solution number11

fault plane: strike= 148. dip= 17. slip=-129. degrees
auxiliary plane: strike= 9. dip= 77. slip= -78. degrees

Moment Mo= 1.4e+23 dyne-cm

slipvector=(.152,-.962, .225) vecaz= -81.8 vecdip= 13.8

moment tensor11:

M11=	-5.9e+21	M12=	1.5e+22	M13=	-2.3e+22	
M21=	1.5e+22	M22=	6.5e+22	M23=	1.2e+23	dyne-cm
M31=	-2.3e+22	M32=	1.2e+23	M33=	-5.9e+22	

Eigenvectors: component 1=N, 2=E, 3=V

eigenvector1=(.811, .857, .516) vecaz.= 89.3 vecdip= 31.8

eigenvector2=(-.978,-.899, .184) vecaz.= -174.2 vecdip= 18.6

eigenvector3=(.288,-.586, .837) vecaz.= -67.6 vecdip= 56.8

m1923

Fault plane solution number12

fault plane: strike= 148. dip= 17. slip=-129. degrees
auxiliary plane: strike= 9. dip= 77. slip= -78. degrees

Moment Mo= 1.4e+23 dyne-cm

slipvector=(.152,-.962, .225) vecaz= -81.8 vecdip= 13.8

moment tensor12:

M11=	-5.9e+21	M12=	1.5e+22	M13=	-2.3e+22	
M21=	1.5e+22	M22=	6.5e+22	M23=	1.2e+23	dyne-cm
M31=	-2.3e+22	M32=	1.2e+23	M33=	-5.9e+22	

Eigenvectors: component 1=N, 2=E, 3=V

eigenvector1=(.811, .857, .516) vecaz.= 89.3 vecdip= 31.8

eigenvector2=(-.978,-.899, .184) vecaz.= -174.2 vecdip= 18.6

eigenvector3=(.288,-.586, .837) vecaz.= -67.6 vecdip= 56.8

m1946

Fault plane solution number13

fault plane: strike= 148. dip= 17. slip=-129. degrees
auxiliary plane: strike= 9. dip= 77. slip= -78. degrees

Moment Mo= 1.4e+23 dyne-cm

slipvector=(.152,-.962, .225) vecaz= -81.8 vecdip= 13.8

moment tensor13:
M11= -5.9e+21 M12= 1.5e+22 M13= -2.3e+22
M21= 1.5e+22 M22= 6.5e+22 M23= 1.2e+23
M31= -2.3e+22 M32= 1.2e+23 M33= -5.9e+22 dyne-cm

Eigenvectors: component i=N, 2=E, 3=V
eigenvector1=(.811, .857, .516) vecaz.= 89.3 vecdip= 31.8
eigenvector2=(-.978, -.899, .184) vecaz.= -174.2 vecdip= 18.6
eigenvector3=(.288, -.586, .837) vecaz.= -67.6 vecdip= 56.8

m1958

Fault plane solution number14
fault plane: strike= 148, dip= 17, slip=-129, degrees
auxiliary plane: strike= 9, dip= 77, slip= -78, degrees
Moment Mo= 1.4e+23 dyne-cm
slipvector=(.152, -.562, .225) vecaz= -81.8 vecdip= 13.8
moment tensor14:
M11= -5.9e+21 M12= 1.5e+22 M13= -2.3e+22
M21= 1.5e+22 M22= 6.5e+22 M23= 1.2e+23
M31= -2.3e+22 M32= 1.2e+23 M33= -5.9e+22 dyne-cm

Eigenvectors: component i=N, 2=E, 3=V
eigenvector1=(.811, .857, .516) vecaz.= 89.3 vecdip= 31.8
eigenvector2=(-.978, -.899, .184) vecaz.= -174.2 vecdip= 18.6
eigenvector3=(.288, -.586, .837) vecaz.= -67.6 vecdip= 56.8

Regional moment tensor:
M11= -2.7e+23 M12= 7.1e+23 M13= -1.8e+24
M21= 7.1e+23 M22= 2.9e+24 M23= 5.3e+24
M31= -1.8e+24 M32= 5.3e+24 M33= -2.7e+24 dyne-cm

Eigenvalues:
sigma1= 6.2e+24 sigma2= -6.5e+24 sigma3= -6.2e+24

Eigenvectors: component i=N, 2=E, 3=V
eigenvector1=(.811, .857, .516) vecaz.= 89.3 vecdip= 31.8
eigenvector2=(-.978, -.899, .184) vecaz.= -174.2 vecdip= 18.6
eigenvector3=(.288, -.586, .837) vecaz.= -67.6 vecdip= 56.8

SYNTHETIC FAULT PLANE SOLUTION:

201

coefficient of internal friction= .888 ==> alpha= 25.7 degrees

slipvec1=(.152, .248, .956) vecaz= 58. vecdip= 73.
nodal plane2: strike= 148, dip= 17.
T1=(.859, .976, .289) vecaz= 93. vecdip= 12.
B=(-.978, -.899, .184) vecaz=-174. vecdip= 11.
P1=(.288, -.194, .968) vecaz=-44. vecdip= 74.

slipvec2=(.148, -.964, .227) vecaz= -82. vecdip= 13.
nodal plane1: strike= 8, dip= 77.
T2=(.879, .641, .763) vecaz= 83. vecdip= 58.
B=(-.978, -.899, .184) vecaz=-174. vecdip= 11.
P2=(.193, -.761, .619) vecaz=-76. vecdip= 38.

DETERMINATION OF THE STRAIN RATE:

The specified volume= 167.2x 38.3x 18.8km³

The strain rates for the last 78 years in the directions of the principal stress
extensional: 2.4e-89/yr = 4.6e-13/sec
intermediate: -2.5e-13/yr = -4.8e-17/sec
compressional: -2.4e-89/yr = -4.6e-13/sec

The horizontal and vertical strain rates:
Maximum horizontal: 1.2e-89/yr = 3.8e-17/sec Azimuth: N78E
Minimum horizontal: -1.6e-18/yr = -5.1e-18/sec Azimuth: N12W
Vertical: -1.8e-89/yr = -3.3e-17/sec

ENTER region boundary rotation

.88888888e+.88
razmax
.7u1332626e+.82

The maximum horizontal deformation rate = .8368 mm/yr

202

COMPUTATION OF A SYNTHETIC FAULT FLARE SOLUTION FROM A REGIONAL MOMENT TENSOR

EAST CACHE REGION

Cheche Valley 1962 #2

Fault plane solution number 1
 fault plane: strike=197. dip= 58. slip=-84. degrees
 auxiliary plane: strike= 5. dip= 35. slip=-181. degrees
 Moment Mo= 7.46E+28 dyn-cm
 slip vector=(.846, -.528, .848) vccaz= -85.8 vcdip= 58.8
 moment tensor 1: M11= 1.9e+23 M12= -1.7e+24 M13= 1.3e+24
 M21= -1.2e+24 M22= 6.1e+24 M23= -2.8e+24
 M31= 1.3e+24 M32= -2.8e+24 M33= -6.3e+24
 dyn-cm
 Eigenvectors: component 1=N, 2=E, 3=V
 eigenvector1=(.214, -.951, .222) vccaz.= -77.3 vcdip= 12.8
 eigenvector2=(.987, .238, .089) vccaz.= 71.8 vcdip= 5.1
 eigenvector3=(-.137, .195, .971) vccaz.= 125.8 vcdip= 76.2

Lugan composite 1974-78

Fault plane solution number 2
 fault plane: strike=196. dip= 38. slip= -85. degrees
 auxiliary plane: strike= 5. dip= 68. slip= -93. degrees
 Moment Mo= 2.6e+22 dyn-cm
 slip vector=(.875, -.863, .588) vccaz= -85.8 vcdip= 38.8
 moment tensor 2: M11= 2.9e+28 M12= -2.8e+21 M13= -3.2e+28
 M21= -2.8e+21 M22= 2.2e+22 M23= 1.3e+22
 M31= -3.2e+28 M32= 1.3e+22 M33= -2.2e+22
 dyn-cm

Eigenvectors: component 1=N, 2=E, 3=V
 eigenvector1=(-.187, .968, .268) vccaz.= 96.3 vcdip= 15.1
 eigenvector2=(.994, -.253, .965) vccaz.= 5.7 vcdip= 2.5
 eigenvector3=(-.816, -.253, .965) vccaz.= -93.5 vcdip= 74.7

Salt Lake City composite 1

Fault plane solution number 3
 fault plane: strike=28. dip= 78. slip= -85. degrees
 auxiliary plane: strike=28. dip= 28. slip=-184. degrees

Moment Mo= 2.6e+22 dyn-cm
 slip vector=(.117, -.321, .948) vccaz= -78.8 vcdip= 78.8
 moment tensor 3: M11= 2.5e+21 M12= 7.1e+21 M13= 1.2e+22
 M21= 7.1e+21 M22= 1.2e+22 M23= -1.6e+22
 M31= 1.2e+22 M32= -1.6e+22 M33= -1.7e+22
 dyn-cm

Eigenvectors: component 1=N, 2=E, 3=V
 eigenvector1=(.489, -.777, .428) vccaz.= -58.9 vcdip= 24.8
 eigenvector2=(.987, .238, .089) vccaz.= 71.8 vcdip= 5.1
 eigenvector3=(-.233, .312, .984) vccaz.= 133.3 vcdip= 64.7

698B thrust composite

Fault plane solution number 4
 fault plane: strike=338. dip= 85. slip= 98. degrees
 auxiliary plane: strike=158. dip= 4. slip= 89. degrees
 Moment Mo= 2.6e+22 dyn-cm
 slip vector=(.826, .885, .998) vccaz= 68.8 vcdip= 86.8
 moment tensor 4: M11= -6.3e+28 M12= -1.6e+21 M13= -9.6e+21
 M21= -1.6e+21 M22= -3.9e+21 M23= -2.4e+22
 M31= -9.6e+21 M32= -2.4e+22 M33= 4.5e+21
 dyn-cm

Eigenvectors: component 1=N, 2=E, 3=V
 eigenvector1=(-.291, -.595, .765) vccaz.= -112.8 vcdip= 58.8
 eigenvector2=(.912, -.418, .687) vccaz.= -24.2 vcdip= .4
 eigenvector3=(.287, .718, .643) vccaz.= 68.8 vcdip= 48.8

n1959

Fault plane solution number 5
 fault plane: strike=197. dip= 58. slip= -84. degrees
 auxiliary plane: strike= 5. dip= 35. slip=-181. degrees
 Moment Mo= 7.46E+28 dyn-cm
 slip vector=(.846, -.528, .848) vccaz= 187.8 vcdip= 12.8
 moment tensor 5: M11= 3.7e+21 M12= -2.4e+22 M13= 2.3e+22
 M21= -2.4e+22 M22= 1.2e+23 M23= -5.2e+22
 M31= 2.3e+22 M32= -5.2e+22 M33= -1.2e+23
 dyn-cm

Eigenvectors: component 1=N, 2=E, 3=V
 eigenvector1=(.211, -.954, .213) vccaz.= -77.5 vcdip= 12.3
 eigenvector2=(.969, .234, .085) vccaz.= 13.6 vcdip= 4.9

eigenvector3=(-.131, .188, .973) vecaz = 1' .9 vecdip = 76.8

n1965

Fault plane solution number 6
fault plane: strike= 6, dip= 33, slip= -99, degrees
auxiliary plane: strike= 187, dip= 58, slip= -84, degrees
Moment Mo= 1.4e+23 dyne-cm
slipvector=(.248, -.111, .538) vecaz= 187.8 vecdip= 32.8
moment tensor 6:
M11= 2.7e+21 M12= -2.4e+22 M13= 2.3e+22
M21= -2.4e+22 M22= 1.2e+23 M23= -5.2e+22
M31= 2.3e+22 M32= -5.2e+22 M33= -1.2e+23 dyne-cm

Eigenvectors: component 1=N, 2=E, 3=V
eigenvector1=(.211, .954, .213) vecaz = 77.5 vecdip = 12.3
eigenvector2=(.969, .238, .973) vecaz = 13.6 vecdip = 4.9
eigenvector3=(-.131, .188, .973) vecaz = 124.9 vecdip = 76.8

n1964

Fault plane solution number 7
fault plane: strike= 6, dip= 33, slip= -99, degrees
auxiliary plane: strike= 187, dip= 58, slip= -84, degrees
Moment Mo= 8.1e+22 dyne-cm
slipvector=(.248, -.111, .538) vecaz= 187.8 vecdip= 32.8
moment tensor 7:
M11= 2.2e+21 M12= -1.4e+22 M13= 1.4e+22
M21= -1.4e+22 M22= 7.1e+22 M23= -3.1e+22
M31= 1.4e+22 M32= -3.1e+22 M33= -7.3e+22 dyne-cm

Eigenvectors: component 1=N, 2=E, 3=V
eigenvector1=(.211, .954, .213) vecaz = 77.5 vecdip = 12.3
eigenvector2=(.969, .238, .973) vecaz = 13.6 vecdip = 4.9
eigenvector3=(-.131, .188, .973) vecaz = 124.9 vecdip = 76.8

n1966

Fault plane solution number 8
fault plane: strike= 6, dip= 33, slip= -99, degrees
auxiliary plane: strike= 197, dip= 58, slip= -84, degrees
Moment Mo= 2.3e+23 dyne-cm

slipvector=(.248, -.111, .538) vecaz= 187.8 vecdip= 32.8
moment tensor 8:
M11= 7.9e+21 M12= -5.1e+22 M13= 5.8e+22
M21= -5.1e+22 M22= 2.5e+23 M23= -2.8e+23
M31= 5.8e+22 M32= -2.8e+23 M33= -2.8e+23 dyne-cm

Eigenvectors: component 1=N, 2=E, 3=V
eigenvector1=(.211, .954, .213) vecaz = 77.5 vecdip = 12.3
eigenvector2=(.969, .238, .973) vecaz = 13.6 vecdip = 4.9
eigenvector3=(-.131, .188, .973) vecaz = 124.9 vecdip = 76.8

Regional moment tensor:
M11= 2.1e+23 M12= -1.4e+24 M13= 1.4e+24
M21= -1.4e+24 M22= 6.7e+24 M23= -3.1e+24
M31= 1.4e+24 M32= -3.1e+24 M33= -6.9e+24 dyne-cm

Eigenvalues:

sigma1= 7.7e+24 sigma2= -1.6e+21 sigma3= -7.7e+24

Eigenvectors: component 1=N, 2=E, 3=V
eigenvector1=(.214, .951, .221) vecaz = 77.3 vecdip = 12.8
eigenvector2=(.967, .238, .987) vecaz = 13.8 vecdip = 5.8
eigenvector3=(-.136, .196, .971) vecaz = 124.7 vecdip = 76.2

SYNTHETIC FAULT PLANE SOLUTION:

coefficient of internal friction= .888 ==> alpha= 25.7 degrees
slipvector=(.655, -.534, .843) vecaz= -84, vecdip= 58.
nodal plane1: strike= 6, dip= 32, slip= -84, degrees
T1=(.247, -.963, -.112) vecaz= -76, vecdip= -6.
S1=(.967, .238, .987) vecaz= 14, vecdip= 5.
P1=(-.857, -.138, .998) vecaz= -114, vecdip= 82.
nodal plane2: strike= 181, dip= 58, slip= 187, degrees 32.
T2=(.157, -.833, .538) vecaz= -79, vecdip= 32.
S2=(.967, .238, .987) vecaz= 14, vecdip= 5.
P2=(-.199, .588, .843) vecaz= 112, vecdip= 57.

DETERMINATION OF THE STRAIN RATE:

The specified volume= 191.8x 78.4x 18.8km3

Eigenvalues:
 sigma1= 2.3e+23 sigma2= 1.5e+15 sigma3= -2.3e+23

Eigenvectors: component 1=N, 2=E, 3=V
 eigenvector1=(-.426, .392, .815) vecaz.= 137.3 vecdip= 54.6
 eigenvector2=(.774, .625, .193) vecaz.= 39.8 vecdip= 5.9
 eigenvector3=(.469, -.675, .678) vecaz.= -55.2 vecdip= 34.7

SYNTHETIC FAULT PLANE SOLUTION:
 coefficient of internal friction= .088 ==> alpha= 25.7 degrees

slipvec1=(.831, -.159, .979) vecaz= -81. vecdip= 78.
 nodal plane2: strike= 9. dip= 12.
 T1=(-.557, .594, .581) vecaz= 133. vecdip= 36.
 B=(-.774, .625, .193) vecaz= 39. vecdip= 6.
 P1=(.382, -.587, .888) vecaz= -59. vecdip= 54.
 slipvec2=(.633, -.754, -.174) vecaz= -58. vecdip= -18.
 nodal plane1: strike= 48. dip= 188.
 T2=(-.246, .147, .958) vecaz= 149. vecdip= 73.
 B=(-.774, .625, .193) vecaz= 39. vecdip= 6.
 P2=(.584, -.766, .268) vecaz= -53. vecdip= 16.

DETERMINATION OF THE STRAIN RATE:

The specified volume= 227.9x 71.5x 18.8km³
 The strain rates for the last 63 years in the directions of the principal stress
 extensional : 3.5e-11/yr = 4.4e-15/sec
 intermediate : 2.2e-19/yr = 2.7e-23/sec
 compressional:-3.5e-11/yr = -4.4e-15/sec

The horizontal and vertical strain rates:
 Maximum horizontal: -1.3e-11/yr = -4.1e-19/sec Azimuth: N66W
 Minimum horizontal: 1.8e-12/yr = 3.2e-28/sec Azimuth: N24E
 Vertical : 1.2e-11/yr = 3.7e-19/sec

ENTER region boundary rotation
 .8H88888888e+88
 raxmax
 .655926598e+82

The maximum horizontal deformation rate = .8818 mm/yr

209

COMPUTATION OF A SYNTHETIC FAULT PLANE SOLUTION FROM A REGIONAL MOMENT TENSOR

SOUTHERN WASATCH FRONT

Central Utah 1963

Fault plane solution number 1
 fault plane: strike= 358. dip= 74. slip=-124. degrees
 auxiliary plane: strike= 238. dip= 48. slip=-29. degrees
 Moment Mo= 1.8e+23 dyne-cm
 slipvector=(.545, -.341, .766) vecaz= 148.8 vecdip= 58.8
 moment tensor 1:
 M11= -3.8e+22 M12= -7.7e+22 M13= 4.9e+22 dyne-cm
 M21= -7.7e+22 M22= 1.1e+23 M23= 1.2e+23
 M31= 4.9e+22 M32= 1.2e+23 M33= -7.8e+22

Eigenvectors: component 1=N, 2=E, 3=V
 eigenvector1=(-.243, .897, .369) vecaz.= 185.2 vecdip= 21.6
 eigenvector2=(.843, .888, .538) vecaz.= .5 vecdip= 32.5
 eigenvector3=(-.479, -.442, .758) vecaz.= -137.3 vecdip= 49.3

Salt Lake City composite 2

Fault plane solution number 2
 fault plane: strike= 171. dip= 68. slip=-79. degrees
 auxiliary plane: strike= 328. dip= 38. slip=-188. degrees
 Moment Mo= 1.3e+24 dyne-cm
 slipvector=(-.258, -.433, .866) vecaz= 248.8 vecdip= 68.8
 moment tensor 2:
 M11= 9.5e+22 M12= 3.8e+23 M13= 2.3e+22 dyne-cm
 M21= 3.8e+23 M22= 1.8e+24 M23= -6.6e+23
 M31= 2.3e+22 M32= -6.6e+23 M33= -1.1e+24

Eigenvectors: component 1=N, 2=E, 3=V
 eigenvector1=(-.283, -.927, .248) vecaz.= -187.8 vecdip= 14.3
 eigenvector2=(.955, -.248, .165) vecaz.= -14.6 vecdip= 9.5
 eigenvector3=(-.892, .283, .955) vecaz.= 188.8 vecdip= 72.7

71 C

Fault plane solution number 3
 fault plane: strike= 355. dip= 85. slip=-185. degrees
 auxiliary plane: strike= 235. dip= 28. slip=-38. degrees

210

Moment No= 1.4e+23 dyne-cm
 slipvector1(-.289,-.196, .948) vecaz= 145.8 vecdip= 78.8
 moment tensor 3
 M11= 5.9e+21 M12= -1.2e+22 M13= 1.4e+22
 M21= -3.2e+22 M22= 2.9e+22 M23= 1.3e+23
 M31= 1.4e+22 M32= 1.3e+23 M33= -2.3e+22
 dyne-cm

Eigenvectors: component 1=N, 2=E, 3=V
 eigenvector1(-.239,-.625, .742) vecaz.= 88.5 vecdip= 38.2
 eigenvector2(-.944,-.862, -.258) vecaz.= 21.7 vecdip= 14.9
 eigenvector3(-.239,-.625, .742) vecaz.= -118.6 vecdip= 47.9

n198B

Fault plane solution number 4
 fault plane: strike= 339, dip= 37, slip=-182, degrees
 auxiliary plane: strike= 175, dip= 54, slip= -88, degrees
 moment No= 4.7e+23 dyne-cm
 slipvector(-.871, .886, .588) vecaz= 85.8 vecdip= 36.8
 moment tensor 4

M11= 1.7e+23 M12= 1.6e+24 M13= 2.7e+23
 M21= 1.8e+24 M22= 4.2e+24 M23= -1.5e+24
 M31= 2.7e+23 M32= -1.5e+24 M33= -4.4e+24
 dyne-cm

Eigenvectors: component 1=N, 2=E, 3=V
 eigenvector1(-.213,-.966, .148) vecaz.= -182.5 vecdip= 8.5
 eigenvector2(-.973,-.196, .125) vecaz.= -11.4 vecdip= 7.2
 eigenvector3(-.892, .171, .981) vecaz.= 118.2 vecdip= 78.8

n191B

Fault plane solution number 5
 fault plane: strike= 339, dip= 37, slip=-182, degrees
 auxiliary plane: strike= 175, dip= 54, slip= -88, degrees
 Moment No= 4.7e+23 dyne-cm
 slipvector(-.871, .886, .588) vecaz= 85.8 vecdip= 36.8
 moment tensor 5

M11= 1.7e+23 M12= 1.6e+24 M13= 2.7e+23
 M21= 1.8e+24 M22= 4.2e+24 M23= -1.5e+24
 M31= 2.7e+23 M32= -1.5e+24 M33= -4.4e+24
 dyne-cm

Eigenvectors: component 1=N, 2=E, 3=V
 eigenvector1(-.213,-.966, .148) vecaz.= -182.5 vecdip= 8.5
 eigenvector2(-.973,-.196, .125) vecaz.= -11.4 vecdip= 7.2
 eigenvector3(-.892, .171, .981) vecaz.= 118.2 vecdip= 78.8

211

eigenvector3(-.892, .171, .981) vecaz.= 118.2 vecdip= 78.8

n192Ba

Fault plane solution number 6
 fault plane: strike= 339, dip= 37, slip=-182, degrees
 auxiliary plane: strike= 175, dip= 54, slip= -88, degrees
 Moment No= 1.4e+23 dyne-cm
 slipvector(-.871, .886, .588) vecaz= 85.8 vecdip= 36.8
 moment tensor 6
 M11= 5.9e+21 M12= 3.6e+22 M13= 7.9e+21
 M21= 3.6e+22 M22= 1.2e+23 M23= -4.2e+22
 M31= 7.9e+21 M32= -4.2e+22 M33= -1.3e+23
 dyne-cm

Eigenvectors: component 1=N, 2=E, 3=V
 eigenvector1(-.213,-.966, .148) vecaz.= -182.5 vecdip= 8.5
 eigenvector2(-.973,-.196, .125) vecaz.= -11.4 vecdip= 7.2
 eigenvector3(-.892, .171, .981) vecaz.= 118.2 vecdip= 78.8

n192Bb

Fault plane solution number 7
 fault plane: strike= 339, dip= 37, slip=-182, degrees
 auxiliary plane: strike= 175, dip= 54, slip= -88, degrees
 Moment No= 1.4e+23 dyne-cm
 slipvector(-.871, .886, .588) vecaz= 85.8 vecdip= 36.8
 moment tensor 7
 M11= 5.9e+21 M12= 3.6e+22 M13= 7.9e+21
 M21= 3.6e+22 M22= 1.2e+23 M23= -4.2e+22
 M31= 7.9e+21 M32= -4.2e+22 M33= -1.3e+23
 dyne-cm

Eigenvectors: component 1=N, 2=E, 3=V
 eigenvector1(-.213,-.966, .148) vecaz.= -182.5 vecdip= 8.5
 eigenvector2(-.973,-.196, .125) vecaz.= -11.4 vecdip= 7.2
 eigenvector3(-.892, .171, .981) vecaz.= 118.2 vecdip= 78.8

n192Bc

Fault plane solution number 8
 fault plane: strike= 339, dip= 37, slip=-182, degrees
 auxiliary plane: strike= 175, dip= 54, slip= -88, degrees
 Moment No= 1.4e+23 dyne-cm

slipvector=(.871, .886, .588) vecaz= 85.8 vecdip= 36.8
 moment tensor 8:
 M11= 5.8e+21 M12= 3.8e+22 M13= 7.9e+21
 M21= 3.8e+22 M22= 1.2e+23 M23= -4.2e+22
 M31= 7.9e+21 M32= -4.2e+22 M33= -1.3e+23
 dyne-cm

Eigenvectors: component 1=N, 2=E, 3=V
 eigenvector1=(-.213, -.965, .148) vecaz= -182.5 vecdip= 8.5
 eigenvector2=(.973, -.196, .125) vecaz= -11.4 vecdip= 7.2
 eigenvector3=(-.892, .171, .981) vecaz= 118.2 vecdip= 78.8

n1938

Fault plane solution number 9
 fault plane: strike= 175, dip= 37, slip=-182, degrees
 auxiliary plane: strike= 175, dip= 54, slip= -88, degrees
 Moment Mo= 1.4e+23 dyne-cm
 slipvector=(.871, .886, .588) vecaz= 85.8 vecdip= 36.8

moment tensor 9:
 M11= 5.8e+21 M12= 3.8e+22 M13= 7.9e+21
 M21= 3.8e+22 M22= 1.2e+23 M23= -4.2e+22
 M31= 7.9e+21 M32= -4.2e+22 M33= -1.3e+23
 dyne-cm

Eigenvectors: component 1=N, 2=E, 3=V
 eigenvector1=(-.213, -.965, .148) vecaz= -182.5 vecdip= 8.5
 eigenvector2=(.973, -.196, .125) vecaz= -11.4 vecdip= 7.2
 eigenvector3=(-.892, .171, .981) vecaz= 118.2 vecdip= 78.8

n1943a

Fault plane solution number 18
 fault plane: strike= 339, dip= 37, slip=-182, degrees
 auxiliary plane: strike= 175, dip= 54, slip= -88, degrees
 Moment Mo= 7.9e+23 dyne-cm
 slipvector=(.871, .886, .588) vecaz= 85.8 vecdip= 36.8

moment tensor 18:
 M11= 2.9e+22 M12= 1.8e+23 M13= 4.6e+22
 M21= 1.8e+23 M22= 7.2e+23 M23= -2.5e+23
 M31= 4.6e+22 M32= -2.5e+23 M33= -7.5e+23
 dyne-cm

Eigenvectors: component 1=N, 2=E, 3=V
 eigenvector1=(.973, -.196, .125) vecaz= -182.5 vecdip= 8.5
 eigenvector2=(-.892, .171, .981) vecaz= -11.4 vecdip= 7.2
 eigenvector3=(.871, .886, .588) vecaz= 118.2 vecdip= 78.8

213

n1943b

Fault plane solution number 11
 fault plane: strike= 339, dip= 37, slip=-182, degrees
 auxiliary plane: strike= 175, dip= 54, slip= -88, degrees
 Moment Mo= 1.4e+23 dyne-cm
 slipvector=(.871, .886, .588) vecaz= 85.8 vecdip= 36.8

moment tensor 11:
 M11= 5.8e+21 M12= 3.8e+22 M13= 7.9e+21
 M21= 3.8e+22 M22= 1.2e+23 M23= -4.2e+22
 M31= 7.9e+21 M32= -4.2e+22 M33= -1.3e+23
 dyne-cm

Eigenvectors: component 1=N, 2=E, 3=V
 eigenvector1=(-.213, -.965, .148) vecaz= -182.5 vecdip= 8.5
 eigenvector2=(.973, -.196, .125) vecaz= -11.4 vecdip= 7.2
 eigenvector3=(-.892, .171, .981) vecaz= 118.2 vecdip= 78.8

n1952

Fault plane solution number 12
 fault plane: strike= 339, dip= 37, slip=-182, degrees
 auxiliary plane: strike= 175, dip= 54, slip= -88, degrees
 Moment Mo= 1.4e+23 dyne-cm
 slipvector=(.871, .886, .588) vecaz= 85.8 vecdip= 36.8

moment tensor 12:
 M11= 5.8e+21 M12= 3.8e+22 M13= 7.9e+21
 M21= 3.8e+22 M22= 1.2e+23 M23= -4.2e+22
 M31= 7.9e+21 M32= -4.2e+22 M33= -1.3e+23
 dyne-cm

Eigenvectors: component 1=N, 2=E, 3=V
 eigenvector1=(-.213, -.965, .148) vecaz= -182.5 vecdip= 8.5
 eigenvector2=(.973, -.196, .125) vecaz= -11.4 vecdip= 7.2
 eigenvector3=(-.892, .171, .981) vecaz= 118.2 vecdip= 78.8

n1955

Fault plane solution number 13
 fault plane: strike= 339, dip= 37, slip=-182, degrees
 auxiliary plane: strike= 175, dip= 54, slip= -88, degrees
 Moment Mo= 1.4e+23 dyne-cm
 slipvector=(.871, .886, .588) vecaz= 85.8 vecdip= 36.8

214

moment tensor13:
M11= 5.8e+21 M12= 3.8e+22 M13= 7.9e+21
M21= 1.5e+23 M22= -4.2e+22 M23= -4.2e+22
M31= 7.9e+21 M32= -4.2e+22 M33= -1.3e+23
dyne-cm

Eigenvalues: component 1=H, 2=E, 3=V
eigenvector1=(-.213, -.966, .148) vecaz = -182.5 vecdip= 8.5
eigenvector2=(.973, -.196, .125) vecaz = -11.4 vecdip= 7.2
eigenvector3=(-.892, -.171, .981) vecaz = 118.2 vecdip= 78.8

n.958a

Fault plane solution number14
fault plane: strike=339, dip= 37, slip=-182, degrees
auxiliary plane: strike=175, dip= 54, slip=-88, degrees
Moment Mo= 1.4e+23 dyne-cm
slipvector=(.871, .886, .588) vecaz = 85.8 vecdip= 36.8
moment tensor14:
M11= 5.8e+21 M12= 3.8e+22 M13= 7.9e+21
M21= 3.8e+22 M22= 1.2e+23 M23= -4.2e+22
M31= 7.9e+21 M32= -4.2e+22 M33= -1.3e+23
dyne-cm

Eigenvalues: component 1=H, 2=E, 3=V
eigenvector1=(-.213, -.966, .148) vecaz = -182.5 vecdip= 8.5
eigenvector2=(.973, -.196, .125) vecaz = -11.4 vecdip= 7.2
eigenvector3=(-.892, -.171, .981) vecaz = 118.2 vecdip= 78.8

n1958b

Fault plane solution number15
fault plane: strike=339, dip= 37, slip=-182, degrees
auxiliary plane: strike=175, dip= 54, slip=-88, degrees
Moment Mo= 1.4e+23 dyne-cm
slipvector=(.871, .886, .588) vecaz = 85.8 vecdip= 36.8
moment tensor15:
M11= 5.8e+21 M12= 3.8e+22 M13= 7.9e+21
M21= 3.8e+22 M22= 1.2e+23 M23= -4.2e+22
M31= 7.9e+21 M32= -4.2e+22 M33= -1.3e+23
dyne-cm

Eigenvalues: component 1=H, 2=E, 3=V
eigenvector1=(-.213, -.966, .148) vecaz = -182.5 vecdip= 8.5
eigenvector2=(.973, -.196, .125) vecaz = -11.4 vecdip= 7.2
eigenvector3=(-.892, -.171, .981) vecaz = 118.2 vecdip= 78.8

Regional moment tensor:
M11= 4.8e+23 M12= 2.8e+24 M13= 7.5e+23
M21= 2.8e+24 M22= 1.1e+25 M23= -4.8e+24
M31= 7.5e+23 M32= -4.8e+24 M33= -1.2e+25
dyne-cm

Eigenvalues:
sigma1= 1.3e+25 sigma2= 1.9e+22 sigma3= -1.3e+25

Eigenvalues: component 1=H, 2=E, 3=V
eigenvector1=(-.213, -.966, .148) vecaz = -182.4 vecdip= 8.6
eigenvector2=(.973, -.196, .126) vecaz = -11.3 vecdip= 7.2
eigenvector3=(-.892, -.171, .981) vecaz = 118.3 vecdip= 78.8

SYNTHETIC FAULT PLANE SOLUTION:

coefficient of internal friction= .888 ==> alpha= 25.7 degrees

slipvec1=(-.215, -.562, .799) vecaz=-111. vecdip= 53.
nodal plane2: strike=-21, dip= 37, slip= 88, vecdip= -11.
P1=(.179, -.988, -.194) vecaz=-11 vecdip= 7.
P1=(-.157, -.158, .975) vecaz=-135, vecdip= 77.
nodal plane1: strike=174, dip= 54, slip= 88, vecdip= 36.
P2=(.971, -.195, .125) vecaz=-11 vecdip= 7.
P2=(-.817, -.481, .876) vecaz= 92, vecdip= 61.

DETERMINATION OF THE STRAIN RATE:

The specified volume= 185.9x 38.3x 18.8m3

The strain rates for the last 78 years in the directions of the principal stress
extensional : 4.4e-89/yr = 8.4e-13/sec
intermediate : 6.4e-12/yr = 1.2e-15/sec
compressional:-4.4e-89/yr = -8.4e-13/sec

The horizontal and vertical strain rates
Maximum horizontal: 4.2e-89/yr = 1.2e-16/sec Azimuth: N76E
Minimum horizontal: -6.6e-11/yr = -2.1e-18/sec
Vertical : -4.1e-89/yr = -1.3e-16/sec
ENTER region boundary rotation

.00000000e+00
raimax
.764978627e+02

The maximum horizontal deformation rate = .1321 mm/yr

217

COMPUTATION OF A SYNTHETIC FAULT PLANE SOLUTION FROM A REGIONAL MOMENT TENSOR

PROVO REGION

Heber City composite 1972

Fault plane solution number 1

fault plane: strike= 323. dip= 64. slip= -71. degrees

auxiliary plane: strike= 118. dip= 38. slip= -128. degrees

Moment Mo= 1.4e+23 dyne-cm

slipvector=(.478, .171, .866) vecaz= 28.8 vecdip= 68.8

moment tensor 1:

M11=	6.9e+22	M12=	5.8e+22	M13=	3.5e+22	dyne-cm
M21=	5.8e+22	M22=	3.3e+22	M23=	7.4e+22	
M31=	3.5e+22	M32=	7.4e+22	M33=	-1.8e+23	

Eigenvectors: component 1=N, 2=E, 3=V

eigenvector1=(.717, .628, .381) vecaz.= 41.2 vecdip= 17.5

eigenvector2=(-.695, .675, .248) vecaz.= 135.8 vecdip= 14.3

eigenvector3=(-.848, -.387, .921) vecaz.= -97.8 vecdip= 67.1

Heber City thrust composite 1a #68

Fault plane solution number 2

fault plane: strike= 184. dip= 88. slip= 92. degrees

auxiliary plane: strike= 353. dip= 18. slip= 79. degrees

Moment Mo= 1.0e+22 dyne-cm

slipvector=(-.821, -.172, .985) vecaz= 263.8 vecdip= 88.8

moment tensor 2:

M11=	5.6e+19	M12=	-1.8e+20	M13=	-1.3e+21	dyne-cm
M21=	-1.8e+20	M22=	-6.2e+21	M23=	1.7e+22	
M31=	-1.3e+21	M32=	1.7e+22	M33=	6.2e+21	

Eigenvectors: component 1=N, 2=E, 3=V

eigenvector1=(-.855, .571, .819) vecaz.= 96.5 vecdip= 55.8

eigenvector2=(.997, .864, .834) vecaz.= 3.7 vecdip= 2.8

eigenvector3=(.833, -.819, .573) vecaz.= -87.7 vecdip= 35.8

Heber City thrust composite 1b #69

Fault plane solution number 3

fault plane: strike= 184. dip= 88. slip= 92. degrees

auxiliary plane: strike= 353. dip= 18. slip= 79. degrees

218

Moment No 1.8e+22 dyne-cm
 slipvector1=(-.821, -.172, .985) vecaz= 263.6 vecdip= 88.8
 moment tensor 3: M11= 5.6e+19 M12= -1.8e+20 M13= -1.3e+21
 M21= -1.8e+20 M22= -6.2e+21 M23= 1.7e+22
 M31= -1.3e+21 M32= 1.7e+22 M33= 6.2e+21 dyne-cm

Eigenvectors: component 1=N, 2=E, 3=V
 eigenvector1=(-.865, .571, .819) vecaz.= 96.5 vecdip= 85.8
 eigenvector2=(-.997, .864, .834) vecaz.= 3.7 vecdip= 2.8
 eigenvector3=(-.833, -.819, .573) vecaz.= -87.7 vecdip= 35.8

Heber City reversed composite 2

Fault plane solution number 4
 fault plane: strike= 297, dip= 98, slip= 98, degrees
 auxiliary plane: strike= 297, dip= 18, slip= 98, degrees
 Moment No 8.8e+22 dyne-cm
 slipvector1=(-.879, -.155, .985) vecaz= -63.8 vecdip= 88.8
 moment tensor 4: M11= -1.3e+21 M12= 2.8e+21 M13= -7.7e+21
 M21= -7.7e+21 M22= -4.3e+22 M23= 6.2e+21
 M31= 2.8e+21 M32= 6.2e+21 M33= 6.2e+21 dyne-cm

Eigenvectors: component 1=N, 2=E, 3=V
 eigenvector1=(-.268, .511, .819) vecaz.= 117.8 vecdip= 85.8
 eigenvector2=(-.977, .952, .296) vecaz.= 85.4 vecdip= 17.2
 eigenvector3=(-.372, -.738, .574) vecaz.= -83.8 vecdip= 38.8

n1915

Fault plane solution number 5
 fault plane: strike= 99, dip= 29, slip= 37, degrees
 auxiliary plane: strike= 335, dip= 73, slip= 114, degrees
 Moment No 7.9e+23 dyne-cm
 slipvector1=(-.484, -.867, .292) vecaz= 245.8 vecdip= 17.8
 moment tensor 5: M11= -3.1e+23 M12= -3.5e+23 M13= -1.7e+23
 M21= -3.5e+23 M22= -9.3e+23 M23= -5.8e+23
 M31= -1.7e+23 M32= -5.8e+23 M33= 4.1e+23 dyne-cm

Eigenvectors: component 1=N, 2=E, 3=V
 eigenvector1=(-.775, .499, .387) vecaz.= -85.8 vecdip= 55.6
 eigenvector2=(-.775, .499, .387) vecaz.= 147.3 vecdip= 22.8

eigenvector3=(-.629, .659, .412) vecaz.= 46.3 vecdip= 24.3

n1916

Fault plane solution number 6
 fault plane: strike= 98, dip= 29, slip= 37, degrees
 auxiliary plane: strike= 335, dip= 73, slip= 114, degrees
 Moment No 1.4e+23 dyne-cm
 slipvector1=(-.484, -.867, .292) vecaz= 245.8 vecdip= 17.8
 moment tensor 6: M11= -5.3e+22 M12= -6.8e+22 M13= -3.8e+22
 M21= -6.8e+22 M22= -1.6e+23 M23= -9.6e+22
 M31= -3.8e+22 M32= -9.6e+22 M33= 6.8e+22 dyne-cm

Eigenvectors: component 1=N, 2=E, 3=V
 eigenvector1=(-.849, .563, .825) vecaz.= -85.8 vecdip= 85.6
 eigenvector2=(-.775, .499, .387) vecaz.= 147.3 vecdip= 22.8
 eigenvector3=(-.629, .659, .412) vecaz.= 46.3 vecdip= 24.3

n1958

Fault plane solution number 7
 fault plane: strike= 98, dip= 29, slip= 37, degrees
 auxiliary plane: strike= 335, dip= 73, slip= 114, degrees
 Moment No 1.2e+23 dyne-cm
 slipvector1=(-.484, -.867, .292) vecaz= 245.8 vecdip= 17.8
 moment tensor 7: M11= -5.3e+22 M12= -6.8e+22 M13= -3.8e+22
 M21= -6.8e+22 M22= -1.6e+23 M23= -9.6e+22
 M31= -3.8e+22 M32= -9.6e+22 M33= 6.8e+22 dyne-cm

Eigenvectors: component 1=N, 2=E, 3=V
 eigenvector1=(-.849, .563, .825) vecaz.= -85.8 vecdip= 85.6
 eigenvector2=(-.775, .499, .387) vecaz.= 147.3 vecdip= 22.8
 eigenvector3=(-.629, .659, .412) vecaz.= 46.3 vecdip= 24.3

n1951

Fault plane solution number 8
 fault plane: strike= 98, dip= 29, slip= 37, degrees
 auxiliary plane: strike= 335, dip= 73, slip= 114, degrees
 Moment No 1.4e+23 dyne-cm

```

slipvector=(-.484,-.867,.292)  vccaz= 245.8  vccdlp= 17.8
moment tensor:
  M11= -5.9e+22  M12= -6.8e+22  M13= -3.8e+22
  M21= -5.9e+22  M22= -9.3e+22  M23= -9.9e+22
  M31= -3.8e+22  M32= -9.3e+22  M33= 6.9e+22
  dyne-cm

```

```

Eigenvectors: component 1=N, 2=E, 3=V
eigenvector1=(.75,-.563,.825)  vccaz=-95.8  vccdlp= 55.6
eigenvector2=(-.775,.499,.387)  vccaz= 147.3  vccdlp= 22.8
eigenvector3=(.629,.659,.412)  vccaz= 46.3  vccdlp= 24.3

```

n1953

```

Fault plane solution number 9
fault plane: strike= 98, dip= 29, slip= 37, degrees
auxiliary plane: strike= 335, dip= 73, slip= 114, degrees
Moment Mo= 1.4e+23 dyne-cm
slipvector=(-.484,-.867,.292)  vccaz= 245.8  vccdlp= 17.8
moment tensor:
  M11= -5.3e+22  M12= -6.8e+22  M13= -3.8e+22
  M21= -6.8e+22  M22= -1.6e+22  M23= -9.9e+22
  M31= -3.8e+22  M32= -9.9e+22  M33= 6.9e+22
  dyne-cm

```

```

Eigenvectors: component 1=N, 2=E, 3=V
eigenvector1=(.849,-.563,.825)  vccaz=-85.8  vccdlp= 55.6
eigenvector2=(-.775,.499,.387)  vccaz= 147.3  vccdlp= 22.8
eigenvector3=(.629,.659,.412)  vccaz= 46.3  vccdlp= 24.3

```

n1958

```

Fault plane solution number 18
fault plane: strike= 98, dip= 29, slip= 37, degrees
auxiliary plane: strike= 335, dip= 73, slip= 114, degrees
Moment Mo= 7.9e+23 dyne-cm
slipvector=(-.484,-.867,.292)  vccaz= 245.8  vccdlp= 17.8
moment tensor:
  M11= -3.1e+23  M12= -3.5e+23  M13= -1.7e+23
  M21= -3.5e+23  M22= -9.3e+22  M23= -9.8e+22
  M31= -1.7e+23  M32= -9.8e+22  M33= 4.1e+22
  dyne-cm

```

```

Eigenvectors: component 1=N, 2=E, 3=V
eigenvector1=(.849,-.563,.825)  vccaz=-85.8  vccdlp= 55.6
eigenvector2=(-.775,.499,.387)  vccaz= 147.3  vccdlp= 22.8
eigenvector3=(.629,.659,.412)  vccaz= 46.3  vccdlp= 24.3

```

321

n1963

```

Fault plane solution number 11
fault plane: strike= 98, dip= 29, slip= 37, degrees
auxiliary plane: strike= 335, dip= 73, slip= 114, degrees
Moment Mo= 6.3e+22 dyne-cm
slipvector=(-.484,-.867,.292)  vccaz= 245.8  vccdlp= 17.8
moment tensor:
  M11= -2.5e+22  M12= -2.8e+22  M13= -1.4e+22
  M21= -2.8e+22  M22= -7.4e+21  M23= -4.6e+22
  M31= -1.4e+22  M32= -4.6e+22  M33= 3.2e+22
  dyne-cm

```

```

Eigenvectors: component 1=N, 2=E, 3=V
eigenvector1=(.75,-.563,.825)  vccaz=-95.8  vccdlp= 55.6
eigenvector2=(-.775,.499,.387)  vccaz= 147.3  vccdlp= 22.8
eigenvector3=(.629,.659,.412)  vccaz= 46.3  vccdlp= 24.3

```

```

Regional moment tensor:
  M11= -7.9e+23  M12= -9.1e+23  M13= -4.5e+23
  M21= -9.1e+23  M22= -2.4e+23  M23= -1.5e+24
  M31= -4.5e+23  M32= -1.5e+24  M33= 1.8e+24
  dyne-cm

```

```

Eigenvectors:
sigma1= 2.6e+24  sigma2= 1.8e+22  sigma3= -2.6e+24

```

```

Eigenvectors: component 1=N, 2=E, 3=V
eigenvector1=(.75,-.563,.825)  vccaz=-95.1  vccdlp= 55.6
eigenvector2=(-.775,.499,.387)  vccaz= 147.2  vccdlp= 22.7
eigenvector3=(.629,.659,.412)  vccaz= 46.3  vccdlp= 24.3

```

SYNTHETIC FAULT PLANE SOLUTION:

```

coefficient of internal friction= .888  => alpha= 25.7 degrees

```

```

slipvec1=(.488,.868,.875)  vccaz= 8.vecdlp= 61.
nodal plane2: strike= 98, dip= 29, slip= 102, vccdlp= 48.
Pl=(.193,-.749,.642)  vccaz= 187.
Pl=(.618,-.435,.682)  vccaz= 35.  vccdlp= 41.

```

```

slipvec2=(.411,.863,-.292)  vccaz= 65.vecdlp= -17.

```

nodal plane: strike= 155. dip= 187.
 P1= .313 .913) vcaz= -51. vcdip= 66.
 P2= -.775 -.386) vcaz= 187. vcdip= 23.
 P3= .578 .088 .116) vcaz= 54. vcdip= 7.
 DETERMINATION OF THE STRAIN RATE:

 The specified volume= 183.8x 71.5x 18.0km³
 The strain rates for the last 83 years in the directions of the principal stress
 extensional: 1) 5.8e-12/yr = 8.3e-14/sec
 2) 7.3e-12/yr = 7.3e-16/sec
 compressional: 1) -6.6e-18/yr = -8.3e-14/sec
 2) -8.3e-14/sec
 The horizontal and vertical strain rates:
 Maximum horizontal: 4.6e-18/yr = 4.6e-18/sec Azimuth: N37E
 Minimum horizontal: .4e-18/yr = 1.1e-17/sec Azimuth: N53W
 Vertical: 1.1e-17/sec
 ENTER region boundary r...ation
 #####
 r1zmax
 .365128483e+82
 The maximum horizontal deformation rate = .#572 mm/yr

COMPUTATION OF A SYNTHETIC FAULT PLANE SOLUTION FROM A REGIONAL MOMENT TENSOR

CENTRAL UTAH REGION

6 S
 Fault plane solution number 1
 fault plane: strike= 178. dip= 86. slip= 185. degrees
 auxiliary plane: strike= 275. dip= 15. slip= 16. degrees
 Moment Mo= 1.3e+24 dyne-cm
 slipvector=(-.259, -.823, .986) vcaz= 185.# vcdip= 75.#
 moment tensor 1
 M11= -1.2e+23 M12= -3.5e+23 M13= 2.8e+23
 M21= -3.5e+23 M22= -5.6e+22 M23= 1.2e+24
 M31= 2.8e+23 M32= 1.2e+24 M33= 1.8e+23
 Eigenvectors: component 1=N, 2=E, 3=V
 eigenvector1=(.948, -.186, .258) vcaz= 85.5 vcdip= 45.9
 eigenvector2=(.198, -.948, -.258) vcaz= -11.1 vcdip= 15.9
 eigenvector3=(-.311, -.718, .632) vcaz= -113.7 vcdip= 39.2

48 C

Fault plane solution number 2
 fault plane: strike= 283. dip= 88. slip= -88. degrees
 auxiliary plane: strike= 348. dip= 14. slip= -132. degrees
 Moment Mo= 1.8e+22 dyne-cm
 slipvector=(-.893, -.227, .978) vcaz= 258.# vcdip= 76.#
 moment tensor 2
 M11= -2.1e+21 M12= -6.9e+19 M13= 1.1e+22
 M21= -6.9e+19 M22= 1.2e+22 M23= -2.5e+22
 M31= 1.1e+22 M32= -2.5e+22 M33= -9.9e+21
 Eigenvectors: component 1=N, 2=E, 3=V
 eigenvector1=(.266, -.888, .563) vcaz= -75.5 vcdip= 34.3
 eigenvector2=(.918, .357, .171) vcaz= 21.2 vcdip= 9.8
 eigenvector3=(-.338, .482, .889) vcaz= 125.# vcdip= 54.#

n19#1

Fault plane solution number 3
 fault plane: strike= 349. dip= 16. slip= 166. degrees
 auxiliary plane: strike= 349. dip= 94. slip= 75. degrees

Moment No 1. 2e+25 dyne-cm
 slipvector=(-.198, -.979, -.878) vecaz= 259.8 vecdip= -4.8
 moment tensor 3:
 M11= -2.8e+25 M12= 3.2e+25 M13= 3.2e+25
 M21= 3.2e+25 M22= 3.2e+25 M23= -1.2e+25
 M31= 3.2e+25 M32= -1.2e+25 M33= 1.6e+25 dyne-cm

Eigenvectors: component 1=N, 2=E, 3=V
 eigenvector1=(.885, -.687, .727) vecaz.= -89.5 vecdip= 46.6
 eigenvector2=(.919, .298, .267) vecaz.= 17.5 vecdip= 15.5
 eigenvector3=(-.395, .666, .633) vecaz.= 128.6 vecdip= 39.2

n192

Fault plane solution number 4
 fault plane: strike=369, dip= 16, slip= 166, degrees
 auxiliary plane: strike=349, dip= 94, slip= 75, degrees
 Moment No 1. 4e+23 dyne-cm
 slipvector=(-.198, -.979, -.878) vecaz= 259.8 vecdip= -4.8
 moment tensor 4:
 M11= -2.1e+22 M12= 3.5e+22 M13= 3.4e+22
 M21= 3.4e+22 M22= 3.7e+21 M23= -1.2e+23
 M31= 3.4e+22 M32= -1.2e+23 M33= 1.7e+22 dyne-cm

Eigenvectors: component 1=N, 2=E, 3=V
 eigenvector1=(.919, -.297, .727) vecaz.= -89.5 vecdip= 46.6
 eigenvector2=(.919, .298, .267) vecaz.= 17.5 vecdip= 15.5
 eigenvector3=(-.395, .666, .633) vecaz.= 128.6 vecdip= 39.2

n191a

Fault plane solution number 5
 fault plane: strike=273, dip= 16, slip= 166, degrees
 auxiliary plane: strike=349, dip= 94, slip= 75, degrees
 Moment No 7. 9e+23 dyne-cm
 slipvector=(-.198, -.979, -.878) vecaz= 259.8 vecdip= -4.8
 moment tensor 5:
 M11= -1.2e+23 M12= 2.1e+23 M13= 2.6e+23
 M21= 2.1e+23 M22= 2.2e+22 M23= -7.3e+23
 M31= 2.6e+23 M32= -7.3e+23 M33= 1.8e+23 dyne-cm

Eigenvectors: component 1=N, 2=E, 3=V
 eigenvector1=(.885, -.687, .727) vecaz.= -89.5 vecdip= 46.6
 eigenvector2=(.919, .298, .267) vecaz.= 17.5 vecdip= 15.5

eigenvector3=(-.395, .666, .633) vecaz.= 128.6 vecdip= 39.2

n191b

Fault plane solution number 6
 fault plane: strike=273, dip= 16, slip= 166, degrees
 auxiliary plane: strike=349, dip= 94, slip= 75, degrees
 Moment No 7. 9e+23 dyne-cm
 slipvector=(-.198, -.979, -.878) vecaz= 259.8 vecdip= -4.8
 moment tensor 6:
 M11= -1.2e+23 M12= 2.1e+23 M13= 2.6e+23
 M21= 2.1e+23 M22= 2.2e+22 M23= -7.3e+23
 M31= 2.6e+23 M32= -7.3e+23 M33= 1.8e+23 dyne-cm

Eigenvectors: component 1=N, 2=E, 3=V
 eigenvector1=(.885, -.687, .727) vecaz.= -89.5 vecdip= 46.6
 eigenvector2=(.919, .298, .267) vecaz.= 17.5 vecdip= 15.5
 eigenvector3=(-.395, .666, .633) vecaz.= 128.6 vecdip= 39.2

n1921a

Fault plane solution number 7
 fault plane: strike=273, dip= 16, slip= 166, degrees
 auxiliary plane: strike=349, dip= 94, slip= 75, degrees
 Moment No 1. 2e+23 dyne-cm
 slipvector=(-.198, -.979, -.878) vecaz= 259.8 vecdip= -4.8
 moment tensor 7:
 M11= -2.1e+22 M12= 3.5e+22 M13= 3.4e+22
 M21= 3.4e+22 M22= 3.7e+21 M23= -1.2e+23
 M31= 3.4e+22 M32= -1.2e+23 M33= 1.7e+22 dyne-cm

Eigenvectors: component 1=N, 2=E, 3=V
 eigenvector1=(.885, -.687, .727) vecaz.= -89.5 vecdip= 46.6
 eigenvector2=(.919, .298, .267) vecaz.= 17.5 vecdip= 15.5
 eigenvector3=(-.395, .666, .633) vecaz.= 128.6 vecdip= 39.2

n1921b

Fault plane solution number 8
 fault plane: strike=273, dip= 16, slip= 166, degrees
 auxiliary plane: strike=349, dip= 94, slip= 75, degrees
 Moment No 1. 4e+23 dyne-cm

```

slipvector1(-.198,-.979,-.878)  vecaz= 259.8  vecdip= -4.8
moment tensor 8
  M11= -2.1e+22  M12= 3.5e+22  M13= 3.4e+22
  M21= 3.5e+22  M22= 3.7e+21  M23= -1.2e+23  dyne-cm
  M31= 3.4e+22  M32= -1.2e+23  M33= 1.7e+22
Eigenvectors: component 1=M, 2=E, 3=V
eigenvector1(.885,-.687,.727)  vecaz.= -89.5  vecdip= 45.6
eigenvector2(.919,.298,.267)  vecaz.= 17.5  vecdip= 15.5
eigenvector3(-.395,.666,.633)  vecaz.= 128.6  vecdip= 39.2

```

n1921c

```

Fault plane solution number 9
fault plane: strike= 273, dip= 16, slip= 166, degrees
auxiliary plane: strike= 349, dip= 94, slip= 75, degrees
Moment No 2.1e+25 dyne-cm
slipvector(-.198,-.979,-.878)  vecaz= 259.8  vecdip= -4.8
moment tensor 8:
  M11= -3.3e+24  M12= 5.5e+24  M13= 5.4e+24
  M21= 5.5e+24  M22= 5.9e+23  M23= -2.8e+25
  M31= 5.4e+24  M32= -2.8e+25  M33= 2.7e+24  dyne-cm
Eigenvectors: component 1=M, 2=E, 3=V
eigenvector1(.885,-.687,.727)  vecaz.= -89.5  vecdip= 45.6
eigenvector2(.919,.298,.267)  vecaz.= 17.5  vecdip= 15.5
eigenvector3(-.395,.666,.633)  vecaz.= 128.6  vecdip= 39.2

```

n1921d

```

Fault plane solution number 16
fault plane: strike= 273, dip= 16, slip= 166, degrees
auxiliary plane: strike= 349, dip= 94, slip= 75, degrees
Moment No 4.7e+24 dyne-cm
slipvector(-.198,-.979,-.878)  vecaz= 259.8  vecdip= -4.8
moment tensor 11:
  M11= -7.3e+23  M12= 1.3e+24  M13= 1.2e+24
  M21= 1.2e+24  M22= 1.3e+23  M23= -4.3e+24  dyne-cm
  M31= 1.2e+24  M32= -4.3e+24  M33= 6.8e+23
Eigenvectors: component 1=M, 2=E, 3=V
eigenvector1(.885,-.687,.727)  vecaz.= -89.5  vecdip= 45.6
eigenvector2(.919,.298,.267)  vecaz.= 17.5  vecdip= 15.5
eigenvector3(-.395,.666,.633)  vecaz.= 128.6  vecdip= 39.2

```

n1921e

```

Fault plane solution number 11
fault plane: strike= 273, dip= 16, slip= 166, degrees
auxiliary plane: strike= 349, dip= 94, slip= 75, degrees
Moment No 2.1e+25 dyne-cm
slipvector(-.198,-.979,-.878)  vecaz= 259.8  vecdip= -4.8
moment tensor 11:
  M11= -3.3e+24  M12= 5.5e+24  M13= 5.4e+24
  M21= 5.5e+24  M22= 5.9e+23  M23= -2.8e+25
  M31= 5.4e+24  M32= -2.8e+25  M33= 2.7e+24  dyne-cm
Eigenvectors: component 1=M, 2=E, 3=V
eigenvector1(.885,-.687,.727)  vecaz.= -89.5  vecdip= 45.6
eigenvector2(.919,.298,.267)  vecaz.= 17.5  vecdip= 15.5
eigenvector3(-.395,.666,.633)  vecaz.= 128.6  vecdip= 39.2

```

n1921f

```

Fault plane solution number 12
fault plane: strike= 273, dip= 16, slip= 166, degrees
auxiliary plane: strike= 349, dip= 94, slip= 75, degrees
Moment No 1.4e+23 dyne-cm
slipvector(-.198,-.979,-.878)  vecaz= 259.8  vecdip= -4.8
moment tensor 12:
  M11= -2.1e+22  M12= 3.5e+22  M13= 3.4e+22
  M21= 3.5e+22  M22= 3.7e+21  M23= -1.2e+23
  M31= 3.4e+22  M32= -1.2e+23  M33= 1.7e+22  dyne-cm
Eigenvectors: component 1=M, 2=E, 3=V
eigenvector1(.885,-.687,.727)  vecaz.= -89.5  vecdip= 45.6
eigenvector2(.919,.298,.267)  vecaz.= 17.5  vecdip= 15.5
eigenvector3(-.395,.666,.633)  vecaz.= 128.6  vecdip= 39.2

```

n.943

```

Fault plane solution number 13
fault plane: strike= 273, dip= 16, slip= 166, degrees
auxiliary plane: strike= 349, dip= 94, slip= 75, degrees
Moment No 1.4e+23 dyne-cm
slipvector(-.198,-.979,-.878)  vecaz= 259.8  vecdip= -4.8

```

moment tensor13:
 M11= -2.1e+22 M12= 3.5e+22 M13= 7.4e+22
 M21= 3.5e+22 M22= 3.7e+22 M23= -1.5e+23
 M31= 3.4e+22 M32= -1.2e+23 M33= 1.7e+22 dyne-cm

Eigenvalues: component 1=N, 2=E, 3=V
 eigenvalue1=.919, .298, .267
 eigenvalue2=(-.395, .666, .633)
 eigenvalue3=(-.395, .666, .633)

n1959

Fault plane solution number14

fault plane: strike= 273, dip= 16, slip= 166, degrees
 auxiliary plane: strike= 349, dip= 94, slip= 75, degrees
 Moment No 1.7e+23 dyne-cm
 slipvector=(-.199, -.979, -.878) vecax= 259.8 vecdip= -4.8

moment tensor14:
 M11= -1.2e+23 M12= 2.1e+23 M13= 2.8e+23
 M21= 2.1e+23 M22= 2.2e+22 M23= -7.3e+23
 M31= 2.8e+23 M32= -7.3e+23 M33= 1.8e+23

Eigenvalues: component 1=N, 2=E, 3=V

eigenvalue1=.885, -.587, .727
 eigenvalue2=(-.919, .298, .267)
 eigenvalue3=(-.395, .666, .633) vecax= 128.6 vecdip= 39.2

n1972a

Fault plane solution number15

fault plane: strike= 273, dip= 16, slip= 166, degrees
 auxiliary plane: strike= 349, dip= 94, slip= 75, degrees
 Moment No 1.7e+23 dyne-cm

slipvector=(-.199, -.979, -.878) vecax= 259.8 vecdip= -4.8

moment tensor15:
 M11= -2.7e+22 M12= 4.5e+22 M13= 4.6e+22
 M21= 4.5e+22 M22= 4.5e+22 M23= 1.6e+23
 M31= 4.4e+22 M32= -1.6e+23 M33= 2.8e+23 dyne-cm

Eigenvalues: component 1=N, 2=E, 3=V

eigenvalue1=.895, -.587, .727
 eigenvalue2=(-.919, .298, .267)
 eigenvalue3=(-.395, .666, .633) vecax= 128.6 vecdip= 39.2

n1972b

Fault plane solution number16

fault plane: strike= 273, dip= 16, slip= 166, degrees
 auxiliary plane: strike= 349, dip= 94, slip= 75, degrees
 Moment No 1.7e+23 dyne-cm

slipvector=(-.199, -.979, -.878) vecax= 259.8 vecdip= -4.8

moment tensor16:
 M11= -9.8e+21 M12= 1.6e+22 M13= 1.6e+22
 M21= 1.6e+22 M22= 1.7e+21 M23= -5.8e+22
 M31= 1.6e+22 M32= -5.8e+22 M33= 8.1e+21 dyne-cm

Eigenvalues: component 1=N, 2=E, 3=V

eigenvalue1=.895, -.687, .727
 eigenvalue2=(-.919, .298, .267)
 eigenvalue3=(-.395, .666, .633) vecax= 128.6 vecdip= 39.2

n1982

Fault plane solution number17

fault plane: strike= 273, dip= 16, slip= 166, degrees
 auxiliary plane: strike= 349, dip= 94, slip= 75, degrees
 Moment No 6.3e+22 dyne-cm

slipvector=(-.199, -.979, -.878) vecax= 259.8 vecdip= -4.8

moment tensor17:
 M11= -9.8e+21 M12= 1.6e+22 M13= 1.6e+22
 M21= 1.6e+22 M22= 1.7e+21 M23= -5.8e+22
 M31= 1.6e+22 M32= -5.8e+22 M33= 8.1e+21 dyne-cm

Eigenvalues: component 1=N, 2=E, 3=V

eigenvalue1=.895, -.687, .727
 eigenvalue2=(-.919, .298, .267)
 eigenvalue3=(-.395, .666, .633) vecax= 128.6 vecdip= 39.2

Regional moment tensor:

M11= -2.8e+25 M12= 4.6e+25 M13= 4.5e+25
 M21= 4.6e+25 M22= 4.8e+24 M23= -1.6e+26
 M31= 4.6e+25 M32= -1.6e+26 M33= 2.3e+25 dyne-cm

Eigenvalues:

sigma1= 1.8e+26 sigma2= 8.3e+21 sigma3= -1.8e+26

Eigenvectors: component 1=N, 2=E, 3=V
eigenvector1=(.000, -.686, .728) vecaz.= -89.4 vecdip= 46.7
eigenvector2=(.918, .294, .267) vecaz.= 17.7 vecdip= 15.5
eigenvector3=(-.397, .666, .632) vecaz.= 128.8 vecdip= 39.2

SYNTHETIC FAULT PLANE SOLUTION:

coefficient of internal friction= .000 ==> alpha= 25.7 degrees

slipvec1=(-.275, -.014, .961) vecaz=-177. vecdip= 74.
nodal plane1: strike= -87. dip= 16.
T1=(.139, -.068, .477) vecaz= -81. vecdip= 29.
B=(.918, .294, .267) vecaz= 18. vecdip= 15.
P1=(-.372, .481, .837) vecaz= 133. vecdip= 57.

slipvec2=(-.286, .956, -.068) vecaz= 187. vecdip= -4.
nodal plane1: strike= 197. dip= 94.
T2=(-.124, -.427, .896) vecaz=-186. vecdip= 64.
B=(.918, .294, .267) vecaz= 18. vecdip= 15.
P2=(-.377, .855, .355) vecaz= 114. vecdip= 21.

DETERMINATION OF THE STRAIN RATE:

The specified volume= 135.9x10¹¹ km³

The strain rates for the last 81 years in the directions of the principal stress
extensional : 2.4e-08/yr = 4.9e-12/sec
intermediate : 1.1e-12/yr = 2.3e-16/sec
compressional:-2.4e-08/yr = -4.9e-12/sec

The horizontal and vertical strain rates:
Maximum horizontal: -8.1e-09/yr = -2.6e-16/sec Azimuth: N35W
Minimum horizontal: 5.8e-09/yr = 1.6e-16/sec Azimuth: N55E
Vertical : 3.1e-09/yr = 9.8e-17/sec

ENTER region boundary rotation
.B:1100000e+00
razmax
.1:1692390e+02

The maximum horizontal deformation rate = 1.3428 mm/yr

231

COMPUTATION OF A SYNTHETIC FAULT PLANE SOLUTION FROM A REGIONAL MOMENT TENSOR

SOUTHERN UTAH REGION

24 5

fault plane solution number 1
fault plane: strike= 345. dip= 65. slip= -75. degrees
auxiliary plane: strike= 136. dip= 38. slip= -116. degrees
Moment Mo= 3.8e+22 dyne-cm
slipvector=(.347, .368, .866) vecaz= 46.8 vecdip= 68.8

moment tensor 1:
M11= 4.9e+21 M12= 1.1e+22 M13= 1.6e+21
M21= 1.1e+22 M22= 1.7e+22 M23= 1.9e+22
M31= 1.6e+21 M32= 1.9e+22 M33= -2.2e+22 dyne-cm

Eigenvectors: component 1=N, 2=E, 3=V
eigenvector1=(.417, .858, .328) vecaz.= 63.9 vecdip= 18.7
eigenvector2=(-.985, .356, .235) vecaz.= 158.5 vecdip= 13.6
eigenvector3=(.086, -.388, .918) vecaz.= -77.5 vecdip= 66.6

n1933

fault plane solution number 2
fault plane: strike= 345. dip= 65. slip= -75. degrees
auxiliary plane: strike= 136. dip= 38. slip= -116. degrees
Moment Mo= 7.9e+23 dyne-cm
slipvector=(.347, .368, .866) vecaz= 46.8 vecdip= 68.8

moment tensor 2:
M11= 1.3e+23 M12= 3.1e+23 M13= 4.4e+22
M21= 3.1e+23 M22= 4.6e+23 M23= 5.8e+23
M31= 4.4e+23 M32= 5.8e+23 M33= -5.9e+23 dyne-cm

Eigenvectors: component 1=N, 2=E, 3=V
eigenvector1=(.417, .858, .328) vecaz.= 63.9 vecdip= 18.7
eigenvector2=(-.985, .356, .235) vecaz.= 158.5 vecdip= 13.6
eigenvector3=(.086, -.388, .918) vecaz.= -77.5 vecdip= 66.6

n1936

fault plane solution number 3
fault plane: strike= 345. dip= 65. slip= -75. degrees
auxiliary plane: strike= 136. dip= 38. slip= -116. degrees

232

Moment Mo= 3.7e+23 dyne-cm
 slipvector3=(.368, .368, .866) vecaz= 46.8 vecdip= 68.8
 moment tensor 3:
 M11= 6.2e+22 M12= 1.4e+23 M13= 2.8e+22
 M21= 1.4e+23 M22= 2.8e+23 M23= 2.3e+23
 M31= 2.8e+22 M32= 2.3e+23 M33= -2.8e+23 dyne-cm

Eigenvalues: component 1=N, 2=E, 3=V
 eigenvector1=(.417, .858, .328) vecaz= 63.9 vecdip= 18.7
 eigenvector2=(-.985, .356, .235) vecaz= 158.5 vecdip= 13.6
 eigenvector3=(.886, -.388, .918) vecaz= -77.5 vecdip= 66.6

n1937

Fault plane solution number 4
 fault plane: strike=135, dip= 65, slip= -75, degrees
 auxiliary plane: strike=136, dip= 38, slip=-116, degrees
 Moment Mo= 1.4e+23 dyne-cm
 slipvector=(.347, .368, .866) vecaz= 46.8 vecdip= 68.8
 moment tensor 4:
 M11= 2.3e+22 M12= 5.2e+22 M13= 7.4e+21
 M21= 5.2e+22 M22= 7.5e+22 M23= 8.5e+22
 M31= 7.4e+21 M32= 8.5e+22 M33= -1.8e+23 dyne-cm

Eigenvalues: component 1=N, 2=E, 3=V
 eigenvector1=(.417, .858, .328) vecaz= 63.9 vecdip= 18.7
 eigenvector2=(-.985, .356, .235) vecaz= 158.5 vecdip= 13.6
 eigenvector3=(.886, -.388, .918) vecaz= -77.5 vecdip= 66.6

n1942a

Fault plane solution number 5
 fault plane: strike=345, dip= 65, slip= -75, degrees
 auxiliary plane: strike=136, dip= 38, slip=-116, degrees
 Moment Mo= 7.9e+23 dyne-cm
 slipvector=(.347, .368, .866) vecaz= 46.8 vecdip= 68.8
 moment tensor 5:
 M11= 1.3e+23 M12= 3.1e+23 M13= 4.4e+22
 M21= 3.1e+23 M22= 4.6e+23 M23= 5.8e+23
 M31= 4.4e+22 M32= 5.8e+23 M33= -5.9e+23 dyne-cm

Eigenvalues: component 1=N, 2=E, 3=V
 eigenvector1=(.417, .858, .328) vecaz= 63.9 vecdip= 18.7
 eigenvector2=(-.985, .356, .235) vecaz= 158.5 vecdip= 13.6

eigenvector3=(.886, -.388, .918) vecaz= -77.5 vecdip= 66.6

n1942b

Fault plane solution number 6
 fault plane: strike=345, dip= 65, slip= -75, degrees
 auxiliary plane: strike=136, dip= 38, slip=-116, degrees
 Moment Mo= 1.4e+23 dyne-cm
 slipvector=(.347, .368, .866) vecaz= 46.8 vecdip= 68.8
 moment tensor 6:
 M11= 2.3e+22 M12= 5.2e+22 M13= 7.4e+21
 M21= 5.2e+22 M22= 7.7e+22 M23= 8.5e+22
 M31= 7.4e+21 M32= 8.5e+22 M33= -1.8e+23 dyne-cm

Eigenvalues: component 1=N, 2=E, 3=V
 eigenvector1=(.417, .858, .328) vecaz= 63.9 vecdip= 18.7
 eigenvector2=(-.985, .356, .235) vecaz= 158.5 vecdip= 13.6
 eigenvector3=(.886, -.388, .918) vecaz= -77.5 vecdip= 66.6

n1942c

Fault plane solution number 7
 fault plane: strike=135, dip= 65, slip= -75, degrees
 auxiliary plane: strike=136, dip= 38, slip=-116, degrees
 Moment Mo= 7.9e+23 dyne-cm
 slipvector=(.347, .368, .866) vecaz= 46.8 vecdip= 68.8
 moment tensor 7:
 M11= 1.3e+23 M12= 3.1e+23 M13= 4.4e+22
 M21= 3.1e+23 M22= 4.6e+23 M23= 5.8e+23
 M31= 4.4e+22 M32= 5.8e+23 M33= -5.9e+23 dyne-cm

Eigenvalues: component 1=N, 2=E, 3=V
 eigenvector1=(.417, .858, .328) vecaz= 63.9 vecdip= 18.7
 eigenvector2=(-.985, .356, .235) vecaz= 158.5 vecdip= 13.6
 eigenvector3=(.886, -.388, .918) vecaz= -77.5 vecdip= 66.6

n1943

Fault plane solution number 8
 fault plane: strike=345, dip= 65, slip= -75, degrees
 auxiliary plane: strike=136, dip= 38, slip=-116, degrees
 Moment Mo= 1.4e+23 dyne-cm


```

slipvector=(.347, .368, .866) vecaz= 46.8 vecdip= 68.8
moment tensor 8:
M11= 2.3e+22 M12= 5.2e+22 M13= 7.4e+21
M21= 7.7e+22 M22= 8.5e+22 M23= 8.5e+22
M31= 7.4e+21 M32= 8.5e+22 M33= -1.8e+23
dyne-cm

```

```

Eigenvalues: component 1=N, 2=E, 3=V
eigenvector1=(.417, .858, .328) vecaz.= 63.9 vecdip= 18.7
eigenvector2=(-.985, .356, .235) vecaz.= 158.5 vecdip= 13.6
eigenvector3=(.886, -.388, .918) vecaz.= -77.5 vecdip= 66.6

```

n1953

```

Fault plane solution number 9
fault plane: strike=345, dip= 65, slip=-75, degrees
auxiliary plane: strike=136, dip= 38, slip=-116, degrees
Moment Mo= 7.9e+23 dyne-cm
slipvector=(.347, .368, .866) vecaz= 46.8 vecdip= 68.8
moment tensor 9:
M11= 2.3e+22 M12= 5.2e+22 M13= 7.4e+21
M21= 7.7e+22 M22= 8.5e+22 M23= 8.5e+22
M31= 7.4e+21 M32= 8.5e+22 M33= -1.8e+23
dyne-cm

```

```

Eigenvalues: component 1=N, 2=E, 3=V
eigenvector1=(.417, .858, .328) vecaz.= 63.9 vecdip= 18.7
eigenvector2=(-.985, .356, .235) vecaz.= 158.5 vecdip= 13.6
eigenvector3=(.886, -.388, .918) vecaz.= -77.5 vecdip= 66.6

```

n1959a

```

Fault plane solution number 18
fault plane: strike=345, dip= 65, slip=-75, degrees
auxiliary plane: strike=136, dip= 38, slip=-116, degrees
Moment Mo= 7.9e+23 dyne-cm
slipvector=(.347, .368, .866) vecaz= 46.8 vecdip= 68.8
moment tensor 18:
M11= 1.3e+23 M12= 2.1e+23 M13= 4.4e+22
M21= 3.1e+23 M22= 4.6e+23 M23= 5.8e+23
M31= 4.4e+22 M32= 5.8e+23 M33= -5.9e+23
dyne-cm

```

```

Eigenvalues: component 1=N, 2=E, 3=V
eigenvector1=(.417, .858, .328) vecaz.= 63.9 vecdip= 18.7
eigenvector2=(-.985, .356, .235) vecaz.= 158.5 vecdip= 13.6
eigenvector3=(.886, -.388, .918) vecaz.= -77.5 vecdip= 66.6

```

n1959b

```

Fault plane solution number 11
fault plane: strike=345, dip= 65, slip=-75, degrees
auxiliary plane: strike=136, dip= 38, slip=-116, degrees
Moment Mo= 2.8e+24 dyne-cm
slipvector=(.347, .368, .866) vecaz= 46.8 vecdip= 68.8
moment tensor 11:
M11= 4.7e+23 M12= 1.1e+24 M13= 1.6e+23
M21= 1.1e+24 M22= 1.6e+24 M23= 1.8e+24
M31= 1.6e+23 M32= 1.8e+24 M33= -2.1e+24
dyne-cm

```

```

Eigenvalues: component 1=N, 2=E, 3=V
eigenvector1=(.417, .858, .328) vecaz.= 63.9 vecdip= 18.7
eigenvector2=(-.985, .356, .235) vecaz.= 158.5 vecdip= 13.6
eigenvector3=(.886, -.388, .918) vecaz.= -77.5 vecdip= 66.6

```

n1966

```

Fault plane solution number 12
fault plane: strike=345, dip= 65, slip=-75, degrees
auxiliary plane: strike=136, dip= 38, slip=-116, degrees
Moment Mo= 8.1e+22 dyne-cm
slipvector=(.347, .368, .866) vecaz= 46.8 vecdip= 68.8
moment tensor 12:
M11= 1.4e+22 M12= 3.2e+22 M13= 4.5e+21
M21= 3.2e+22 M22= 5.1e+22 M23= 5.1e+22
M31= 4.5e+21 M32= 5.1e+22 M33= -6.8e+22
dyne-cm

```

```

Eigenvalues: component 1=N, 2=E, 3=V
eigenvector1=(.417, .858, .328) vecaz.= 63.9 vecdip= 18.7
eigenvector2=(-.985, .356, .235) vecaz.= -37.5 vecdip= 13.6
eigenvector3=(.886, -.388, .918) vecaz.= -77.5 vecdip= 66.6

```

n1981

```

Fault plane solution number 13
fault plane: strike=345, dip= 65, slip=-75, degrees
auxiliary plane: strike=136, dip= 38, slip=-116, degrees
Moment Mo= 2.3e+23 dyne-cm
slipvector=(.347, .368, .866) vecaz= 46.8 vecdip= 68.8

```

moment tensor13:
M11= 3.9e+22 M12= 9.8e+22 M13= 1.3e+22
M21= 9.8e+22 M22= 1.3e+23 M23= 1.5e+23
M31= 1.3e+22 M32= 1.5e+23 M33= -1.7e+23 dyn-cm

Eigenvectors: component 1=N, 2=E, 3=V
eigenvector1=(.417, .858, .328) vecaz.= 63.9 vecdip= 18.7
eigenvector2=(-.985, .356, .235) vecaz.= 158.5 vecdip= 13.6
eigenvector3=(.886, -.388, .918) vecaz.= -77.5 vecdip= 66.6

Regional moment tensor:
M11= 1.2e+24 M12= 2.8e+24 M13= 4.8e+23
M21= 2.8e+24 M22= 4.2e+24 M23= 4.6e+24
M31= 4.8e+23 M32= 4.6e+24 M33= -5.4e+24 dyn-cm

Eigenvalues:
sigma1= 7.3e+24 sigma2= -7.2e+16 sigma3= -7.3e+24

Eigenvectors: component 1=N, 2=E, 3=V
eigenvector1=(.417, .858, .328) vecaz.= 63.9 vecdip= 18.7
eigenvector2=(-.985, .356, .235) vecaz.= 158.5 vecdip= 13.6
eigenvector3=(.886, -.388, .918) vecaz.= -77.5 vecdip= 66.6

SYNTHETIC FAULT PLANE SOLUTION:

coefficient of internal friction= .888 ==> alpha= 25.7 degrees

slipvec1=(.356, .327, .875) vecaz= 43. vecdip= 61.

nodal plane2: strike= 133. dip= 29.

T1=(.365, .931, -.882) vecaz= 69. vecdip= .

B=(-.985, .356, .235) vecaz= 159. vecdip= 14.

P1=(.219, -.884, .972) vecaz= -21. vecdip= 76.

slipvec2=(-.235, -.875, .423) vecaz=-185. vecdip= 25.

nodal plane1: strike= -15. dip= 65.

T2=(.422, .674, .686) vecaz= 58. vecdip= 37.

B=(-.985, .356, .235) vecaz= 159. vecdip= 14.

P2=(-.857, -.647, .768) vecaz= -95. vecdip= 49.

DETERMINATION OF THE STRAIN RATE:

The specified volume= 94.4x138.6x 18.8km³

237

The strain rates for the last 48 years in the directions of the principal stress
extensional : 1.7e-8/yr = 1.3e-13/sec
intermediate : -1.7e-17/yr = -1.3e-21/sec
compressional : -1.7e-8/yr = -1.3e-13/sec

The horizontal and vertical strain rates:
Maximum horizontal: 1.4e-8/yr = 4.5e-17/sec Azimuth: N59
Minimum horizontal: -1.2e-18/yr = -3.8e-18/sec Azimuth: N31W
Vertical : -1.3e-8/yr = -4.1e-17/sec

ENTER region boundary rotation

razmax
.588121918e+82

The maximum horizontal deformation rate = .2298 mm/yr

238

COMPUTATION OF A SYNTHETIC FAULT PLANE SOLUTION FROM A REGIONAL MOMENT TENSOR

UTAH-NEVADA BORDER REGION

5 5

Fault plane solution number 1
 fault plane: strike= 298. dip= 88. slip= 12. degrees
 auxiliary plane: strike= 194. dip= 88. slip= 169. degrees
 Moment Mo= 2.3e+25 dyne-cm
 slipvector=(.238,-.956, .174) vecaz= 184.# vecdip= 18.#
 moment tensor 1:

M11= 1.3e+25	M12= -1.8e+25	M13= -5.7e+24	
M21= -1.8e+25	M22= -1.5e+25	M23= 2.2e+24	dyne-cm
M31= -5.7e+24	M32= 2.2e+24	M33= 1.7e+24	

 Eigenvectors: component 1=N, 2=E, 3=V
 eigenvector1=(-.867, .421, .268) vecaz.= 154.1 vecdip= 15.5
 eigenvector2=(.231,-.137, .963) vecaz.= -38.8 vecdip= 74.4
 eigenvector3=(.442, .897, .822) vecaz.= 63.8 vecdip= 1.3

n192a

Fault plane solution number 2
 fault plane: strike= 298. dip= 88. slip= 12. degrees
 auxiliary plane: strike= 194. dip= 88. slip= 169. degrees
 Moment Mo= 2.1e+25 dyne-cm
 slipvector=(.238,-.956, .174) vecaz= 184.# vecdip= 18.#
 moment tensor 2:

M11= 1.2e+25	M12= -1.6e+25	M13= -5.2e+24	
M21= -1.6e+25	M22= -1.3e+25	M23= 2.8e+24	dyne-cm
M31= -5.2e+24	M32= 2.8e+24	M33= 1.5e+24	

 Eigenvectors: component 1=N, 2=E, 3=V
 eigenvector1=(-.867, .421, .268) vecaz.= 154.1 vecdip= 15.5
 eigenvector2=(.231,-.137, .963) vecaz.= -38.8 vecdip= 74.4
 eigenvector3=(.442, .897, .822) vecaz.= 63.8 vecdip= 1.3

n192b

Fault plane solution number 3
 fault plane: strike= 298. dip= 88. slip= 12. degrees
 auxiliary plane: strike= 194. dip= 88. slip= 169. degrees

Moment Mo= 7.9e+23 dyne-cm
 slipvector=(.238,-.956, .174) vecaz= 184.# vecdip= 18.#
 moment tensor 3:

M11= 4.4e+23	M12= -6.8e+23	M13= -1.9e+23	
M21= -6.8e+23	M22= -5.8e+23	M23= 7.4e+22	dyne-cm
M31= -1.9e+23	M32= 7.4e+22	M33= 5.6e+22	

 Eigenvectors: component 1=N, 2=E, 3=V
 eigenvector1=(-.867, .421, .268) vecaz.= 154.1 vecdip= 15.5
 eigenvector2=(.231,-.137, .963) vecaz.= -38.8 vecdip= 74.4
 eigenvector3=(.442, .897, .822) vecaz.= 63.8 vecdip= 1.3

n1914

Fault plane solution number 4
 fault plane: strike= 298. dip= 88. slip= 12. degrees
 auxiliary plane: strike= 194. dip= 88. slip= 169. degrees
 Moment Mo= 1.4e+23 dyne-cm
 slipvector=(.238,-.956, .174) vecaz= 184.# vecdip= 18.#
 moment tensor 4:

M11= 7.5e+22	M12= -1.8e+23	M13= -3.3e+22	
M21= -1.8e+23	M22= -8.5e+22	M23= 1.3e+22	dyne-cm
M31= -3.3e+22	M32= 1.3e+22	M33= 9.6e+21	

 Eigenvectors: component 1=N, 2=E, 3=V
 eigenvector1=(-.867, .421, .268) vecaz.= 154.1 vecdip= 15.5
 eigenvector2=(.231,-.137, .963) vecaz.= -38.8 vecdip= 74.4
 eigenvector3=(.442, .897, .822) vecaz.= 63.8 vecdip= 1.3

n1966

Fault plane solution number 5
 fault plane: strike= 298. dip= 88. slip= 12. degrees
 auxiliary plane: strike= 194. dip= 88. slip= 169. degrees
 Moment Mo= 3.7e+23 dyne-cm
 slipvector=(.238,-.956, .174) vecaz= 184.# vecdip= 18.#
 moment tensor 5:

M11= 2.1e+23	M12= -2.8e+23	M13= -9.8e+22	
M21= -2.8e+23	M22= -2.3e+23	M23= 3.5e+22	dyne-cm
M31= -9.8e+22	M32= 3.5e+22	M33= 2.6e+22	

 Eigenvectors: component 1=N, 2=E, 3=V
 eigenvector1=(-.867, .421, .268) vecaz.= 154.1 vecdip= 15.5
 eigenvector2=(.231,-.137, .963) vecaz.= -38.8 vecdip= 74.4

eigenvector3=(.442, .897, .822) vecaz.= 63.8 vecdip= 1.3

Regional moment tensor:
 M11= 2.6e+25 M12= 3.5e+25 M13= -1.1e+25
 M21= -5.5e+25 M22= -2.5e+25 M23= 4.3e+24 dyne-cm
 M31= -1.1e+25 M32= 4.3e+24 M33= 3.3e+24

Eigenvalues:
 sigma1= 4.6e+25 sigma2= -1.6e+18 sigma3= -4.6e+25

Eigenvectors: component | = M, 2 = E, 3 = V
 eigenvector1=(-.867, .421, .268) vecaz.= 154.1 vecdip= 15.5
 eigenvector2=(.231, -.137, .963) vecaz.= -38.8 vecdip= 74.4
 eigenvector3=(.442, .897, .822) vecaz.= 63.8 vecdip= 1.3

SYNTHETIC FAULT PLANE SOLUTION:

coefficient of internal friction= .888 ==> alpha= 25.7 degrees

slipvec1=(-.381, .932, .285) vecaz= 188 vecdip= 12.

nodal plane2: strike= 198, dip= 78, vecaz= 188, vecdip= 12.

T1=(-.964, .188, .245) vecaz= 174, vecdip= 14.

S=(-.231, -.137, .963) vecaz= -31, vecdip= 74.

P1=(.138, .985, .189) vecaz= 82, vecdip= 6.

slipvec2=(.925, .337, -.174) vecaz= 28, vecdip= -18.

nodal plane1: strike= 118, dip= 188,

T2=(-.672, .594, .268) vecaz= 134, vecdip= 15.

S=(-.231, -.137, .963) vecaz= -31, vecdip= 74.

P2=(.784, .787, -.868) vecaz= 45, vecdip= -4.

DETERMINATION OF THE STRAIN RATE:

The specified volume= 94.4x 65.8x 18.8km³

The strain rates for the last 88 years in the directions of the principal stress

extensional: 1.4e-88/yr = 2.9e-12/sec

intermediate: -2.2e-16/yr = -6.5e-20/sec

compressional: -1.4e-88/yr = -2.9e-12/sec

The horizontal and vertical strain rates:

Maximum horizontal: -1.4e-88/yr = -4.5e-16/sec Azimuth: N64E

Minimum horizontal: 1.3e-88/yr = 4.2e-16/sec Azimuth: N26W

Vertical boundary rotation
 ENTER: 1.4e-88/yr = 3.2e-17/sec

 rmax
 .6393889e+82

The maximum horizontal deformation rate = 1.6293 mm/yr



APPENDIX E
EARTHQUAKE RECURRENCE RATES

The main earthquake catalog, by study area, was used to determine a- and b-values from the equation

$$\log(N) = a - bM \quad (20)$$

where N is the number of earthquakes of magnitude M or greater occurring within the time period examined. The b-values were determined using the maximum likelihood estimate method discussed by Aki [1965] with confidence limits set at 95%:

$$b = \frac{\log_{10} e}{\bar{M} - M_0} \quad (21)$$

where \bar{M} = mean magnitude of the events considered, M_0 = the minimum magnitude considered, and the error can be determined using

$$\frac{1 - d_L \sqrt{n}}{\sum_{i=1}^{i=n} M_i / n - M_0} \leq b' \leq \frac{1 + d_U \sqrt{n}}{\sum_{i=1}^{i=n} M_i / n - M_0} \quad (22)$$

where $b' = \frac{b}{\log_{10} e}$, $d_L = 1.96$ ($+d_U$ are confidence limits used by Aki [1965] to develop equation (22)) and n is the number of events considered [Aki, 1965]. Typically, the minimum magnitude used was M_L 3.0, although occasionally, when the sampling completeness differed, larger or smaller minimum magnitudes were used. Results are shown in Figures 17-22.

a- and b- values were determined using the entire data set from 1900 to 1981. Consequently, the results are biased by variable network coverage early in the century. The lack of recorded small events probably accounts for the low b-values determined for the Utah region (~5.0 in this study, compared to 0.75-1.2 from Arabasz et al. [1980])

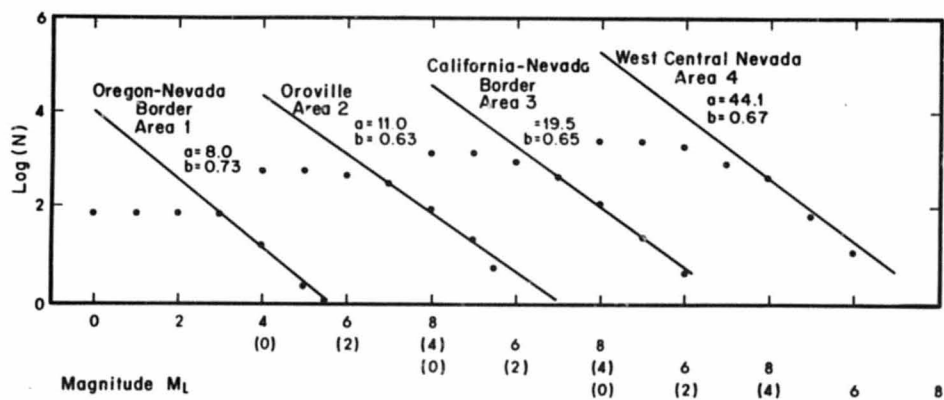


Figure 17. Area 1-4 a - and b -value graphs.

245

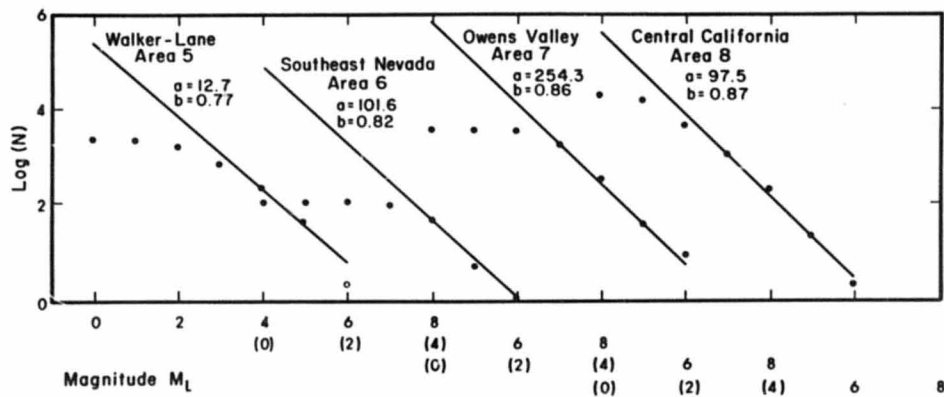


Figure 18. Area 5-8 a - and b -value graphs.

246

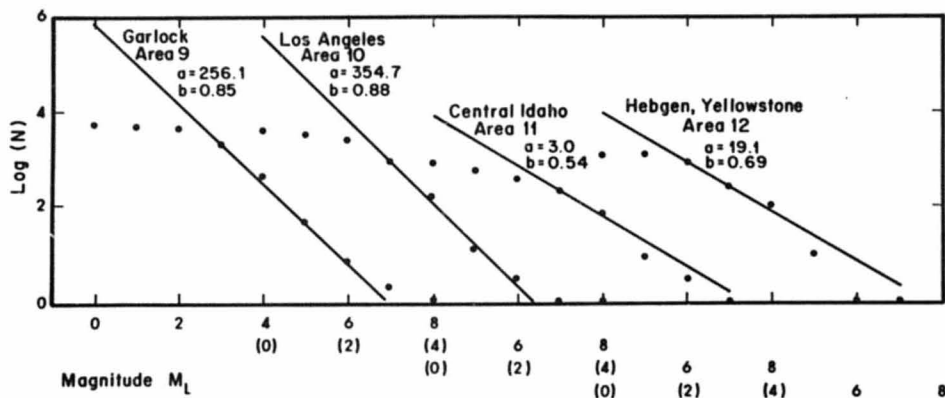


Figure 19. Area 9-12 a- and b-value graphs.

247

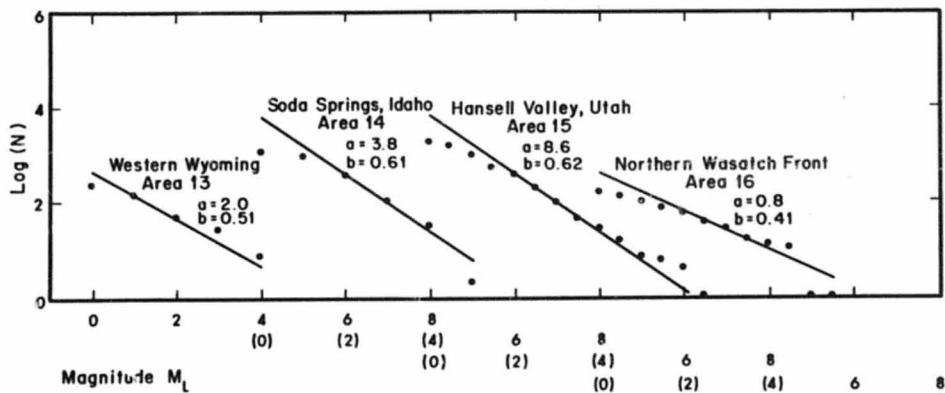


Figure 20. Area 13-16 a- and b-value graphs.

248

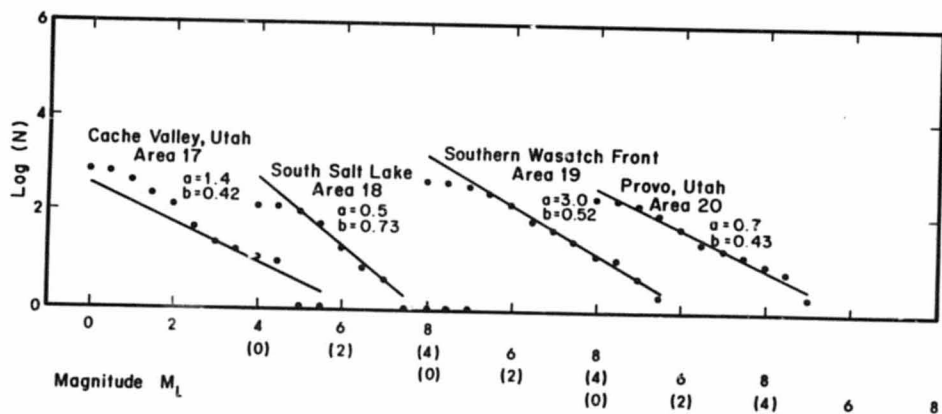


Figure 21. Area 17-20 a- and b-value graphs.

249

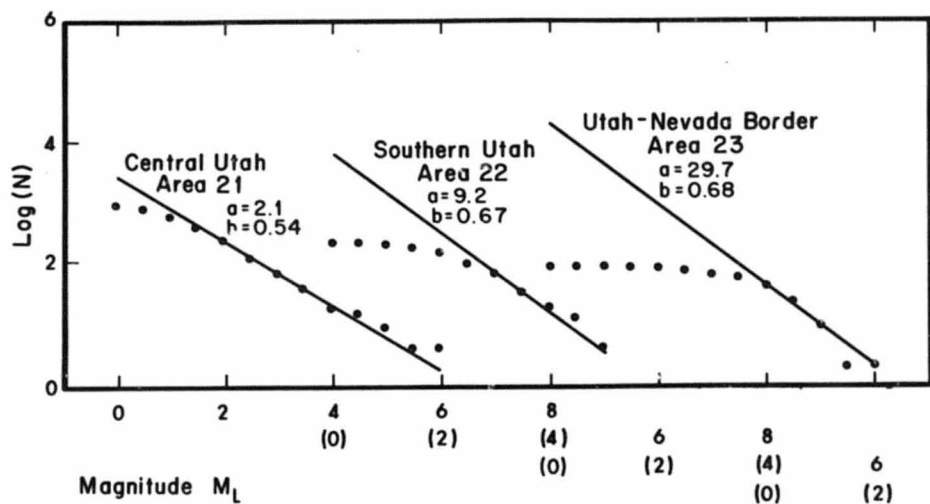


Figure 22. Area 21-23 a- and b-value graphs.

250

APPENDIX F

LITHOSPHERE DEFORMATION MODEL

Finite Element Modeling

Strain rates obtained from the earthquake data along with measured vertical strain rates [Brown, et al, 1980] were used to constrain two-dimensional, viscoelastic, finite element modeling of the Great Basin. The finite element program used ('nrift'), by Lynch [1983], considers the lithosphere of the earth to be symmetric with respect to the axis of a rift. It also assumes that structure is fixed perpendicular to the rift axis (assuming a plane-strain, two-dimensional configuration). The model is symmetric about the center of the Great Basin along an east - west cross-section of the lithosphere loaded perpendicular to the rift axis (Figure 23).

The program allows the lithosphere to deform under a given stress field according to the viscosities which develop in materials with different properties. Thus, the input rock types may deform brittlely, plastically, elastically, or according to some intermediate flow law depending on the temperature, stress field, and material properties.

'Nrift' allowed for model evolution through time by recalculating stresses, strains, and deformation style for each time step using the previous time step results as an initial model. The size of the time step was calculated by 'nrift' from the viscosity term to provide the maximum step size which would produce numerically stable results [Lynch, 1983].

Limiting Assumptions

Simplifying assumptions are made in 'nrift' which limit the reliability of the program's results. These are 1) bilateral symmetry of the rift modeled, 2) two-dimensional, plane-strain stress-strain laws, 3) far-field loading of the right hand edge of a model crust, and 4) deformation only by simple stretching, i.e no thermal doming, addition of mantle

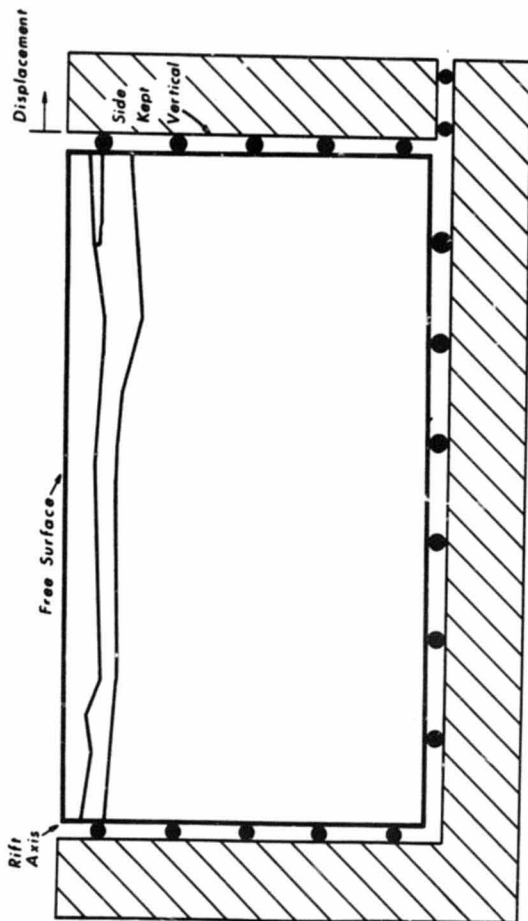


Fig. 23. Diagram showing boundary assumptions used to model the right (east) half of an E-W symmetric Great Basin lithosphere. The load is applied to the east edge, which is maintained vertical throughout modeling.

material, etc.

The most appropriate of these assumptions is bilateral symmetry perpendicular to the rift axis. As noted in the section on regional geology and geophysics, the Great Basin does display remarkable east-west symmetry. However, this symmetry is not exact and so 'nrift' imposes some artificial symmetry on the Great Basin model.

Another simplification which can be quite confidently applied is the plane-strain case. 'Nrift' models a one meter thick, east-west cross-section of the crust. Since one meter is very much less than the north-south length of the Great Basin, plane-strain stress-strain laws are a valid assumption.

The third simplifying condition addressed above cannot be applied with as much confidence as were the first two. This third assumption is that the crust is loaded along a right hand edge that is so far from the rift that spurious effects are minimal. This is a fair assumption when using 'nrift' to model narrow rift zones. In those cases, the right hand edge can be 2-3 times the rift radius away from the rift. Unfortunately, the extreme width of the Great Basin made it necessary to decrease this distance. Numerical stability in 'nrift' requires the model to be only 2-2.5 times as wide as it is thick [Lynch, 1984]. This means that for rifts as wide as the Great Basin, it is impractical to put the right hand edge of the crust more than about one tenth of a rift radius away from the rift itself. The result is edge effect contamination of the model. The loaded edge must be maintained as a vertical edge throughout the modeling. Also, the lowest point on this edge must be fixed for the finite element equations to have a unique solution. Consequently, unreasonably high stress is concentrated along the edge changing deformation styles (less ductile), and increasing displacement rates.

The fourth assumption is that of the simple stretching model. Lachenbruch and Sass [1978] pointed out that this mode of deformation is inefficient from a thermal standpoint. Unfortunately, there is no provision in 'nrift' for any addition of material once modeling has begun. Consequently, neither magma intrusion, mantle convection, nor cru-

stal underplating can be modeled using this program.

Model Parameters

The model tested in this study, shown in Figure 24, came from a lithospheric cross-section of the western United States from Continental Transects Profile C-2 by Blake, et al. (unpublished data, 1985). Material properties for the rocks were taken from Smith and Bruhn [1984] and from Turcotte and Schubert [1982]. Heat flow and heat generation used to determine temperature depth profiles were taken from Lachenbruch and Sams [1978] and Turcotte and Schubert [1982]. The model used is presented along with the temperature-depth profile and a diagram of rock properties in Figure 25.

Results of Finite Element Modeling

Figure 26a shows the the results of the model after 660 years of lateral crustal stretching. The vertical displacements have been grossly exaggerated to make them visible. Figure 26b is a graph of surface horizontal deformation rate versus horizontal distance. Using these two figures, meaningful effects and model assumption artifacts can be segregated to some degree.

The largest deformation rates were found in the center and toward the left edge of the model and are connected by a dotted line in Figure 26b. These deformation rates are considered to be products of localized, upper crust doming in the model. This local folding is associated with the simple stretching assumption and hence has been omitted from the solid line in Figure 26b which represents true model results.

The crust in these areas of high deformation has fallen rather rapidly due to crustal stretching and subsequent "necking down" of the mantle. Any mantle upwarps under the crust acted as pivots over which the crust draped. Directly over these pivots, the upper crust exhibited its most pronounced deformation. Between the folds, upper crustal extension dropped to zero. Mantle upwelling and the possible addition of material to the crust

MODEL WESTERN U.S. CROSS-SECTION

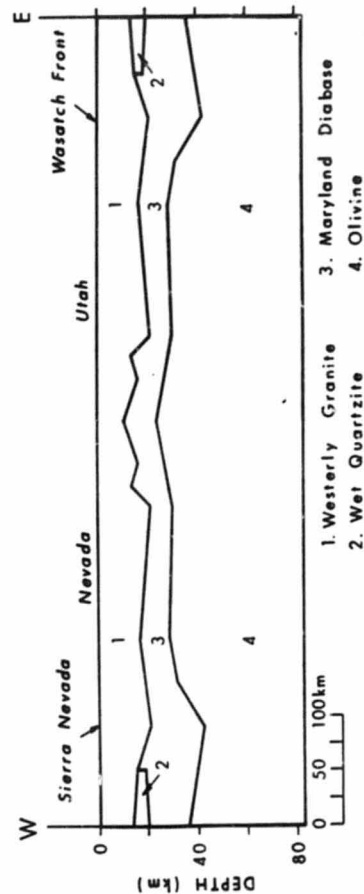


Fig. 24. E-W symmetric, simplified Great Basin lithospheric model.

MODEL CRUSTAL STRUCTURE AND TEMPERATURE PROFILE

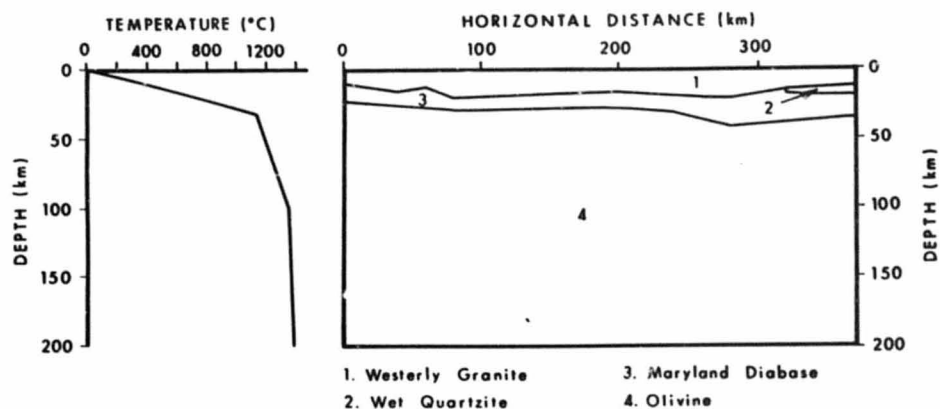


Fig. 25. Model material and temperature depth assumptions.

257

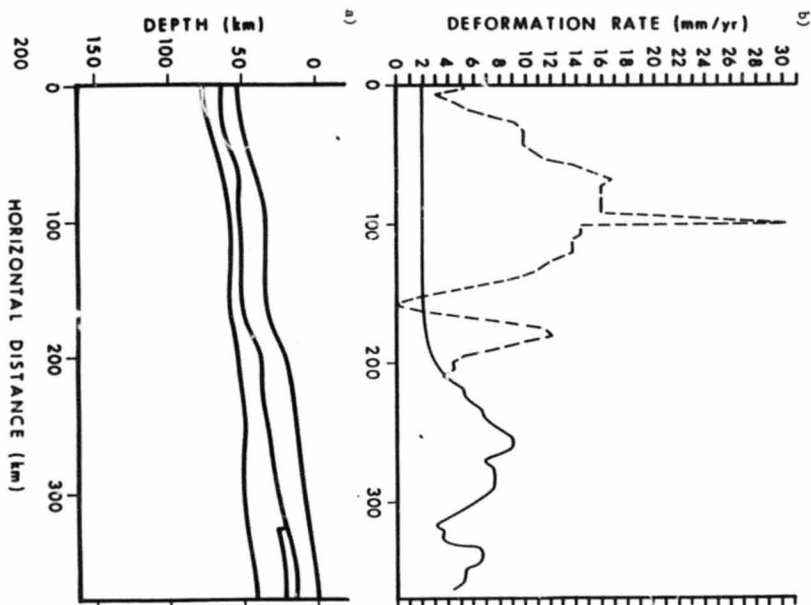


Fig. 26. Modeling results showing a) relative magnitudes of vertical deformation and b) surface horizontal deformation rates per element versus distance across the Great Basin. The dashed line refers to results assumed to be model artifacts.

258

here would have counteracted this vertical drop and thus eliminated the folding of the crust described above. Brown et al. [1980] have shown through leveling studies that the central Great Basin crust has indeed been uplifted not down-dropped in the past 60 years.

Another area of high deformation rate is found on the extreme right hand margin of the model. This zone of deformation is probably a loaded edge effect. To accommodate both a deviatoric stress and gravity induced stresses, the right edge must be maintained in a vertical position and no vertical motion can be allowed (otherwise the model would extend at the base and slump at the top - something like a melting butter cube). Still, it is not clear how edge effects are expressed in the model, so this deformation high was left in the solid line curve in Figure 26b.

The most significant feature left in the solid line graph of Figure 26b is a band of high deformation about 100 km wide located at the east side of the graph. This zone of high deformation rate compares very well with the location of the diffuse band of seismicity and deformation which marks the borders of the Great Basin and could be caused by lithospheric thinning occurring at the margins of the Great Basin where the depth to the "olivine" mantle rocks increases from ~30 km to ~40 km.

The type of deformation is another important factor to be considered. Figure 27 maps the deformational styles found throughout the model crust. Note that significant brittle deformation is only found at depth beneath the zone of high deformation corresponding to the Great Basin margin seismicity belts. This corresponds to locations of large earthquakes and major faults (such as the Wasatch fault) located within these belts.

Figure 27 also shows that deformation style changes from brittle to ductile with depth within a given material and then commonly goes through this cycle again when a new material is encountered. This effect is predicted in Smith and Bruhn [1984] and helps explain depths of earthquake nucleation as discussed earlier in this work.

Note that edge effects can be seen in Figure 27 as a 20 km wide zone of mostly elastic deformation located on the right edge of the model.

MODEL RESULTS-DEFORMATION STYLES

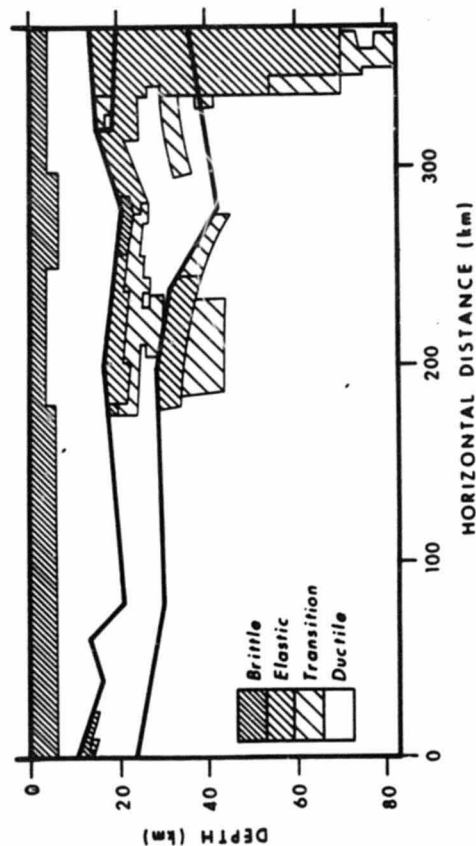


Fig. 27. Modeling results showing deformational style throughout the lithosphere.

The general conclusion derived from this modeling experiment is that the crustal model stretching employed [Figure 2] accounted well for the surface horizontal deformation trends and the changes in deformation style associated with the Great Basin.

REFERENCES

- Aki, K., Maximum likelihood estimate of b in the formula $\log N = a - bm$ and its confidence limits, *Bull. of the Earthquake Res. Inst. Tokyo Univ.*, 43, 237-239, 1965.
- Aki, K., Generation and propagation of G waves from the Niigata earthquake of June 16, 1964. 2. Estimation of earthquake moment, release energy, and stress drop from the G-wave spectrum, *Bull. of the Earthquake Res. Inst. Tokyo Univ.*, 44, 73-88, 1966.
- Aki, K. and P. Richards, *Quantitative Seismology*, pp. 105-119, W. H. Freeman, San Francisco, Calif., 1980.
- Anderson, J. G., Estimating the seismicity from geological structure for seismic-risk studies, *Bull. Seismol. Soc. Am.*, 69, 135-158, 1979.
- Anderson, J. G. and J. E. Luco, Consequences of slip rate constraints on earthquake occurrence relations, *Bull. Seismol. Soc. Am.*, 73, 471-496, 1983.
- Arabasz, W. J., R. B. Smith and W. S. Richins, Earthquake studies along the Wasatch Front, Utah: Network monitoring, seismicity and seismic hazards, *Bull. Seismol. Soc. Am.*, 70, 1479-1499, 1980.
- Archuleta, R. J., E. Cranswick, C. Mueller and P. Spudich, Source parameters of the 1980 Mammoth Lakes, California earthquake sequence, *J. Geophys. Res.*, 87, 4595-4607, 1982.
- Askew, B. and S. T. Algermissen, An earthquake catalog for the Basin and Range province 1803-1977, *U. S. Geol. Surv. Open-File Rep.*, 83-86, 1983.
- Atwater, T., Implications of plate tectonics for the Cenozoic tectonic evolution of western North America, *Bull. Geol. Soc. Am.*, 81, 3513-3535, 1970.
- Best, M. G. and W. K. Hamblin, Origin of the northern Basin and Range province: Implications from the geology of its eastern boundary, *Mem. Geol. Soc. Am.*, 152, 313-340, 1978.
- Brown, L. D., R. E. Reillinger and G. P. Citron, Recent vertical crustal movements in the U. S.: Evidence from precise levelling, in *Earth Rheology, Isostasy and Eustasy*, edited by N. Morner, pp. 389-405, John Wiley & Sons, New York, New York, 1980.
- Caristan, Y. and W. F. Brace, Experimental study of the brittle ductile transition in a basaltic rock (abstract), paper presented at AGU, 1980 fall meeting, *EOS, Transactions AGU*, 61, 1131-1132, 1980.

- Doser, D. I., Source parameters and faulting processes of the August 1959 Hebgen Lake, Montana earthquake sequence, PhD dissertation, 152 pp., University of Utah, Salt Lake City, Utah, 1984.
- Doser, D. I., Source parameters and faulting processes of the 1959 Hebgen Lake, Montana earthquake sequence, *J. Geophys. Res.*, 90, 4537-4556, 1985.
- Doser, D. I. and R. B. Smith, Seismic moment rates in the Utah region, *Bull. Seismol. Soc. Am.*, 72, 525-551, 1982.
- Easton, G. P., R. R. Wahl, H. J. Prostka, D. R. Mabey and M. D. Kleinkopf, Regional gravity and tectonic patterns: Their relation to late Cenozoic epeirogeny and lateral spreading in the western Cordillera, *Mem. Geol. Soc. Am.*, 152, 51-91, 1978.
- Forsythe, G. E., M. A. Malcolm and C. B. Moler, *Computer Methods for Mathematical Computations*, pp.49-55, Prentice Hall, Englewood Cliffs, New Jersey, 1977.
- Gilbert, F., Excitation of the normal modes of the earth by earthquake sources, *Geophys. J. R. Astr. Soc.*, 22, 223-226, 1970.
- Greensfelder, R. W., Kintzer, F. C. and M. R. Somerville, Seismotectonic regionalization of the Great Basin, and comparison of moment rates computed from Holocene strain and historic seismicity: Summary, *Bull. Geol. Soc. Am.*, 97, 518-523, 1980.
- Gutenberg, B. and C. F. Richter, Earthquake magnitude, intensity, energy, and acceleration, *Bull. Seismol. Soc. Am.*, 46, 105-145, 1956.
- Hamilton, W. and W. B. Myers, Cenozoic tectonics of the western United States, *Rev. Geophys.*, 5, 509-549, 1966.
- Hanks, T. C. and H. Kanamori, A moment magnitude scale, *J. Geophys. Res.*, 84, 2348-2350, 1979.
- Hanks, T. C. and D. M. Boore, Moment-magnitude relations in theory and practice, *J. Geophys. Res.*, 89, 6229-6235, 1984.
- Hanks, T. C., J. A. Hileman and W. Thatcher, Seismic moments of the larger earthquakes of the southern California region, *Geol. Soc. Am. Bull.*, 86, 1131-1139, 1975.
- Hyndman, R. D. and D. H. Weichert, Seismicity and rates of relative motion on the plate boundaries of western North America, *Geophys. J. R. Astr. Soc.*, 72, 59-82, 1983.
- Jordan, T. H., J. B. Minster, D. C. Christodoulidis and D. E. Smith, Constraints on western U. S. deformation from satellite laser ranging, preprint, 1985.
- Kostrov, V. V., Seismic moment and energy of earthquakes, and seismic flow of rock, *Izv. Earth Phys.*, 1, 23-40, 1974.
- Lynch, H. D., Numerical models of the formation of continental rifts by processes of lithospheric necking, PhD dissertation, 290 pp. New Mexico State Univ., Las Cruces, New Mexico, 1983.
- Lachenbruch, A. H. and J. H. Sass, Models of an extending lithosphere and heat flow in the

- Basin and Range province, *Mem. Geol. Soc. Am.*, 152, 209-250, 1978.
- Minster, J. B. and T. H. Jordan, Vector constraints on Quaternary deformation of the western United States east and west of the San Andreas fault. Tectonics and Sedimentation Along the California Margin, *S.E.P.M. Pac. Sect.*, 33, 1984.
- Molnar, P., Earthquake recurrence intervals and plate tectonics, *Bull. Seismol. Soc. Am.*, 69, 115-133, 1979.
- Patton, H. J., P-wave fault-plane solutions and the generation of surface waves by earthquakes in the Western United States, preprint, 1984.
- Proffett, J. M., Jr., Cenozoic geology of the Yerington district, Nevada and implications for the nature of and origin of Basin and Range faulting, *Bull. Geol. Soc. Am.*, 88, 247-266, 1977.
- Renggli, C. and R. B. Smith, Estimates of crustal extension for the Basin-Range/southern San Andreas associated with active seismicity (abstract), *Earthquake Notes*, 55, 29, 1984.
- Richins, W. D., R. B. Smith, C. J. Langer, J. E. Zollweg, J. J. King and J. C. Pechmann, The 1983 Borah Peak, Idaho earthquake: Relationship of aftershocks to the main shock, surface faulting, and regional tectonics, *U. S. Geol. Surv. Open-File Rep.*, 85-290, 285-310, 1985.
- Savage, J. C., Strain accumulation in western United States, *Ann. Rev. Earth Planet. Sci.*, 11, 11-43, 1983.
- Savage, J. C., M. Lisowski and W. H. Prescott, Strain accumulation in the Rocky Mountain states, preprint, 1985.
- Scholz, C. H., M. Barazangi and M. L. Sbar, Late Cenozoic evolution of the Great Basin, Western United States, as an ensialic intrarc basin, *Geol. Soc. Am. Bull.*, 82, 2979-2990, 1971.
- Schwartz, D. P. and K. J. Coppersmith, Fault behavior and characteristic earthquakes: Examples from the Wasatch and San Andreas fault zones, *J. Geophys. Res.*, 89, 5681-5698, 1984.
- Scott, W. E., K. L. Pierce and M. H. Hait, Jr., Quaternary tectonic setting of the 1983 Borah Peak earthquakes, Central Idaho, preprint, 1984.
- Sibson, R. H., Roughness at the base of the seismogenic zone: Contributing factors, *J. Geophys. Res.*, 89, 5791-5799, 1984.
- Sieh, K. E., A study of Holocene displacement history along the south-central reach of the San Andreas fault, PhD dissertation, Stanford Univ., Stanford, California, 1977.
- Smith, R. B., Regional geophysics and intraplate tectonics of the Wyoming-Idaho-Utah thrust belt (abstract), paper presented at 29th Ann. Field Conf. and Sympos., Joint Wyoming-Montana-Utah Geol. Assoc., Jackson, Wyoming, 1977.
- Smith, R. B., Seismicity, crustal structure, and intraplate tectonics of the interior of the

- western Cordillera, *Mem. Geol. Soc. Am.*, 152, 111-144, 1978.
- Smith, R. B., Intraplate seismo-tectonics and mechanisms of extension in the western United States (abstract), paper presented at Chapman Conference on Fault Behavior and the Earthquake Generation Process, AGU, Snowbird, Utah, 1982.
- Smith, R. B., Kinematics and dynamics of an extending lithosphere: The Basin-Range (abstract), paper presented at Continental Extensional Tectonics conf., Geol. Soc. London, Univ. of Durham, U.K., 1985.
- Smith, R. B. and M. Sbar, Contemporary tectonics and seismicity of the western United States with emphasis on the Intermountain Seismic Belt, *Bull. Geol. Soc. of Am.*, 85, 1205-1218, 1974.
- Smith, R. B. and A. G. Lindh, Fault-plane solutions of the Western United States: A compilation, *Mem. Geol. Soc. Am.*, 152, 107-109, 1978.
- Smith, R. B. and R. L. Bruhn, Intraplate extensional tectonics of the Western U. S. cordillera: Inferences on structural style from seismic reflection data, regional tectonics and thermal/mechanical models of brittle/ductile deformation, *J. Geophys. Res.*, 89, 5733 - 5762, 1984.
- Smith, R. B. and W. Richins, Seismicity and earthquake hazards of Utah and the Wasatch Front: Paradigm and paradox, *U. S. Geol. Surv. Open-File Rep.*, 84-763, 73-112, 1984.
- Smith, R. B., P. K. Eddington and L. Leu, Strain rates in Utah from seismic moments, paleostrip and geodetic surveys (expanded abstract), *U. S. Geol. Surv. Open-File Rep.*, 84-763, 422-435, 1984a.
- Smith, R. B., W. D. Richins, D. I. Doser and J. C. Pechmann, The 1983 Borah Peak, Idaho, earthquake: A model for active crustal extension (abstract), paper presented at 97th Annual Meeting of The Geol. Soc. Am., Reno, Nevada, 1984b.
- Smith, R. L. and R. G. Luedke, Potentially active volcanic lineaments and loci in western conterminous United States, in *Explosive Volcanism: Inception, Evolution, and Hazards*, pp. 47-66, Nat. Res. Council, National Academy Press, Wash. D. C., 1984.
- Seay, R. A., R. B. Smith and T. Soler, Horizontal strain across the Wasatch Front near Salt Lake City, Utah, *J. Geophys. Res.*, 89, 1113-1122, 1984.
- Stewart, J. H., Basin-range structure in western North America: A review, *Mem. Geol. Soc. Am.*, 152, 1 - 31, 1978.
- Thatcher, W. and T. C. Hanks, Source parameters of southern California earthquakes, *J. Geophys. Res.*, 78, 8547-8576, 1973.
- Thenhaus, P. C. and C. M. Wentworth, Map showing zones of similar ages of surface faulting and estimated maximum earthquake size in the Basin and Range province and selected adjacent areas, *U. S. Geol. Surv. Open-File Rep.*, 82-742, 1982.
- Thompson, G. A. and D. B. Burke, Regional geophysics of the Basin and Range province, *A. Rev. Earth Planet. Sci.*, 2, 213-238, 1974.

- Tocher, D., The Dixie Valley-Fairview Peak earthquakes of December 16, 1954: Introduction, *Bull. Seismol. Soc. Am.*, 47, 299-300, 1957.
- Tarcotte, D. L. and G. Schubert, *Geodynamics: Applications of Continuum Physics to Geological Problems*, pp. 192, 432-433, John Wiley and Sons, New York, New York, 1982.
- Von Tish, D. B., R. W. Allmendinger and J. W. Sharp, History of Cenozoic extension in central Sevier Desert, west-central Utah, from COCORP seismic reflection data, *Bull. Am. Assoc. Petrol. Geol.*, 69, 1077-1087, 1985.
- Wallace, R. E., Patterns and timing of late Quaternary faulting in the Great Basin province and relation to some regional tectonic features, *J. Geophys. Res.*, 89, 5763-5769, 1984.
- Wernoucky, S. G., C. H. Scholz and K. Shimazaki, Deformation of an island arc: Rates of moment release and crustal shortening in intraplate Japan determined from seismicity and Quaternary fault data, *J. Geophys. Res.*, 87, 6829-6852, 1982a.
- Wernoucky, S. G., C. H. Scholz, K. Shimazaki and T. Matsuda, Earthquake frequency distribution and the mechanics of faulting, *J. Geophys. Res.*, 88, 9331-9340, 1982b.
- Wright, L., Late Cenozoic fault patterns and stress fields in the Great Basin and westward displacement of the Sierra Nevada block, *Geology*, 4, 489-494, 1976.
- Zoback, M. L. and Zoback, M. D., Faulting patterns in north central Nevada and strength of the crust, *J. Geophys. Res.*, 85, 275-284, 1980.
- Zoback, M. L., R. E. Anderson and G. A. Thompson, Cainozoic evolution of the state of stress and style of tectonism of the Basin and Range province of the Western United States, *Philos. Trans. R. Soc. London Ser. A*, 300, 407 - 434, 1981.

Preprints available from R. B. Smith, Department of Geology and Geophysics, University of Utah.

B5=(-0.0885,-0.084,-0.111) accs=-132° accqb=-10°
 B=(-0.113,0.194,0.931) accs=103° accqb=28°
 L5=(-0.018,-0.926,0.382) accs=-93° accqb=20°
 Uobj diuwei zflrke=521° qib=116° accs=193° accqb=-59°
 aibvac5=(-0.821,0.501,-0.482)

b1=(-0.819,-0.492,0.242) accs=-120° accqb=50°
 B=(-0.113,0.194,0.931) accs=103° accqb=28°
 l1=(-0.203,-0.441,0.104) accs=-36° accqb=42°
 Uobj diuwei zflrke=-26° qib=25° accs=-156° accqb=28°
 aibvac1=(-0.489,-0.915,0.919)

coefficient of inflexion (t1ctfow=0.800 ==> a1bpa=52.3 qadlase

SYNTHETIC EARLY PLANE SOLUTION

a1dunvecfo12=(-.035,-.561,0.045) accs=-192° accqb=21.2
 a1dunvecfo15=(-.113,0.194,0.931) accs=103° accqb=28°
 a1dunvecfo1=(-0.521,-.232,0.118) accs=-99° accqb=21.1
 E1dunvecfo1 combounef l=M, S=E, 2=0

a1dwa1=3.9e+5P a1dwa5=-5.5e+5I a1dwa2=-5.9e+5P
 E1dunv1nna1:

M21= 3.4e+5R M25= -1.1e+5P M22= 1.1e+5P q1ue-cw
 M31= -1.1e+5P M35= 9.2e+5R M32= -1.1e+5P
 M11= -5.5e+5P M15= -1.1e+5P M12= 3.4e+5R

Central Cellouls

 FROM A REGIONAL MOMENT TENSOR
 COMPUTATION OF A SYNTHETIC EARLY PLANE SOLUTION

The wavelength for sourceq dequomfion k2fs = 2.9e+01 mmyA

144.534
k2swr1:

--P4 0700
ENEE Ledou dompnaA kofr10:

A1 f1r1 1 1.1e+01VA 2.7e+12vec
 A1u1w1w1 souf1r1 1.1e+01VA 2.7e+12vec
 A1u1w1w1 souf1r1 1.1e+01VA 2.7e+12vec A1u1w1w1 INBLF
 The polarizati and vertical eflrke:

comb1er1r1r1:-1.5e-01VA = -4.9e-11vec
 inflexw1r1r1: 3.2e-14VA = 3.8e-11vec
 r1r1r1r1r1: 1.5e-01VA = 4.2e-11vec
 of the principal eflrke:

The absc1t1ed w1r1w1= 352.4815e+38 12.06w2

 DETERMINATION OF THE SLEWIN RATE:

OF POOR QUALITY
 ORIGINAL PAGE IS

B=1.0E+01 0.0E+00 0.0E+00 0.0E+00 1.0E+00 0.0E+00
 B=1.0E+01 0.0E+00 0.0E+00 0.0E+00 0.0E+00 1.0E+00
 L=1.0E+01 0.0E+00 0.0E+00 0.0E+00 0.0E+00 1.0E+00
 u=0.0E+00 0.0E+00 0.0E+00 0.0E+00 0.0E+00 0.0E+00
 a1b=0.0E+00 0.0E+00 0.0E+00 0.0E+00 0.0E+00 0.0E+00
 B=1.0E+01 0.0E+00 0.0E+00 0.0E+00 1.0E+00 0.0E+00
 B=1.0E+01 0.0E+00 0.0E+00 0.0E+00 0.0E+00 1.0E+00
 L=1.0E+01 0.0E+00 0.0E+00 0.0E+00 0.0E+00 1.0E+00
 u=0.0E+00 0.0E+00 0.0E+00 0.0E+00 0.0E+00 0.0E+00
 a1b=0.0E+00 0.0E+00 0.0E+00 0.0E+00 0.0E+00 0.0E+00
 coefficient of reference pressure = 0.000 (= 0) q1bpa = 0.000 q1dava =

GAUSSIAN ELEMENT PLANE SOLUTION:

e1p=0.0E+00 0.0E+00 0.0E+00 0.0E+00 0.0E+00 1.0E+00
 e1d=0.0E+00 0.0E+00 0.0E+00 0.0E+00 0.0E+00 0.0E+00
 e1d=0.0E+00 0.0E+00 0.0E+00 0.0E+00 0.0E+00 0.0E+00
 E1d=0.0E+00 0.0E+00 0.0E+00 0.0E+00 0.0E+00 0.0E+00

e1d=0.0E+00 0.0E+00 0.0E+00 0.0E+00 0.0E+00 0.0E+00
 E1d=0.0E+00 0.0E+00 0.0E+00 0.0E+00 0.0E+00 0.0E+00

M21 = 1.2E+03 M22 = 0.0E+00 M23 = 0.0E+00
 M21 = 2.0E+03 M22 = 0.0E+00 M23 = 0.0E+00
 M11 = -0.4E+03 M12 = 2.0E+03 M13 = 1.2E+03
 Regional moment tensor:

g=1.0E+00

COMPUTATION OF A REGIONAL MOMENT TENSOR SOLUTION

FROM A REGIONAL MOMENT TENSOR

The maximum horizontal deformation rate = 1.1E+00 mm/yr

85.8426
L=0.0000

ENTER REGIONAL DEFORMATION LOGSTATION

Vertical 1 2.4E+06/yr = 1.1E+19/sec
 Minimum horizontal 3.2E+06/yr = 1.0E+13/sec
 Maximum horizontal -2.0E+06/yr = -1.8E+19/sec
 The horizontal and vertical strain rates:

compression -2.0E+06/yr = -1.7E+13/sec
 extension 1.0E+06/yr = 0.7E+13/sec
 extension 1.2E+06/yr = 1.1E+13/sec

The strain rates for the test 80.0 years in the direction

The specified volume = 205.34194 cm³ @ 0.96 g/cm³

DETERMINATION OF THE STRAIN RATE


```

B5=(-0.201, 0.110, 0.828)  accs= 188.  accqb= 26.
B=(-0.433,-0.832, 0.324)  accs= -82.  accqb= 31.
L5=( 0.129, 0.224, 0.215)  accs= 29.  accqb= 35.
uobj1 b1uobj1 q1r1k= -80.  q1b= 25.
  atbvec5=(-0.114,-0.124, 0.815)  accs=-130.  accqb= 28.
b1=( 0.081, 0.433, 0.402)  accs= 141.  accqb= 82.
B=( 0.433,-0.832, 0.324)  accs= -82.  accqb= 31.
L=( 0.402, 0.225, 0.249)  accs= 31.  accqb= -14.
uobj1 b1uobj1 q1r1k= 126.  q1b= 42.
  atbvec1=( 0.484, 0.224, 0.303)  accs= 46.  accqb= 42.
coefficient of internal friction= 0.800  =>  atbpa= 32.1  qdulse
SYNTHETIC ENFLT PLANE SOLUTION:
  eidauvecfor_2=(-.332,0.582,0.823)  accs= 158.2  accqb= 88.9
  eidauvecfor_5=(0.433,-.832,0.324)  accs= -82.5  accqb= 30.1
  eidauvecfor_1=(0.832,0.435,0.093)  accs= 58.5  accqb= 2.8
  eidauvecfor_4 compound I=M, S=e, Z=A
  atdwa1= 2.2e+5p  atdwa5= -2.0e+50  atdwa2= -2.2e+5p
  eidauvecfor_3=
M21= 8.8e+52  M23= -1.1e+52  M22= -5.9e+5p  qvne-cw
M31= 1.9e+5p  M33= 4.1e+52  M32= -1.1e+52
M11= 5.9e+5p  M13= 1.9e+5p  M12= 8.8e+52
Reduobj1 mouuef fauobj1
Comp[r]1 qsbpc
*****

```

COMPUTATION OF A REGIONAL MOMENT TENSOR

FROM A REGIONAL MOMENT TENSOR

COMPUTATION OF A SYNTHETIC ENFLT PLANE SOLUTION

The maximum horizontal displacement rate = 1.5e+00 mm/yr

NAZREV
L22000

ENTER region parameters

Velocity : 4.8e 03/yr 1.9e 1p/sec utime: 10.7E
 Minimum horizontal : 1.2e 10/yr 5.3e 1p/sec utime: 10.7E
 Maximum horizontal : 2.0e 03/yr 1.9e 1p/sec utime: 10.7E

The horizontal and vertical strain rates:

comp[er]at[ion]: 4.2e 03/yr 1.2e 1p/sec
 t[er]m[inal] r[ate]: 2.1e 12/yr -4.1e 1p/sec
 of the principal stresses

The strain rates for the 1st 3d of vectors in the directions

The specified volume= 1.4e 48.52.2e 12.01m³

 DETERMINATION OF THE STRAIN RATE:


```

B3=( 0.4237,-0.2847, 0.816)   accel= -45.   accelb= 22.
B=( 0.6247, 0.1267, 0.008)   accel= 44.   accelb= 0.
L5=(-0.6507, 0.2207, 0.218)   accel= 134.  accelb= 22.
uobj1 b1uobj1 accel= 44.  q1b= 41.   accel= -41. accelb= 54.
a1bvecS=( 0.6247,-0.2207, 0.482)   accel= 140. accelb= 41.

b1=( -0.0447, 0.0327, 0.448)   accel= 141.  accelb= 81.
B=( 0.6247, 0.1267, 0.008)   accel= 44.   accelb= 0.
L1=(-0.1227, 0.8247,-0.028)   accel= 124.  accelb= -2.
uobj1 b1uobj1 accel= 220.  q1b= 54.   accel= 140. accelb= 41.
a1bvec1=(-0.217, 0.215, 0.812)   accel= 140. accelb= 41.

coefficients of inflexion (injection=0.800 =>) a1bvec= 52.1 qobj= 44

```

SYNTHETIC EWLFL PLANE SOLUTION

```

a1dnuvecfcl_3=( 0.5027,-.181, 0.461)   accel= -45.4  accelb= 24.0
a1dnuvecfcl_5=( 0.6247, 0.1267, 0.008)   accel= 44.1  accelb= 0.2
a1dnuvecfcl_1=(-.1287, 0.8237, 0.224)   accel= 124.2  accelb= 14.0
a1dnuvecfcl_1=comboufcl_1=M*5=4.2=4
a1dnuvecfcl_1=1.54+54 a1dnuvecfcl_1=4.94+11 a1dnuvecfcl_1=-1.54+54

```

EIDNUVSIJNANI

```

M21= -4.94+52 M25= 4.14+52 M22= -6.44+52 q1dnu-cw
M31= -4.94+52 M35= 4.54+52 M32= 4.14+52
M11= 2.24+52 M15= -4.94+52 M12= -4.94+52
Regional moment tensor:

```

M20MUD

```

*****
FROM A REGIONAL MOMENT TENSOR
COMPUTATION OF A SYNTHETIC EWLFL PLANE SOLUTION

```

The maximum horizontal deformation rate = $4.3e+00$ mm/yr
10.2225
L5obj1:

ENTER leftou ponuqkA Lofajclou

Vertical : -3.0e-03VA = 1.1e-12/sec

Minimum horizontal: -3.0e-12VA = 1.1e-12/sec

Maximum horizontal: 3.0e-03VA = 1.1e-12/sec

The horizontal and vertical strain rates:

comb1 eastonj1: -4.1e-08VA = -2.3e-12/sec

inf1 westonj1: 5.1e-14VA = 2.3e-12/sec

inf2 westonj1: 4.1e-08VA = 2.3e-12/sec

The strain rates for the 1987 40.0 years in the direction

The specified values = 12.4e+00 or 12.0km/yr

DETERMINATION OF THE STRAIN RATE

```

k3=( 0.44e+0.288, 0.80e)      vccs3=-41.      vccq1b= 24.
B=(-0.842,-0.524, 0.72e)      vccs4=-144.     vccq1b= 55.
L3=(-0.09e+0.884, 0.4e2)      vccs5= 44.      vccq1b= 58.
L2q1 b1uq1s1 r1r1e= 20. q1b= 28.
e1b1vccs=( 0.421,-0.122, 0.25) vccs6=-40. vccq1b= 25.
B1=( 0.201, 0.344, 0.41e)      vccs7= 24.      vccq1b= 41.
B=(-0.842,-0.524, 0.72e)      vccs8=-144.     vccq1b= 55.
L1=(-0.220, 0.422,-0.142)      vccs9= 104.     vccq1b= -8.
L2q1 b1uq1s1 r1r1e= 168. q1b= 40. vccs10= 18. vccq1b= -8.
e1b1vccs=( 0.124, 0.654, 0.14e) vccs11= 18. vccq1b= 20.
coefficient of inflexion {r1r1e}=0.800 ==> q1b1u= 52.1 qe1e=
SYNTHETIC ENFLI PLANE SOLUTION
e1d1u1vccf1=2=(0.244,-0.014, 0.414) vccs12=-10.2 vccq1b= 44.1
e1d1u1vccf1=3=(-.842,-.524,0.72e) vccs13=-142.8 vccq1b= 51.4
e1d1u1vccf1=4=(-.510,0.492,0.19e) vccs14= 105.2 vccq1b= 4.8
E1d1u1vccf1=compouf1=M1, S=1, 2=1
e1d1u1= 1.2e+52 e1d1u2=-5.6e+14 e1d1u3=-1.2e+52
E1d1u1v1n=1
M21= -2.78e+54 M23=- 2.4e+54 M22= -1.58e+52 q1u1e-cw
M31= -5.2e+54 M33= 1.2e+52 M32= 2.4e+54
M11= -1.2e+54 M13= -5.2e+54 M12= -2.78e+54
Regions1 uowouf feuo1.1
Boq1 qbl1u1d
*****
FROM A REGIONAL MOMENT TENSOR
COMPUTATION OF A SYNTHETIC ENFLI PLANE SOLUTION

```

```

The maximum horizontal displacement rate = 4.6e-05 mm/yr
4.0-2313
L2SWK
ENTER nodon number, location
of
vertical displacement rate = -1.4e-11/sec
Minimum horizontal displacement rate = -1.4e-11/sec
Maximum horizontal displacement rate = 1.4e-11/sec
of the direction of strain rate
The horizontal and vertical strain rates
compr1=0.2e-10/yr = -2.4e-12/sec
inflex1=4.2e-10/yr = 4.6e-11/sec
exp1=0.2e-10/yr = 2.4e-12/sec
of the direction of strain rate
The specified volume= 111.14111111111111 12.04e2
*****
DETERMINATION OF THE STRAIN RATE:

```

```

B2=( 0.433, 0.223, 0.041)   accs= 50.   accqib= 2.
B=(-0.122, 0.110, 0.082)   accs= 141.  accqib= 80.
L3=( 0.235, -0.632, 0.143)  accs=-31.  accqib= 4.
uobj1 b1uobj1 eflr1a= 122. q1b= 80.
ajlvacc5=( 0.302, 0.304, 0.013)  accs= 42. accqib= 1.
b1=( 0.433, -0.230, 0.194)   accs= -14.  accqib= 4.
B=(-0.122, 0.110, 0.082)   accs= 141.  accqib= 80.
uobj1 b1uobj1 eflr1a= 122. q1b= 80.
ajlvacc1=( 0.498, -0.498, 0.114)  accs= -42. accqib= 10.
coefficients of inflexion t1c1c1a= 0.800 ==> ajlvacc= 32.3 qdvacc=
SYNTHETIC EARTH PLWME SOLUTION!
ajlvaccfor2=( 0.441, 0.004, 0.122)  accs= 0.2   accqib= 3.8
ajlvaccfor3=( -1.22, 0.110, 0.082)  accs= 140.3  accqib= 80.0
ajlvaccfor1=( -1.008, -1.044, 0.111)  accs= -40.2  accqib= 4.4
Eidlvaccfor1 combouanf 1a1, 3aE, 2aV
ajlvacc1= 1.2a+3p   ajlvacc2= 2.2a+1b   ajlvacc3= -1.2a+3p
Eidlvacc1a1

```

```

M21= -1.8a+3z   M25= -1.2a+3z   M22= -1.4a+3z
M31= -4.0a+3z   M33= 1.2a+3p   M32= -1.2a+3z
M11= -1.2a+3p   M13= -4.0a+3z   M12= -1.8a+3z
Regional moment tensor,

```

Northrup Cal. Nevada porqer.

FROM A REGIONAL MOMENT TENSOR
COMPUTATION OF A SYNTHETIC EARTH PLWME SOLUTION

```

The maximum horizontal displacement is: a = 4.2a-01 mm/VL
BP. 3000
L. 2aax
0.
ENTER region parameters, a1a1a1a1
velcty 1 -5.3a-0aVL = -8.9a-13.3acc
Minimum horizontal 1 -8.3a-13.3VL = -5.8a-14.4acc
Maximum horizontal 5.3a-0aVL = 8.9a-13.3acc
Azimuthal 182W
The horizontal and vertical first lags:
combouanf1-5.8a-0aVL = -2.3a-12.3acc
inflexion1 1-2.3a-12.3VL = -1.1a-50.3acc
ax1a1a1a1 1 5.8a-0aVL = 2.3a-12.3acc
of the principal stresses
The first lags for the first 80.0 years in the direction
The specified volume 199.3a199.3a 12.0km2
*****
DETERMINATION OF THE STRAIN RATE!

```


B5=(-0.222'-0.263' 0.000) accs=-135' accqib= 25'
 B = (0.020' 0.199' 0.145) accs= 14' accqib= 48'
 L5=(-0.245' 0.182' 0.200) accs= 152' accqib= 15'
 uobj1 b1uobj1 sfl1k1=-19' qib= 99' accs=-109' accqib= 54'
 a1b1uobj5=(-0.549'-0.818' 0.411) accs= 138' accqib= 41'
 b1=(-0.122' 0.352' 0.029) accs= 14' accqib= 48'
 B = (0.020' 0.199' 0.145) accs= 82' accqib= -8'
 L1=(-0.040' 0.089' -0.141) accs= 28' qib= 28'
 uobj1 b1uobj1 sfl1k1= 528' qib= 28' accs= 148' accqib= 25'
 a1b1uobj1=(-0.119' 0.449' 0.220) accs= 148' accqib= 25'
 coefficient of refraction= 0.800 => a1b1s= 52.3 qel1s=

SYNTHETIC FRONT PROFILE SOLUTION

a1duv1uobj2=(-.085'-1.207'0.002) accs'= -129'-1' accqib= 41.7'
 a1duv1uobj5=(0.020'0.199'0.145) accs'= 14'2" accqib= 45.6'
 a1duv1uobj1=(-.222'0.228'0.084) accs'= 109'9" accqib= 4.8'
 E1duv1uobj1 combouurf 1=M' 5=E' 2=V
 a1duv1uobj1= 1.4e+53 a1duv1s= 1.2e+53 a1duv1z= -1.4e+53
 E1duv1uobj1=

M21= 9.1e+39 M23= 4.0e+39 M22= -9.2e+39 q1u1e-cu
 M31= -1.2e+39 M33= 1.1e+33 M32= 4.0e+39
 M11= -2.1e+39 M13= -1.2e+39 M12= 9.1e+39

Morf-Gouf1j1 j1e1q3

FROM A REGIONAL MOMENT TENSOR
 COMPUTATION OF A SYNTHETIC FRONT PROFILE SOLUTION

The maximum horizontal displacement r1s = 1.0e+00 mm/VL

52.9133

L23W3X

-94.0000

ENTER led1u ponuq1A Lof1c1u

vef1c1j

Maximum horizontal displacement = -1.5e-18Vacc

Maximum horizontal displacement = -5.0e-19Vacc Az1m1g1h1 N OE

The horizontal and vertical surface waves:

comb1e1o1u1j1-9.0e-04VL = -1.5e-15Vacc

1u1e1u1e1q1i1 5.1e-19VL = 4.8e-50Vacc

sk1e1u1o1u1j 1 9.0e-04VL = 1.5e-15Vacc

of the principal stresses:

The stress r1s for the first 12.0 years in the direction

The absolute value= 52.9133 in 12.0yr

DETERMINATION OF THE STRAIN RATE

b5=(-0.2227,-0.263, 0.000) vecs5=-125. vecq1b= 23.
 B=(-0.020, 0.199, 0.143) vecs4= 14. vecq1b= 48.
 L5=(-0.245, 0.182, 0.200) vecs3= 152. vecq1b= 13.
 uobj1 b1uobj1 q1r1k=-19. q1b= pp.
 a1bvec3=(-0.349,-0.838, 0.411) vecs2=-109. vecq1b= 54.

b1a(-0.332, 0.032, 0.029) vecs1= 138. vecq1b= 41.
 B=(-0.020, 0.199, 0.143) vecs2= 14. vecq1b= 48.
 L1a(-0.040, 0.089,-0.141) vecs3= 62. vecq1b= -8.
 uobj1 b1uobj1 q1r1k= 528. q1b= 28.
 a1bvec1=(-0.319, 0.449, 0.220) vecs2= 148. vecq1b= 25.

coefficients of inflexion t1c1c1on= 0.800 ==> a1b1u= 527.3 qed1ee

SYNTHETIC ENFLI PLANE SOLUTION:

a1dauvecfoc2a=(-.985,-.302,0.092) vecs1=-129.1 vecq1b= 41.3
 a1dauvecfoc3a=(0.920,0.199,0.143) vecs2=- 14.2 vecq1b= 43.6
 E1dauvecfoc1a=(-.222,0.022,0.084) vecs3=- 109.9 vecq1b= 4.8
 E1dauvecfoc1a1 compound 1=M. S=E. 2=V
 a1dwa1= 1.3e+53 a1dwa2=-2.1e+51 a1dwa3=-1.3e+53
 E1dauv1nwa1

M21= 3.4e+59 M25= 4.9e+59 M22= -3.9e+59
 M31= -6.0e+59 M35= 1.4e+53 M32= 4.4e+59 q1ue-cw
 M11= -9.1e+59 M15= -6.0e+59 M12= 3.4e+59

Heef-Couf1a1 Nawaq (1ar1e wad1ur1eae)

FROM A REGIONAL MOMENT TENSOR

COMPUTATION OF A SYNTHETIC ENFLI PLANE SOLUTION

The maximum horizontal deformation rate = 3.2e+00 mm/yr

4.81436
L5w1w

-94.0000

ENTER REGION POINTS AND LOCATIONS

Velocities 1 -1.4e-08/yr. = -4.4e-19/sec

Minimum horizontal 1-1.8e-08/yr. = -2.9e-19/sec V1u1n1f1 N1S1E

Maximum horizontal 2.5e-08/yr. = 1.0e-12/sec V1u1n1f1 N1W1M

The horizontal and vertical strain rates

comp1a1a1a1a1-2.5e-08/yr. = -2.7e-13/sec

1u1e1w1e1r1e 1 2.0e-12/yr. = 2.4e-13/sec

ex1t1e1n1o1n1 1 2.5e-08/yr. = 2.7e-13/sec

of the horizontal extension

the strain rates for the last 2e+0 years in the direction

The specified volume 529.2K524.9K 12.0Kw2

DETERMINATION OF THE STRAIN RATE

```

B3=( 0.000, 0.010, 0.000)   aaccs= 52.   aecqb= 0.
B=( -0.000,-0.010, 1.000)   aaccs= -d1.  aecqb= B0.
L3=( -0.010, 0.000, 0.010)   aaccs= 112.  aecqb= 1.
uobj b1uaj1 g1k1k= B0. q1b= d0.
a1bvacc5=( 1.000,-0.010, 0.000)   aaccs= -1. aecqb= 0.

```

```

b1=( 0.000, 0.000, 0.010)   aaccs= q2.   aecqb= 1.
B=( -0.000,-0.010, 1.000)   aaccs= -d1.  aecqb= B0.
L1=( -0.000, 0.000, 0.000)   aaccs= 122.  aecqb= 0.
uobj b1uaj1 g1k1k= 120. q1b= B0.
a1bvacc1=( 0.010, 1.000, 0.010)   aaccs= B0. aecqb= 1.

```

coefficient of internal friction= 0.000 ==> a1bu= 52.0 qeclacc

SYNTHETIC EARTH PLANE SOLUTION:

```

a1dvaccfor2=( 0.010, 0.000, 0.010)   aaccs= 44.0   aecqb= 0.0
a1dvaccfor3=( -0.000,-0.010, 1.000)   aaccs= -d1.0   aecqb= B0.0
a1dvaccfor1=( -0.000, 0.010, 0.010)   aaccs= 124.0   aecqb= 0.0
E1dvaccfor1= combouf 1=M1. S= E1. 2=V
a1dvacc1= 1.2e+39   a1dvacc2= -1.4e+10   a1dvacc3= -1.2e+39
E1dvacc1=

```

```

M21= -5.2e+39   M22= 4.1e+33   M23= -4.1e+10   qvacc=cm
M31= -1.2e+39   M32= 4.3e+34   M33= 4.1e+33
M11= -4.2e+39   M12= -1.2e+39   M13= -5.2e+39
Region1= combouf feouf1

```

Major Axis

 COMPUTATION OF A REGIONAL MOMENT TENSOR
 FROM A REGIONAL PLANE SOLUTION

The maximum horizontal deformation rate = 0.1e+00 mm/yr

4.81442
 L=mm

-P4.0000
 ENTER region number location

```

A=cc1c1   1 -1.1e-08\yr = -2.4e-19\sec
Minimum horizontal: 5.2e-08\yr = -0.8e-19\sec
Maximum horizontal: 2.8e-08\yr = 1.2e-12\sec
Minimum horizontal: 1.2e-08\yr = 0.2e-15\sec
Maximum horizontal: 2.8e-08\yr = 1.2e-12\sec
Minimum horizontal: 1.2e-08\yr = 0.2e-15\sec

```

Combination1-2.0e-08\yr = -0.0e-15\sec
 Internal rate 1-1.1e-12\yr = -5.0e-13\sec
 expansion 1 2.0e-08\yr = 0.0e-15\sec
 of the principal stresses
 The strain rates for the 1st 12.0 year in the direction

The absolute value= 32e.2x524.0x 12.0km2

 DETERMINATION OF THE STRAIN RATE

```

b3=( 0.90d+0.41\ 0.008)   vacas= 32.   vacqib= 0.
B=(-0.000,-0.01\ 1.000)   vacas=-d1.   vacqib= Bb.
L3=(-0.41\ 0.90d+0.01e)   vacas=112.   vacqib= 1.
uqaj b1uaj sp1k= Bb' qib= d0.   vacas= -1.   vacqib= 0.
a1bvac5=( 1.000+0.01\ 0.000)   vacas= 0.
b1=( 0.44d+0.8d\ 0.01e)   vacas= p2.   vacqib= 1.
B=(-0.000,-0.01\ 1.000)   vacas=-d1.   vacqib= Bb.
uqaj b1uaj sp1k= 1\3' qib= Bb'.   vacas=122.   vacqib= 0.
a1bvac1=( 0.01\ 1.000+0.01\ 1.000)   vacas= Bb'.   vacqib= 1.
coefficients of inflexion treflexion= 0.800 ==> a1b1u= 32.1 qad= 32

```

SYNTHETIC EWL1 PLANE SOLUTION

```

a1duvacfor3=(0.1d+0.9d\ 0.015)   vacas= 44.0   vacqib= 0.1
a1duvacfor5=(-0.000,-0.01\ 1.000)   vacas= -d1.0   vacqib= Bb.0
a1duvacfor1=(-.9d+0.1d\ 0.015)   vacas= 124.0   vacqib= 0.1
Eiduvacfor1= compouf 1=H' S=H' 2=H
a1duaj= 1.2e+3e a1duaj5= -1.2e+1\ a1duaj2= -1.2e+3e
Eiduvaj1uaj

```

```

M21= -5.3e+3d M22= 2.8e+35 M23= -2.8e+1\ qvuc=cw
M31= -1.2e+3e M32= 4.4e+3d M33= 2.8e+35
M1= -4.4e+3d M12= -1.2e+3e M13= -5.3e+3d
Radiouj mouuf fawor1

```

W1k= 1.0u (H+ avuuf ouj\)

FROM A REGIONAL MOMENT TENSOR
COMPUTATION OF A SYNTHETIC EWL1 PLANE SOLUTION

The maximum horizontal deformation rate = 5.3e+00 mm\yr

```

-18.0000
Lazwax
-94.0000
ENTER latlon poudary location
vertics 1 -1.2e-1\yr = -4.1e-32\sec Astimf1 NENE
Minimum horizontal 4.3e-0d\yr = -1.2e-1e\sec Astimf1 NENE
Maximum horizontal 4.3e-0d\yr = 1.2e-1e\sec Astimf1 NENE
The horizontal and vertical strain rates

```

```

comb= a1uaj1-4.3e-0d\yr = -0.1e-12\sec
inflexion1= 4.2e-18\yr = -0.1e-35\sec
exp= a1uaj1 4.3e-0d\yr = 4.3e-12\sec

```

of the principal stresses

The strain rates for the last 11.0 years in the directions

The abscissed volume p1.4k pB.6x 12.0kx2

DETERMINATION OF THE STRAIN RATE

DETERMINATION OF THE STRAIN RATE:

The specified volume = 661.4x 68.6x 12.0km³

The strain rates for the last 71.0 years in the directions of the principal stresses:

extensional: 2.9e-09/yr = 6.7e-13/sec
intermediate: -4.0e-18/yr = -6.4e-22/sec
compressional: -2.9e-09/yr = -6.7e-13/sec

The horizontal and vertical strain rates:

Maximum horizontal: 2.9e-09/yr = 1.2e-16/sec
Minimum horizontal: -2.9e-09/yr = -1.2e-16/sec
Vertical: -1.2e-17/yr = -3.8e-25/sec

ENTER region boundary rotation
-64.0000
-18.0000
-44.0000
-18.0000

The maximum horizontal deformation rate = 2.7e+00 mm/yr

COMPUTATION OF A SYNTHETIC FAULT PLANE SOLUTION
FROM A REGIONAL MOMENT TENSOR

Southeast Nevada

Regional moment tensor:

M11 = 1.9e+25	M12 = -1.8e+25	M13 = -5.6e+24
M21 = -1.8e+25	M22 = -1.7e+25	M23 = -6.5e+24
M31 = -5.6e+24	M32 = -6.5e+24	M33 = -1.9e+24

Eigenvalues:

sigma1 = 2.6e+25 sigma2 = 5.0e+17 sigma3 = -2.6e+25

Eigenvectors component i=N, 2=E, 3=W

eigenvector 1 = (-.927, 0.272, 0.002)	vecax = 128.0	vecby = 0.1
eigenvector 2 = (-.098, -.249, 0.964)	vecax = -111.2	vecby = 74.2
eigenvector 3 = (0.282, 0.892, 0.287)	vecax = 67.9	vecby = 12.2

SYNTHETIC FAULT PLANE SOLUTION:

coefficient of internal friction = 0.800 ==> alpha = 32.7 degrees

nodal planes: strike = 112. dip = 79. vecax = 129. vecby = 2. vcp = 74.2

12 = (-0.922, 0.620, 0.091) vecax = 129. vecby = 2. vcp = 74.2

8 = (-0.098, -0.249, 0.964) vecax = -111.2 vecby = 74.2 vcp = 12.2

P1 = (0.022, 0.647, 0.252) vecax = 88. vecby = 12.2 vcp = 11.1

nodal planes: strike = 504. dip = 79. vecax = 114. vecby = 11.1

11 = (-0.299, 0.897, 0.191) vecax = 114. vecby = 11.1

LE (0.0025, 0.0005, 0.0170) 0.0000 0.0000 0.0000
B (0.0000, 0.0000, 0.0000) 0.0000 0.0000 0.0000
L (0.0114, 0.0000, 0.0000) 0.0000 0.0000 0.0000
UR (0.0000, 0.0000, 0.0000) 0.0000 0.0000 0.0000
E (0.0000, 0.0000, 0.0000) 0.0000 0.0000 0.0000

LE (0.0112, 0.0000, 0.0000) 0.0000 0.0000 0.0000
B (0.0000, 0.0000, 0.0000) 0.0000 0.0000 0.0000
L (0.0000, 0.0000, 0.0000) 0.0000 0.0000 0.0000
UR (0.0000, 0.0000, 0.0000) 0.0000 0.0000 0.0000
E (0.0000, 0.0000, 0.0000) 0.0000 0.0000 0.0000

coefficient of refraction (refractive index) = 1.0000
coefficient of refraction (refractive index) = 1.0000
coefficient of refraction (refractive index) = 1.0000

EMITTER POSITION SOLUTION:

OF BOOK QUALITY
ORIGINAL PAGE 18

E (0.0000, 0.0000, 0.0000) 0.0000 0.0000 0.0000
B (0.0000, 0.0000, 0.0000) 0.0000 0.0000 0.0000
L (0.0000, 0.0000, 0.0000) 0.0000 0.0000 0.0000
UR (0.0000, 0.0000, 0.0000) 0.0000 0.0000 0.0000
E (0.0000, 0.0000, 0.0000) 0.0000 0.0000 0.0000

E (0.0000, 0.0000, 0.0000) 0.0000 0.0000 0.0000
B (0.0000, 0.0000, 0.0000) 0.0000 0.0000 0.0000
L (0.0000, 0.0000, 0.0000) 0.0000 0.0000 0.0000
UR (0.0000, 0.0000, 0.0000) 0.0000 0.0000 0.0000
E (0.0000, 0.0000, 0.0000) 0.0000 0.0000 0.0000

COMPUTATION OF A GEOMETRIC MOMENT VECTOR
FROM A GEOMETRIC MOMENT VECTOR

The maximum horizontal deflection rate = 3.5e-01 um/yr

53.0P31

Lasnik

0°

ENTER REGION POINTS LIST

Vertical 1 -5.5e-10/yr = -0.9e-18/sec
Minimum horizontal 2.0e-08/yr = 0.9e-13/sec
Maximum horizontal 2.0e-08/yr = 0.9e-13/sec
Vertical 2.0e-08/yr = 0.9e-13/sec
Minimum horizontal 2.0e-08/yr = 0.9e-13/sec
Maximum horizontal 2.0e-08/yr = 0.9e-13/sec

Combined 2.0e-08/yr = -3.7e-12/sec
Vertical 1 3.5e-11/yr = 1.9e-51/sec
Horizontal 1 3.0e-08/yr = 3.7e-12/sec
Combined 2.0e-08/yr = -3.7e-12/sec

The strain rate for the first 43.0 years in the direction
the specified volume is 1.2e-04

DETERMINATION OF THE STRAIN RATE

```

aug
  lefmlu
20  p(i) = p(i)\v(i,i)
40  coufjune
20  coufjune
    p(i) = p(i) + a(i,k)ef
    go 20 i = i + kmj
    f = -p(k)
    p(k) = p(k)\v(k,k)

```

```

    k = kmj+1
    kmj = n-kp
    go 40 kp = i+umj
50  coufjune
    p(i) = p(i) + a(i,k)ef
    go 10 i = i+1 u
    p(k) = f
    p(w) = p(k)
    f = p(w)
    w = i+vc(k)
    kbi = k+1
    go 50 k = i + umj
    umj = n-1
    i = (u + ed - 1) do fo 20
  lemj f
  iufedek kp kmj umj kbi i k w
  lemj a(i0,i0)p(u)
  iufedek u ibvf(u)
  erploofjune sojve(u' s' p' ibvf)
  c sojve iz {low s wafj iip,sla
  *****
aug
  lefmlu
20  coug = 1.0e+25
    i = (i+1) *um' 0.0) lefmlu
80  coug = 1.0
  lefmlu
    i = (coug *if' 1.0) coug = 1.0
    coug = suolwastuolw\Aulow
  coufjune
    suolw = suolw + spe(mol,k(i))
    go 20 i = i + u
    suolw = 0.0
  eaj sojve(u' s' mol,k' ibvf)

```

relations associated with α and the two nodal planes. This is done using:

It is to find the matrix of direction cosines needed to produce the two possible principal stress orientations.

Now that the principal stresses have been found, we can use a coefficient of friction.

Use of the Mohr circle to solve systems of linear equations [Fitzpatrick et al. 1951].

and then solved using the matrix inversion, 'descent', and 'solve'. These operations

$$\begin{bmatrix} b_{11} & b_{12} & b_{13} \\ b_{21} & b_{22} & b_{23} \\ b_{31} & b_{32} & b_{33} \end{bmatrix} \begin{bmatrix} z_1 \\ z_2 \\ z_3 \end{bmatrix} = \begin{bmatrix} \cos 42 \\ 0 \\ \cos(42 + (1-1)(90)) \end{bmatrix} \quad (12)$$

which can be rearranged for solution as

$$I = I'Z \quad (\text{C. Kenney, unpublished data 1982})$$

$$z_1 \cdot b_{11} = \cos 42$$

$$z_1 \cdot b_{12} = \cos(42 + (1-1)(90)) \quad (14)$$

$$z_1 \cdot b_{13} = 0$$

Then, for each nodal plane, find a slip vector using

referred to now as b_1 , b_2 , and b_3 (found in matrix, through diagonalization of the moment

in order to find the slip plane solution, then identify the b_1 , b_2 and b_3 axes (the eigenvectors

$z =$ slip vector.

$b_1 =$ compression axis

$b_2 =$ intermediate axis

$b_3 =$ tension axis

Then, note the slip plane for the vectors used:

Slip plane solution using the principal stress axes determined either by the program or following:

matrix, is able to generate slip plane solutions and construct a slip plane

Constructing a Slip Plane Solution

stress and strain.

Now, to the construction of the slip plane solution, not in conjunction of

which nodal plane is considered to be the slip plane. Note that it is only allowed to be

two possible sets of b_1 , b_2 and b_3 axes. Which set of axes is considered correct depends on

In Fig 2, the information on the slip plane solution is given along with

and solved for b_1 and b_2 , then as done for b_3 , respectively.

$$\begin{bmatrix} z_1 & z_2 & z_3 \\ b_1 & b_2 & b_3 \\ b_4 & b_5 & b_6 \end{bmatrix} \begin{bmatrix} z_1 \\ z_2 \\ z_3 \end{bmatrix} = \begin{bmatrix} \cos(90 + (-1), \alpha) \\ 0 \\ \cos(42 - \alpha) \end{bmatrix} \quad (15)$$

and

$$\begin{bmatrix} z_1 & z_2 & z_3 \\ b_1 & b_2 & b_3 \\ b_4 & b_5 & b_6 \end{bmatrix} \begin{bmatrix} z_1 \\ z_2 \\ z_3 \end{bmatrix} = \begin{bmatrix} \cos \alpha \\ 0 \\ \cos(42 - \alpha) \end{bmatrix} \quad (16)$$

which can be written as

$$I = I'Z \quad (\text{C. Kenney, unpublished data 1982})$$

$$c) \quad b_1 \cdot z_1 = \cos \alpha \quad \quad b_2 \cdot z_1 = \cos(90 + (-1), \alpha)$$

$$d) \quad b_1 \cdot b_2 = 0 \quad \quad b_1 \cdot b_3 = 0 \quad (17)$$

$$e) \quad b_1 \cdot b_4 = \cos(42 - \alpha) \quad \quad b_1 \cdot b_5 = \cos(42 - \alpha)$$

and the equations

$$\alpha = \frac{\sum_{i=1}^n \tau_i}{I} \quad (18)$$

ΕΛΛΗΝΙΚΗ ΓΕΩΓΡΑΦΙΚΗ ΕΤΑΙΡΕΙΑ
ΕΛΛΗΝΙΚΟ ΓΕΩΓΡΑΦΙΚΟ ΚΕΝΤΡΟ ΣΤΑΘΙΩΝ ΚΑΙ
ΑΡΧΕΙΩΝ

ΑΠΕΝΔΙΧΙΟ C

- 1: 1928-1980 ΕΠΕ (ΠΣΟΟ2-ΠΣΟ2)
 - 2: 1928-1980 ΕΠΕ (ΠΣΟΟ2-ΠΣΟ2)
 - 3: Εθνικό Γεωφυσικό και Σεισμολογικό Κέντρο - Β. Μ. Κινητήρι - 4 Είδη κειμένων
- 1900 - 1980 σεισμικά κείμενα από 1900 - 1930
- 2) Πανεπιστήμιο Μεταλλωρύχων, Λεωφόρος
- 1900 - 1981 συμπεριλαμβανομένου 1983 Βόρειο Επείρω: 1980 σεισμικά κείμενα
- 1) Πανεπιστήμιο Μεταλλωρύχων, Σεισμολογικό Κέντρο

Είδη κειμένων:

κείμενα που είναι 10 δευτερόλεπτα και μικρότερα από 12 km με καταγεγραμμένα σεισμογράμματα

1983 Βόρειο Επείρω: 1980 κείμενα που είναι από 10000 κείμενα: Αυτά είναι σεισμικά κείμενα που είναι καταγεγραμμένα με τον σεισμολογικό κωδικό. Τα κείμενα που είναι σε χρονολογική σειρά, κείμενα που είναι καταγεγραμμένα και τα κείμενα που είναι σε χρονολογική σειρά. Τα κείμενα που είναι καταγεγραμμένα (1983) είναι καταγεγραμμένα στο Εθνικό Κέντρο.

(ΠΣΟΟ2 - ΠΣΟ2), που είναι καταγεγραμμένα από Κινητήρι στο Εθνικό Γεωφυσικό και Σεισμολογικό Κέντρο. Όταν τα κείμενα είναι καταγεγραμμένα, το κλειδί που είναι καταγεγραμμένο ΕΠΕ καταγεγραμμένο το κ. Κείμενα από άλλα κείμενα που είναι καταγεγραμμένα στο κλειδί που είναι καταγεγραμμένα στο κείμενο της δημιουργίας του κειμένου, ένα κείμενο που είναι καταγεγραμμένο και τα κείμενα που είναι καταγεγραμμένα στο κείμενο της δημιουργίας του κειμένου.

Το κείμενο είναι η βάση του κειμένου που είναι καταγεγραμμένο σύμφωνα με τα κείμενα που είναι καταγεγραμμένα.


```

b5=(-0.139,-0.099, 0.133)   aaccs=-102.   aacqib= 49.
B=(-0.404, 0.181, 0.288)   aaccs= 11.   aacqib= 52.
L3=(-0.281, 0.151, 0.212)   aaccs= 118.   aacqib= 22.
uobj biuasi acli= 1. qib= pp.
aibvac3=( 0.010,-0.012, 0.403)   aaccs=-80. aacqib= 54.

```

```

b1=(-0.283,-0.012, 0.431)   aaccs=-196.   aacqib= 91.
B=( 0.404, 0.181, 0.288)   aaccs= 11.   aacqib= 52.
L1=(-0.132, 0.081,-0.002)   aaccs= 101.   aacqib= -0.
uobj biuasi acli= 520. qib= 2d.
aibvac1=(-0.438, 0.228, 0.833)   aaccs= 140. aacqib= 29.

```

```

coefficients of integrals i=1:cfou= 0.800 ==> aibw= 52.1 qadl=ee

```

```

SAMMETRIC FMT1 BEFORE SORTITION

```

```

aibuavacfoa2=(-.369,-.262,0.811)   aaccs=-159.4   aacqib= 90.2
aibuavacfoa3=(0.404,0.181,0.288)   aaccs=- 11.2   aacqib= 52.4
aibuavacfoa1=(-.210,0.405,0.205)   aaccs= 108.0   aacqib= 11.9
Eiduavacfoa1 compouarf 1=M, 3=V
aibuasi= 1.3e+52 aibuw3=-1.2e+18 aibuw2=-1.3e+52
Eiduavasi=aei

```

```

M21= 1.6e+54 M25= 1.1e+54 M22= -1.1e+54 qAve--cw
M31= -4.9e+54 M35= 1.9e+54 M32= 1.1e+54
M11= 1.0e+52 M15= -4.9e+54 M12= 1.6e+54
rediouarf mouarf fauor1

```

```

Odedu-keavqs bolqel.

```

```

*****
FROM A REGIONAL MOMENT TENSOR
COMPUTATION OF A SAMMETRIC FMT1 BEFORE SORTITION

```

STKAM KATE RESULIS

APPENDIX D

```

B5=( 0.020, 0.444, 0.842)   vccs=- 80.   accqib= 64.
B=( -0.448, -0.042, 0.022)   vccs=-18.   accqib= 2.
L5=( 0.082, -0.842, 0.443)   vccs=-80.   accqib= 50.
uobji bisuasi #frik= 180. qib= 25.
#ibvcs=(-0.000, 0.188, 0.419)   vccs= 60. accqib= 28.

b1=( 0.082, -0.315, 0.412)   vccs=-12.   accqib= 11.
B=(-0.448, -0.042, 0.022)   vccs=-18.   accqib= 2.
L1=( 0.020, -0.419, -0.314)   vccs=-88.   accqib=-15.
uobji bisuasi #frik= 0. qib= 28.   vccs=-84. accqib= 25.
#ibvcs=( 0.020, -0.419, 0.188)

coefficuef ut iufelusi ffricium= 0.800 ==> #bpa= 52.3 qedleee
SYNTHETIC ENGLI PLANE ROTULION:
#idauvccfoc-2=(0.046,0.133,0.441)   vccs=- 80.1   accqib= 80.4
#idauvccfoc-3=( -0.448, -0.042, 0.022)   vccs=-111.2   accqib= 2.2
#idauvccfoc-1=(0.046, -0.441, 0.131)   vccs=- 81.5   accqib= 0.4
#idauvccfoc-1 combouarf 1=M. 3=E. 2=A)
#idwaj= 0.1e+52   #idwaj5=-1.3e+18   #idwaj2=-0.1e+52
#idauvajmazi

```

```

M21= -3.4e+54   M25= -1.2e+52   M22= -2.4e+52   qvuc-cu
M31= -2.4e+54   M35= 2.4e+52   M32= -1.2e+52
M11= 2.4e+11   M15= -2.4e+54   M12= -5.4e+54
#edjousi wouarf feurok1

```

Dr./file

 FROM A REGIONAL MOMENT TENSOR
 COMPUTATION OF A SYNTHETIC ENGLI PLANE ROTULION

The maximum horizontal deformation rate = 1.9e-01 mm\A

04.0110
 LAZWA

0.

ENGLI REGIONAL MOMENT TENSOR

```

#edficsj 1 -0.0e-10\A = -1.9e-11\sec
Minimum horizontal 1.9e-10\A = -2.1e-18\sec Astimfisi NSSE
The horizontal and vertical strain rates 5.4e-11\sec Astimfisi NPSM

```

```

combouarf-1-B.4e-10\A = -8.0e-14\sec
#ufelwajife 1-1.2e-10\A = -1.0e-20\sec
#ufelwajouaj 1 B.4e-10\A = 8.0e-14\sec

```

of the horizontal strains

The strain rates for the year 22.0 years in the direction

The specified volume 111.1x55.5x 12.0km³

 DETERMINATION OF THE STRAIN RATE


```

121 couffine
    abel(1)=awf(1)\(S*2.2e11*vol*fabu)
do 121 i=1*2
c
c find afloat rases from Koflora' 1212
c
c JUDICIAL SECTION C) Find afloat and Determination Refee
c
120 forwaf(2x', comb,eejrouaj', 'l'beg',1',\k = 'l'beg',1',\sec.)
148 forwaf(2x', iufak,eqisafe', 'l'beg',1',\k = 'l'beg',1',\sec.)
148 forwaf(2x', wafarajouaj', 'l'beg',1',\k = 'l'beg',1',\sec.)
waf(e(120) afloat(2) *afwaf(2)
waf(e(148) afloat(3) *afwaf(3)
waf(e(148) afloat(1) *afwaf(1)
I. in fine direction, \k' of the principal afloat(1.)
143 forwaf(1, the afloat rases for the 1stf. '42.1'. \ksec.',
waf(e(143) fabu
148 couffine
    afwaf(1)=abel(1)\2.12e12*fabu
    afwaf(1)=abel(1)\fabu
do 148 i=1*2
c
c l' abajou23= 'l'beg',1'\
c 142 forwaf(\', abajou1= 'l'beg',1'2x', abajou3= 'l'beg',1'2x',
c waf(e(142) abaj(1)'i=1*2)
c
c leaq(2*'s) fabu
c
c leaq in fine aflu and nse fo find brinctu / afloat-rases
c
140 couffine
    abaj(1)=ajdew(1)\(p'qel1evoj)
do 140 i=1*2
c Ajoudu' e' wofine' is p'qel1 - uof vka' accrafes' dou' f' nse
c find brinctaj afloat br' nuf' volms' sezmind' ejsafic' wafaraj

```

```

c
c vol=jeaqdaj12
122 forwaf(\', the abajctiqd volms= '42.1'. \k' '42.1'. \k' '42.1'. \k2. \)
waf(e(122) 1e'w'q
leaq(2*'s) 1e'w'q
c
c leaq and eajou aflu dimensions and find the volume
c
c waf(e(1' (.....))
123 forwaf(, DETERMINATION DE THE BIRVIN RATE. )
waf(e(123)
c
c and afloat afloat rases=
c compare afloat rases in direction of brinctaj afluases and hor'oufaj
c
c close(1)
124 couffine
    forwaf(34p'1)
132 waf(e(132) ubax(1)'ubqtb(1)
do 132 i=1*2
    waf(e(1' (.....))
133 forwaf(2x', B' 2x' 2411'p)
waf(e(133) pas'pqib
c
c waf(e onf (B) fo the foraj wachuram tije
c
130a couffine
1310 couffine
1311 couffine
    waw+1
do 1311 i=1*2
    w(k'1)=v(m)
do 1310 k=1*2

```



```

92  coufins
    Auok w = Auok w + spe(mok.k(1))
    qo q2 i = 1' u
    Auok w = 0*0
    coufins
90  mok.k(k) = f
    mok.k(w) = mok.k(k)
    f = mok.k(w)
    i4 (w .sed- k) do fo p0
    w = ibaf(k)
    mok.k(k) = f
22  coufins
    f = f + s(i'k)*mok.k(k)
    qo 22 i = p0 i' u
    kb1 = k+1
    f = 0*0
    k = u - kp
    qo p0 kp = 1' uwi
20  coufins
    mok.k(k) = -(ek + f)\s(k'k)
    i4 (s(i'k) .sed- 0*0) do fo 20
    i4 (f .if- 0*0) ek = -1*0
    ek = 1*0
42  coufins
40  f = f + s(i'k)*mok.k(1)
    qo 40 i = 1' kwi
    kwi = k-1
    i4 (k .sed- 1) do fo 42
    f = 0*0
    qo 20 k = 1' u
32  coufins
30  coufins
32  coufins
    s(i'1) = s(i'1) + s(i'k)*f
    qo 32 i = kb1'u

```

```

30  i4 (f .sed- 0*0) do fo 30
    s(k'1) = f
    s(w'1) = s(k'1)
    f = s(w'1)
    qo 30 i = kb1'u
    coufins
    s(i'k) = -s(i'k)\f
    qo 50 i = p0 i' u
    i4 (f .sed- 0*0) do fo 32
    s(k'k) = f
    s(w'k) = s(k'k)
    f = s(w'k)
    i4 (w .us- k) ibaf(u) = -ibaf(u)
    ibaf(k) = w
12  coufins
    i4 (spe(s(i'k)) .df- spe(s(w'k))) w = i
    qo 12 i = kb1'u
    w = k
    kb1 = k+1
    qo 22 k = 1' uwi
10  coufins
    i4 (f .df- suok w) suok w = f
    coufins
    f = f + spe(s(i'1))
    qo 2 i = 1' u
    f = 0*0
    qo 10 i = 1' u
    suok w = 0*0
    uwi = u - i
    i4 (u .sed- 1) do fo 80
    ibaf(u) = 1
    lesi ek f' suok w' Auok w' suok w
    lesi ek f' suok w' Auok w' suok w
    lesi s(i0'10)'couq'mok.k(u)

```


suq
 afcb
 cfoae (2)
 cfoae (5)
 coufums
 32 tok.waf (1.0'2pm'42'S)
 34 tok.waf (1.0pm'1)
 32 tok.waf (1.4'.'.'12'.'.'14)
 33 tok.waf (5.20)
 31 dofo 12
 tok.waf (2'53) woa

12 w.life (2'53) afc.S'qibS'L'wkeS
 w.life (2'53) afc.l'qib'L'wkeS
 w.life (2'54) awauf
 woa=10'wefcawd+q
 Lesq (S'54'auq=22) awauf'wad
 w.life (2'51) fifeS
 Lesq (2'4) afc.S'qibS'L'wkeS
 w.life (2'4) .EMER: uqwi S afc.ike'qib'L'wke.
 Lesq (2'4) afc.l'qib'L'wkeS
 w.life (2'4) .EMER: uqwi l afc.ike'qib'L'wke.
 Lesq (2'2) fifeS
 w.life (2'4) .EMER: fife of radjou.
 I. radnoufij. tok.w.= tok.wafedq. 'pi'auk= s.a.o.)
 obau (2'4) radnoufij. efafne. uwa. 'accera=
 tok.waf (4)
 Lesq (2'2) onfijj
 w.life (2'4) .EMER: uwa of onfijj.
 Lesq (2'4) c'q
 w.life (2'4) .EMER: c suq q.
 L'auwq S

2 I. radnoufij. tok.w.= tok.wafedq. 'pi'auk= s.a.o.)
 obau (S'4) radnoufij. efafne. oiq. 'accera=
 Lesq (2'2) radnij
 w.life (2'4) .EMER: aw.tudnake tije uwa.
 iufedak. awauf
 c.ue. s.cra. 20 fife' onfijj' radnij
 iufedak. afc.l' afc.S'qib'L'wkeS'L'wkeS
 Lesj woa'wad'c'q
 radnoufij. awajipje tok. fhe radjou.
 c. uerfajiu. nezid fhe emesq t'ouf b'isue
 c suq w.life if fo su tubnf tije tok. brad
 c couwak' if fo s woauf' vis' iolho=cawd+q'
 c brad. fo Lesq radnijmde tok.w. e.d. tije'
 c woauf. t


```

      swf(7)=swf(7)\2M0
    do 100 i=1,9
  C
  C q1v1q0 out the scale factor for diagonalization
  C
    I.M22=. '1b015'1)
    do 100 swf(1)k', M21=. '1b015'1'Sk', M25=. '1b015'1'Sk'
      mlrfe(p'80) swf(4)'swf(2)'swf(4)
      I.MS2=. '1b015'1', qlus-cw.)
    B2 100 swf(1)k', M31=. '1b015'1'Sk', M35=. '1b015'1'Sk'
      mlrfe(p'82) swf(3)'swf(2)'swf(2)
      I.M12=. '1b015'1)
    B0 100 swf(1)k', M11=. '1b015'1'Sk', M15=. '1b015'1'Sk'
      mlrfe(p'80) swf(1)'swf(5)'swf(4)
    12 100 swf(1)k', M11=. '1b015'1'Sk', M15=. '1b015'1'Sk'
      mlrfe(p'82)
  C
  C mlrfe out the summed diagonal moment tensor
  C
    10 continue
      2M0=2M0+M(K)
      do 10 k=1,unmp
        2M0=0
  C
  C sum the scalar moments to give a scale factor
  C
    92 continue
      dofo 90
        k=k+1
        11 k'ed'unmp) dofo 92
      90 swf(1)'swf(1)'swf(1)'k'
        k=1
        swf(1)=0
      do 92 i=1,9
  C

```

```

  C add moment tensors vectorially for all events
  C
  C end of loop over each event
  C
    22 continue
    29 100 swf(1)k'
      mlrfe(p'29)
      11 (m'1e'1) dofo 22
      k=k+1
      11 '12'2', '1k', 'lvcas'=. '1p'1'Sk', 'lvcqib'=. '12'1)
    24 100 swf(1)k', 'lvcas'=. '11', '12'2', '12'2'
      mlrfe(p'24) k'n(m-2)'n(m-5)'n(m-1)'lvcas'lvcqib
      call exqib(n'u'lvcas'lvcqib)
  C
  C end bluf estimates of the and components
  C find the estimates and of the three eigenvalues
  C
      u=1
    28 continue
      w=w+1
      n(u)=n(w)
    22 do 28 u=1,2
      w=1
    21 100 swf(1)k', 'lvcas'=. '11', '12'2', '12'2'
      mlrfe(p'21)
      call exqib(n'u'lvcas'lvcqib)
  C
  C calculate eigenvalues and eigenvalues for each moment tensor
  C
    25 continue
      swf(7)=swf(7)\M0(1)
      do 25 i=1,9
        11 i'ed=0
  C

```

```

130 forwaf(\,coefficients of infernal triction='10.2', ==) a1bpa.'
w1fe(p,130) an,a1bp
a1bp=a1bpa\sq
a1bpa=-2*afau(1.\um)
lswq(2.*a) an
c lswq coeff. of triction' an' and find a1bpa
c
134 forwaf(\, SYNTHETIC EVALI PLANE SOLUTION:.)
w1fe(p,134)
c q1b' and lswq.
c uoqaj 83 qafa' puf comes from uoqaj b1ane 81 a1rike'
c uofaj uoqaj b1ane 83. is not calculated neid indntf
c infernal triction an'
c pofu uoqaj b1ane are calculated according to the coefficient of
c que fo the empidnta in the snif b1ane' the use b-and l-swiz for
c
Generalize a Synthetic snif b1ane solution
c
111.10.3) dofo 112
130 k-k+1
p1b=accq1b
p2=veces
c qe1tne the B (inferwajq1fe) swiz found and b1ande
c
111-3.um-4) dofo 130
w1fe(p,24) p'v(1-2)'v(1-3)'v(1-1)'veces'vecq1b
c1j sq1b(u'n,veces'vecq1b)
u=1
110 couf1une
1=1+1
na(u)=v(1)
112 qo 110 u=1+2

```

```

1=1
k=1
c find and b1anf frende and b1ande of the eigenvectore we before
c
w1fe(\,2) ledu3
110a=forwafed.)
obau(\,11e-onf111'efgne='1M.'veces='redneuf1aj.'
c obau synthetic snif b1ane solution 111s
c
w1fe(p,21)
c
END OF TUTORIAL SECTION B)
c
110a=1.\v)
110 forwaf(.e1dwa1='1beq.'.'3x'.e1dwa3='1beq.1'.'3x'.e1dwa2='
w1fe(p,110) (e1dwa(1)'1=1'2)
10P forwaf(\,E1deuvs1neat.)
w1fe(p,10P)
c
w1fe onf the b1and1aj afreasee
c
102 couf1une
e1dwa(1)=e1dwa(1)*Bk10
qo 102 1=1+2
c snif1b1a pa the e1dwa 1afcor fo dive b1and1aj afreasee
c
c1j e1du(emf,111d,e1dwa'\v)
111e=0
c calculate eigenvalues and eigenvectore for answaq woreuf feuro
c
100 couf1une

```

```

C qecombase .9. se before
C
1313 coufims
      z(1)=p(1)
      a(2,1)=p(1)
      a(5,1)=a(1)+2
      a(1,1)=a(1)
      qo 1315 f=1,2
C
      wbase (81)= zibvecfor (1)
C request the .9. matrix to include vectors (10), (8), and (81)
C
1308 forwef(,uogaj bbase, '11', : zflks=, '42'0', qib=, '42'0)
      wbase(p,1308) w'ubx(1)'ubqib(1)
      f(1,ed,5) w=1
      w=5
      ubqib(1)=d0'-zqib
      ubx(1)=es+d0'
C
C find and brief zflks and qib of the coujndase uogaj bbase
C
      f(2,1), '42', aexs=, '42'0', aecqib=, '42'0)
1303 forwef(, zibvec, '11', =, '42'2', , '42'2', , ,
      wbase(p,1303) f' p(1)'f=1,2)'es+eqib
      call szqib(f'p'es+eqib)
      f=1
C
C combine fbase and bbase of solution vector p' the zib-vector
C
      call solve(u'9'p'ibaf)
C
      oufo the RH2' p'
C solve the system and overwite the solution' the zib-vector'
C
      f(,couqib,ed, couq) zfab

```

```

      couqib=couq+1
1302 forwef(,w'w' wflks iz zindnra for mokriud bbasezrou)
      f(,couqib,ed, couq) wbase(p,1302)
      couqib=couq+1
C
C check for zindnra, fA
C
      call qecomb(u'9'couq'ibaf'work)
C
C qecombase .9. info 9 f'zindnra wflks
C
      f(1,ed,5) p(1)=-p(1)
      p(2)=p(1)
      p(3)=0'0
      p(1)=-cos(b1\4')
      qo 1306 f=1,5
C
C ref nb the riduf-nsud side of the system
C
1400 coufims
      zef(1)=zef(1)+zfab
      qo 1400 f=1,p
      u=2
116 coufims
      coufims
      u=ub+1
      w(k+1)=v(u)
      qo 131 f=1,2
      u=1
C
C blucibaj zbase xzie (10)' (8)' or (80)
C ref nb 9 linear system wflks' w'f esch lom = f f'wubbaseq
      f(2,1, qed,es, '\)

```

12020002

104

ειδυλαςτολ 2=(-5δ9°-2δ2°0'811) λςσς°=-159°δ λςστβ= 90°2
 ειδυλαςτολ 5=(0°δ04°0'181°0'288) λςσς°= 11°2 λςστβ= 33°δ
 ειδυλαςτολ 1=(-210°0'δ05°0'205) λςσς°= 10δ°0 λςστβ= 1Δ°9
 Ειδυλαςτολ ε: κομβουε 1-Η' 5=Ε' 2=Α

M21=	8°56+50	M25=	2°16+51	M22=	-2°26+51	qλυε-ςω
M51=	5°06+51	M55=	2°26+51	M52=	2°16+51	
M11=	4°46+1δ	M15=	-5°09+51	M12=	8°56+50	

κωμυε τειλολ 22'
 ετβλςτολ=(0°019°-δ12°0'40Δ) λςσς=-8δ°0 λςστβ= 54°0
 κωμυε κ0= 2°06+51 qλυε-ςω
 κωμυε κ1= 2°06+51 ετβλς= 1° qτβ= 99° ετβ= -114° qεδλςεε
 ετβλς τειλολ: ετβλς= 520° qτβ= 24° ετβ= -49° qεδλςεε
 ετβλς τειλολ ετβλς τειλολ κωμυε 22

OF BOOK QUANTITY ORIGINAL PAGE 18

12020010

ειδυλαςτολ 2=(-5δ9°-2δ2°0'811) λςσς°=-159°δ λςστβ= 90°2
 ειδυλαςτολ 5=(0°δ04°0'181°0'288) λςσς°= 11°2 λςστβ= 33°δ
 ειδυλαςτολ 1=(-210°0'δ05°0'205) λςσς°= 10δ°0 λςστβ= 1Δ°9
 Ειδυλαςτολ ε: κομβουε 1-Η' 5=Ε' 2=Α

M21=	1°46+51	M25=	2°16+51	M22=	-2°26+51	qλυε-ςω
M51=	-2°26+51	M55=	2°26+51	M52=	2°16+51	
M11=	Δ°26+1δ	M15=	-2°26+51	M12=	1°46+51	

κωμυε τειλολ 24'
 ετβλςτολ=(0°019°-δ12°0'40Δ) λςσς=-8δ°0 λςστβ= 54°0
 κωμυε κ0= 8°26+51 qλυε-ςω
 κωμυε κ1= 8°26+51 ετβλς= 1° qτβ= 99° ετβ= -114° qεδλςεε

ετβλς τειλολ: ετβλς= 520° qτβ= 24° ετβ= -49° qεδλςεε
 ετβλς τειλολ ετβλς τειλολ κωμυε 24

12020208

103

ειδυλαςτολ 2=(-5δ9°-2δ2°0'811) λςσς°=-159°δ λςστβ= 90°2
 ειδυλαςτολ 5=(0°δ04°0'181°0'288) λςσς°= 11°2 λςστβ= 33°δ
 ειδυλαςτολ 1=(-210°0'δ05°0'205) λςσς°= 10δ°0 λςστβ= 1Δ°9
 Ειδυλαςτολ ε: κομβουε 1-Η' 5=Ε' 2=Α

M21=	5°26+51	M25=	8°96+51	M22=	-δ°26+51	qλυε-ςω
M51=	-2°26+51	M55=	δ°56+51	M52=	8°96+51	
M11=	1°56+50	M15=	-2°26+51	M12=	5°26+51	

κωμυε τειλολ 22'
 ετβλςτολ=(0°019°-δ12°0'40Δ) λςσς=-8δ°0 λςστβ= 54°0
 κωμυε κ0= 1°46+55 qλυε-ςω
 κωμυε κ1= 1°46+55 ετβλς= 1° qτβ= 99° ετβ= -114° qεδλςεε
 ετβλς τειλολ: ετβλς= 520° qτβ= 24° ετβ= -49° qεδλςεε
 ετβλς τειλολ ετβλς τειλολ κωμυε 22

OF BOOK QUANTITY ORIGINAL PAGE 18

12020210

ειδυλαςτολ 2=(-5δ9°-2δ2°0'811) λςσς°=-159°δ λςστβ= 90°2
 ειδυλαςτολ 5=(0°δ04°0'181°0'288) λςσς°= 11°2 λςστβ= 33°δ
 ειδυλαςτολ 1=(-210°0'δ05°0'205) λςσς°= 10δ°0 λςστβ= 1Δ°9
 Ειδυλαςτολ ε: κομβουε 1-Η' 5=Ε' 2=Α

M21=	5°26+51	M25=	8°96+51	M22=	-δ°26+51	qλυε-ςω
M51=	-2°26+51	M55=	δ°56+51	M52=	8°96+51	
M11=	1°56+50	M15=	-2°26+51	M12=	5°26+51	

κωμυε τειλολ 25'
 ετβλςτολ=(0°019°-δ12°0'40Δ) λςσς=-8δ°0 λςστβ= 54°0

ei deuaecfoi 1=(-210'0'0.005'0'0.205) aeccs' = 109'0 aecrib= 13'0
Ei deuaecfoi: combouuf 1=M' 3=E' 3=0

M21= p'4e+50 M25= 5'4e+51 M23= -5'9e+51
M31= -1'2e+51 M35= 5'9e+51 M32= 5'4e+51 qAue-cw
M11= 2'4e+10 M15= -1'2e+51 M12= p'4e+50

womeuf feuzoi 20: aeccs= -89'0 aecrib= 54'0

ei bvaecfoi=(0'01p'-'012'0'403) aeccs= -89'0 aecrib= 54'0
Houuef qA= 2'0e+51 qAue-cw
xoujixA biuue: efrifk= 1' qib= pp' efrb=-114' qeqlsee
Lemf biuue: efrifk= 520' qib= 24' efrb= -40' qeqlsee
Lemf biuue: eoujifou umpef 20

1A035A012

ei deuaecfoi 2=(-'59p'-'262'0'8A1) aeccs' = -159'0 aecrib= 90'2
ei deuaecfoi 3=(0'004'0'181'0'288) aeccs' = 11'2 aecrib= 55'0
ei deuaecfoi 1=(-210'0'0.005'0'0.205) aeccs' = 109'0 aecrib= 13'0
Ei deuaecfoi: combouuf 1=M' 3=E' 3=0

M21= 5'2e+50 M25= 8'9e+50 M23= -0'2e+50 qAue-cw
M31= -2'2e+50 M35= 0'3e+50 M32= 8'9e+50
M11= 1'5e+10 M15= -2'2e+50 M12= 5'2e+50

womeuf feuzoi 20: aeccs= -89'0 aecrib= 54'0

ei bvaecfoi=(0'01p'-'012'0'403) aeccs= -89'0 aecrib= 54'0
Houuef qA= 1'4e+51 qAue-cw
xoujixA biuue: efrifk= 1' qib= pp' efrb=-114' qeqlsee
Lemf biuue: efrifk= 520' qib= 24' efrb= -40' qeqlsee
Lemf biuue: eoujifou umpef 20

1A035B032

ei deuaecfoi 2=(-'59p'-'262'0'8A1) aeccs' = -159'0 aecrib= 90'2
ei deuaecfoi 3=(0'004'0'181'0'288) aeccs' = 11'2 aecrib= 55'0
ei deuaecfoi 1=(-210'0'0.005'0'0.205) aeccs' = 109'0 aecrib= 13'0
Ei deuaecfoi: combouuf 1=M' 3=E' 3=0

M21= 8'5e+50 M25= 2'1e+51 M23= -2'2e+51
M31= -5'0e+51 M35= 2'2e+51 M32= 2'1e+51 qAue-cw
M11= 4'4e+10 M15= -5'0e+51 M12= 8'5e+50

womeuf feuzoi 23: aeccs= -89'0 aecrib= 54'0

ei bvaecfoi=(0'01p'-'012'0'403) aeccs= -89'0 aecrib= 54'0
Houuef qA= 2'0e+51 qAue-cw
xoujixA biuue: efrifk= 1' qib= pp' efrb=-114' qeqlsee
Lemf biuue: efrifk= 520' qib= 24' efrb= -40' qeqlsee
Lemf biuue: eoujifou umpef 23

1A0102005

ei deuaecfoi 2=(-'59p'-'262'0'8A1) aeccs' = -159'0 aecrib= 90'2
ei deuaecfoi 3=(0'004'0'181'0'288) aeccs' = 11'2 aecrib= 55'0
ei deuaecfoi 1=(-210'0'0.005'0'0.205) aeccs' = 109'0 aecrib= 13'0
Ei deuaecfoi: combouuf 1=M' 3=E' 3=0

M21= 8'5e+50 M25= 2'1e+51 M23= -2'2e+51
M31= -5'0e+51 M35= 2'2e+51 M32= 2'1e+51 qAue-cw
M11= 4'4e+10 M15= -5'0e+51 M12= 8'5e+50

womeuf feuzoi 20: aeccs= -89'0 aecrib= 54'0

ei bvaecfoi=(0'01p'-'012'0'403) aeccs= -89'0 aecrib= 54'0
Houuef qA= 2'0e+51 qAue-cw
xoujixA biuue: efrifk= 1' qib= pp' efrb=-114' qeqlsee
Lemf biuue: efrifk= 520' qib= 24' efrb= -40' qeqlsee
Lemf biuue: eoujifou umpef 20

πωμεν γωνία ρ2:
 εγβλυστρολ=(0°019'--δ12'0'40λ) λσγρσ=-8δ°0 λσγρβ= 54°0
 ηωμεν ηω= 1°16+55 γλυσ-σ
 σπκττλκλ βγμε: εγλττκ= 1° γτβ= ρρ° εγτβ=-114° γεδλσεε
 τσνττ βγμε: εγλττκ= 520° γτβ= 24° εγτβ=-49° γεδλσεε
 Εσνττ βγμε εσντττου σμμερ ρ2

80041100P

εγβλυστρολ2=(-°5δρ°--2δ2'0'8λ1) λσγρσ=-15ρ°δ λσγρβ= 90°2
 εγβλυστρολ5=(0°δ04'0'181'0'288) λσγρσ= 11°2 λσγρβ= 55°δ
 εγβλυστρολ1=(-°210'0'δ05'0'205) λσγρσ= 10δ°0 λσγρβ= 1λ°ρ
 Εγβλυστρολ: σωμμενττ 1=η° 5=Ε° 2=Λ°
 η21= 1°16+51 η25= 4°06+51 η22= -4°26+51 γλυσ-σ
 η51= -5°96+51 η55= 4°26+51 η52= 4°06+51
 η11= 2°λ6+1δ η15= -5°26+51 η12= 1°16+51

πωμεν γωνία ρ5:
 εγβλυστρολ=(0°019'--δ12'0'40λ) λσγρσ=-8δ°0 λσγρβ= 54°0
 ηωμεν ηω= 4°26+51 γλυσ-σ
 σπκττλκλ βγμε: εγλττκ= 1° γτβ= ρρ° εγτβ=-114° γεδλσεε
 τσνττ βγμε: εγλττκ= 520° γτβ= 24° εγτβ=-49° γεδλσεε
 Εσνττ βγμε εσντττου σμμερ ρ5

λ8021P050

εγβλυστρολ2=(-°5δρ°--2δ2'0'8λ1) λσγρσ=-15ρ°δ λσγρβ= 90°2
 εγβλυστρολ5=(0°δ04'0'181'0'288) λσγρσ= 11°2 λσγρβ= 55°δ
 εγβλυστρολ1=(-°210'0'δ05'0'205) λσγρσ= 10δ°0 λσγρβ= 1λ°ρ
 Εγβλυστρολ: σωμμενττ 1=η° 5=Ε° 2=Λ°

η21= 1°06+55 η25= 2°δ6+55 η22= -4°56+55 γλυσ-σ
 η51= -5°26+55 η55= 4°16+55 η52= 2°δ6+55
 η11= 2°96+50 η15= -5°26+55 η12= 1°06+55
 πωμεν γωνία ρ1:
 εγβλυστρολ=(0°019'--δ12'0'40λ) λσγρσ=-8δ°0 λσγρβ= 54°0
 ηωμεν ηω= 4°26+55 γλυσ-σ
 σπκττλκλ βγμε: εγλττκ= 1° γτβ= ρρ° εγτβ=-114° γεδλσεε
 τσνττ βγμε: εγλττκ= 520° γτβ= 24° εγτβ=-49° γεδλσεε
 Εσνττ βγμε εσντττου σμμερ ρ1

λ20δ05014

εγβλυστρολ2=(-°5δρ°--2δ2'0'8λ1) λσγρσ=-15ρ°δ λσγρβ= 90°2
 εγβλυστρολ5=(0°δ04'0'181'0'288) λσγρσ= 11°2 λσγρβ= 55°δ
 εγβλυστρολ1=(-°210'0'δ05'0'205) λσγρσ= 10δ°0 λσγρβ= 1λ°ρ
 Εγβλυστρολ: σωμμενττ 1=η° 5=Ε° 2=Λ°
 η21= 4°46+50 η25= 5°46+51 η22= -5°96+51 γλυσ-σ
 η51= -1°26+51 η55= 5°96+51 η52= 5°46+51
 η11= 2°46+1δ η15= -1°26+51 η12= 4°46+50

πωμεν γωνία ρ0:
 εγβλυστρολ=(0°019'--δ12'0'40λ) λσγρσ=-8δ°0 λσγρβ= 54°0
 ηωμεν ηω= 2°δ6+51 γλυσ-σ
 σπκττλκλ βγμε: εγλττκ= 1° γτβ= ρρ° εγτβ=-114° γεδλσεε
 τσνττ βγμε: εγλττκ= 520° γτβ= 24° εγτβ=-49° γεδλσεε
 Εσνττ βγμε εσντττου σμμερ ρ0

λ4151P051

εγβλυστρολ2=(-°5δρ°--2δ2'0'8λ1) λσγρσ=-15ρ°δ λσγρβ= 90°2
 εγβλυστρολ5=(0°δ04'0'181'0'288) λσγρσ= 11°2 λσγρβ= 55°δ

BO0415012

eiDeuacfoa_2=(-.589^-.282^0^8X1) accs5'=-159^d accqib= 90^2
 eiDeuacfoa_3=(0^d04^0^181^0^288) accs5' = 11^2 accqib= 55^d
 eiDeuacfoa_1=(-.210^0^d05^0^205) accs5' = 109^0 accqib= 15^p
 EiDeuacfoa: combouanf 1=M^ 5=E^ 2=A

 M21= 5^2e+5i M25= 8^9e+5i M22= -6^2e+5i
 M31= -2^2e+5i M35= 6^3e+5i M32= 8^4e+5i
 M11= 1^5e+50 M15= -2^2e+5i M12= 5^2e+5i
 wouanf feura pp
 eiDvaefoa=(0^01p^-.d12^0^40X) accs5'=-86^0 accqib= 54^0
 Housuf Mo: 1^4e+5i qAue-cw
 srxijrA bjsue: efrife= 1^ qib= pp^ e1ib=-114^ qeDee
 Enif bjsue: efrife= 520^ qib= 24^ e1ib= -49^ qeDee
 Enif bjsue: efrife= 520^ qib= 24^ e1ib= -49^ qeDee
 Enif bjsue: efrife= 520^ qib= 24^ e1ib= -49^ qeDee

BO0415012

eiDeuacfoa_2=(-.589^-.282^0^8X1) accs5'=-159^d accqib= 90^2
 eiDeuacfoa_3=(0^d04^0^181^0^288) accs5' = 11^2 accqib= 55^d
 eiDeuacfoa_1=(-.210^0^d05^0^205) accs5' = 109^0 accqib= 15^p
 EiDeuacfoa: combouanf 1=M^ 5=E^ 2=A

 M21= 1^4e+5i M25= 2^1e+5i M22= -2^2e+5i
 M31= -2^2e+5i M35= 2^2e+5i M32= 2^1e+5i
 M11= 5^2e+1d M15= -2^2e+5i M12= 1^4e+5i
 wouanf feura pp
 eiDvaefoa=(0^01p^-.d12^0^40X) accs5'=-86^0 accqib= 54^0
 Housuf Mo: 8^2e+5i qAue-cw

BO041100A

srxijrA bjsue: efrife= 1^ qib= pp^ e1ib=114^ qeDee
 Enif bjsue: efrife= 520^ qib= 24^ e1ib= -49^ qeDee
 Enif bjsue: efrife= 520^ qib= 24^ e1ib= -49^ qeDee
 EiDeuacfoa: combouanf 1=M^ 5=E^ 2=A

 M21= 1^1e+5i M25= 4^0e+5i M22= -4^2e+5i
 M31= -5^9e+5i M35= 4^2e+5i M32= 4^0e+5i
 M11= 2^3e+1d M15= -5^9e+5i M12= 1^1e+5i
 wouanf feura pp
 eiDvaefoa=(0^01p^-.d12^0^40X) accs5'=-86^0 accqib= 54^0
 Housuf Mo: 2^2e+5i qAue-cw
 srxijrA bjsue: efrife= 1^ qib= pp^ e1ib=-114^ qeDee
 Enif bjsue: efrife= 520^ qib= 24^ e1ib= -49^ qeDee
 Enif bjsue: efrife= 520^ qib= 24^ e1ib= -49^ qeDee

BO041100P

eiDeuacfoa_2=(-.589^-.282^0^8X1) accs5'=-159^d accqib= 90^2
 eiDeuacfoa_3=(0^d04^0^181^0^288) accs5' = 11^2 accqib= 55^d
 eiDeuacfoa_1=(-.210^0^d05^0^205) accs5' = 109^0 accqib= 15^p
 EiDeuacfoa: combouanf 1=M^ 5=E^ 2=A

 M21= 1^8e+5i M25= 6^9e+5i M22= -3^2e+5i
 M31= -4^4e+5i M35= 3^3e+5i M32= 6^9e+5i
 M11= 8^3e+1d M15= -4^4e+5i M12= 1^8e+5i

εἰς δὴ ἀνατολῆς 5 = (0° 04' 0" 181' 0" 288) Ἀνατολῆς = 11' 2" Ἀνατολῆς = 33' δ
 εἰς δὴ ἀνατολῆς 1 = (-210' 0" 05' 0" 205) Ἀνατολῆς = 10δ' 0" Ἀνατολῆς = 13' ρ
 Εἰς δὴ ἀνατολῆς: συνόλου 1=Ν' 3=Ε' 2=Λ

Μ21 = 9' 58+51 Μ25 = 5' 28+53 Μ22 = -5' 28+53 ἄλλο-α
 Μ31 = -1' 28+53 Μ35 = 5' 28+53 Μ32 = 5' 28+53
 Μ11 = 2' 48+50 Μ15 = -1' 28+53 Μ12 = 9' 58+51

ὠκεῖοι ἄντα
 εἰς δὴ ἀνατολῆς = (0° 019' - 212' 0" 403) Ἀνατολῆς = -8δ' 0" Ἀνατολῆς = 54' 0"
 ὠκεῖοι ἄντα: 2' 88+53 ἄλλο-α
 ἄλλοι ἄντα: ἄλλοι = 1' ἄντα = 99' ἄντα = -114' ἄλλοι
 ἄλλοι ἄντα: ἄλλοι = 320' ἄντα = 24' ἄντα = -49' ἄλλοι
 ἄλλοι ἄντα: ἄλλοι ἄντα ἄλλοι 30

800438013

εἰς δὴ ἀνατολῆς 2 = (-3δρ' - 2δ2' 0" 831) Ἀνατολῆς = -15ρ' δ Ἀνατολῆς = 90' 2"
 εἰς δὴ ἀνατολῆς 5 = (0° 04' 0" 181' 0" 288) Ἀνατολῆς = 11' 2" Ἀνατολῆς = 33' δ
 εἰς δὴ ἀνατολῆς 1 = (-210' 0" 05' 0" 205) Ἀνατολῆς = 10δ' 0" Ἀνατολῆς = 13' ρ
 Εἰς δὴ ἀνατολῆς: συνόλου 1=Ν' 3=Ε' 2=Λ

Μ21 = 1' 08+53 Μ25 = 2' δ8+53 Μ22 = -4' 38+53 ἄλλο-α
 Μ31 = -5' 28+53 Μ35 = 4' 18+53 Μ32 = 2' δ8+53
 Μ11 = 2' 48+50 Μ15 = -5' 28+53 Μ12 = 1' 08+53

ὠκεῖοι ἄντα
 εἰς δὴ ἀνατολῆς = (0° 019' - 212' 0" 403) Ἀνατολῆς = -8δ' 0" Ἀνατολῆς = 54' 0"
 ὠκεῖοι ἄντα: 9' 28+53 ἄλλο-α
 ἄλλοι ἄντα: ἄλλοι = 1' ἄντα = 99' ἄντα = -114' ἄλλοι
 ἄλλοι ἄντα: ἄλλοι = 320' ἄντα = 24' ἄντα = -49' ἄλλοι
 ἄλλοι ἄντα: ἄλλοι ἄντα ἄλλοι 9δ

800438013

εἰς δὴ ἀνατολῆς 2 = (-3δρ' - 2δ2' 0" 831) Ἀνατολῆς = -15ρ' δ Ἀνατολῆς = 90' 2"
 εἰς δὴ ἀνατολῆς 5 = (0° 04' 0" 181' 0" 288) Ἀνατολῆς = 11' 2" Ἀνατολῆς = 33' δ
 εἰς δὴ ἀνατολῆς 1 = (-210' 0" 05' 0" 205) Ἀνατολῆς = 10δ' 0" Ἀνατολῆς = 13' ρ
 Εἰς δὴ ἀνατολῆς: συνόλου 1=Ν' 3=Ε' 2=Λ

Μ21 = 5' 18+53 Μ25 = 8' 08+53 Μ22 = -8' 18+53 ἄλλο-α
 Μ31 = -2' 18+53 Μ35 = 8' 08+53 Μ32 = 8' 08+53
 Μ11 = 1' 18+51 Μ15 = -2' 18+53 Μ12 = 5' 18+53

ὠκεῖοι ἄντα
 εἰς δὴ ἀνατολῆς = (0° 019' - 212' 0" 403) Ἀνατολῆς = -8δ' 0" Ἀνατολῆς = 54' 0"
 ὠκεῖοι ἄντα: 1' 28+52 ἄλλο-α
 ἄλλοι ἄντα: ἄλλοι = 1' ἄντα = 99' ἄντα = -114' ἄλλοι
 ἄλλοι ἄντα: ἄλλοι = 320' ἄντα = 24' ἄντα = -49' ἄλλοι
 ἄλλοι ἄντα: ἄλλοι ἄντα ἄλλοι 98

800438012

εἰς δὴ ἀνατολῆς 2 = (-3δρ' - 2δ2' 0" 831) Ἀνατολῆς = -15ρ' δ Ἀνατολῆς = 90' 2"
 εἰς δὴ ἀνατολῆς 5 = (0° 04' 0" 181' 0" 288) Ἀνατολῆς = 11' 2" Ἀνατολῆς = 33' δ
 εἰς δὴ ἀνατολῆς 1 = (-210' 0" 05' 0" 205) Ἀνατολῆς = 10δ' 0" Ἀνατολῆς = 13' ρ
 Εἰς δὴ ἀνατολῆς: συνόλου 1=Ν' 3=Ε' 2=Λ

Μ21 = 5' 88+53 Μ25 = 1' 08+52 Μ22 = -1' 18+52 ἄλλο-α
 Μ31 = -9' 18+53 Μ35 = 1' 08+52 Μ32 = 1' 08+52
 Μ11 = 1' 28+51 Μ15 = -9' 18+53 Μ12 = 5' 88+53

ὠκεῖοι ἄντα
 εἰς δὴ ἀνατολῆς = (0° 019' - 212' 0" 403) Ἀνατολῆς = -8δ' 0" Ἀνατολῆς = 54' 0"
 ὠκεῖοι ἄντα: 1' 18+52 ἄλλο-α
 ἄλλοι ἄντα: ἄλλοι = 1' ἄντα = 99' ἄντα = -114' ἄλλοι
 ἄλλοι ἄντα: ἄλλοι = 320' ἄντα = 24' ἄντα = -49' ἄλλοι
 ἄλλοι ἄντα: ἄλλοι ἄντα ἄλλοι 93

ENTER LEADIN PONDRA X TOGRAIN
 Deflect: -6.0e-10VA = -1.6e-11Vsec V1strngt MS2E
 Minimum hor isoufaj: -1.9e-10VA = -2.1e-11Vsec V1strngt MS2E
 Maximum hor isoufaj: 3.9e-10VA = 5.4e-11Vsec V1strngt MS2M
 The hor isoufaj and deflctaj strain rates:

comb eestrouj: 8.9e-10VA = -8.0e-11Vsec
 infuavectaj: -1.5e-10VA = -1.0e-50Vsec
 er: frouj: 8.9e-10VA = 8.0e-11Vsec
 of the principal stresses:

The strain rates for the loc: 23.0 Vcm² in the directions
 The abedcted volms= 111.1853558 12.01W2

 DETERMINATION OF THE STRAIN RATE

B3=(0.13e-0.99d, 0.233) aecst=-102. aecqtb= 46.
 B=(0.604, 0.181, 0.288) aecst= 11. aecqtb= 32.
 L3=(0.261, 0.251, 0.233) aecst= 118. aecqtb= 22.
 uobj bjsuaj: eflkms= 1. qtb= 40.
 efbvacs=(0.010, -0.912, 0.403) aecst= -89. aecqtb= 34.
 b1=(-0.283, -0.032, 0.231) aecst=-199. aecqtb= 43.
 B=(-0.404, 0.181, 0.288) aecst= 11. aecqtb= 32.
 L1=(-0.182, 0.281, -0.002) aecst= 101. aecqtb= -0.
 uobj bjsuaj: eflkms= 320. qtb= 24.
 efbvacs=(-0.439, 0.228, 0.839) aecst= 140. aecqtb= 29.
 coefficients of infuaj friction= 0.800 ==> qbps= 32.3 qeclsee

SYNTHETIC ENVI PLWME BOTTLING:

eiduavectaj= (-.59e⁴, -.262⁰, 0.811) aecst= -159.9 aecqtb= 90.2

eiduavectaj= (0.604⁰, 0.181⁰, 0.288) aecst= 11.2 aecqtb= 32.9
 eiduavectaj= (-.210⁰, 0.205⁰, 0.202) aecst= 109.0 aecqtb= 13.4
 Eiduavectaj: combouef I=M⁴ S=E⁷ Z=V

eidwaj= 1.5e+52 eidwaj= -1.2e+18 eidwaj= -1.5e+52

Eidwajmeat:

M21=	1.9e+54	M25=	3.1e+54	M29=	-3.3e+54
M31=	-4.9e+54	M35=	3.9e+54	M39=	3.1e+54
M11=	1.0e+52	M15=	-4.9e+54	M19=	1.0e+54

Redrouj womeuf feuraj:

eiduavectaj= (-.59e⁴, -.262⁰, 0.811) aecst=-159.9 aecqtb= 90.2
 eiduavectaj= (0.604⁰, 0.181⁰, 0.288) aecst= 11.2 aecqtb= 32.9
 eiduavectaj= (-.210⁰, 0.205⁰, 0.202) aecst= 109.0 aecqtb= 13.4
 Eiduavectaj: combouef I=M⁴ S=E⁷ Z=V

M21=	5.9e+55	M25=	1.0e+52	M29=	-1.1e+52
M31=	-9.3e+55	M35=	1.1e+52	M39=	1.0e+52
M11=	1.2e+51	M15=	-9.3e+55	M19=	5.9e+55

womeuf feuraj: V1:
 efbvacs=(0.01e⁴, -.912⁰, 0.403) aecst=-89.0 aecqtb= 34.0
 womeuf qe: 1.3e+53 qvuc-cw
 smuaj bjsuaj: eflkms= 320. qtb= 24. efb= -114. qeclsee
 fmsf bjsuaj: eflkms= 320. qtb= 24. efb= -40. qeclsee

B00202000

eiduavectaj= (-.59e⁴, -.262⁰, 0.811) aecst= -159.9 aecqtb= 90.2

The maximum horizontal deflection ratio = 1.36-01 mm/Vc
P4.0110
L. 12550
0°

СОМПУТЕР ПРОГРАММ

ЪБЪЕНДИХ В

980921059

εἰς τὴν ἀστρολόγησιν 2 (-589° - 262' 0" ΒΔ) Ἀστρολ. = -159' δ Ἀστρολ. = 90' 2
 εἰς τὴν ἀστρολόγησιν 5 (0' 404' 0" 181' 0" 288) Ἀστρολ. = 11' 2 Ἀστρολ. = 33' δ
 εἰς τὴν ἀστρολόγησιν 1 (-210' 0" 405' 0" 205) Ἀστρολ. = 10δ' 0 Ἀστρολ. = 13' 9
 Εἰς τὴν ἀστρολόγησιν: συνδυασμῶν 1=Η' 3=Ε' 2=Λ

Η21= 1' 46+51 Η25= 2' 16+51 Η22= -2' 26+51
 Η51= -2' 26+51 Η55= 2' 26+51 Η52= 2' 16+51
 Η11= 3' 26+1δ Η15= -2' 26+51 Η12= 1' 46+51

q lus-cw

ἡμερῶν 21
 εἰς τὴν ἀστρολόγησιν (0' 019' - 412' 0" 403) Ἀστρολ. = -8δ' 0 Ἀστρολ. = 54' 0
 ἡμερῶν 19= 8' 26+51 q lus-cw
 ἡμερῶν 19 βῆμα: εἰς τὴν 1' qib= 99' εἰς τὴν -114' qed lwee
 εἰς τὴν βῆμα: εἰς τὴν 320' qib= 24' εἰς τὴν -49' qed lwee
 εἰς τὴν βῆμα: εἰς τὴν 21

980921001

εἰς τὴν ἀστρολόγησιν 2 (-589° - 262' 0" ΒΔ) Ἀστρολ. = -159' δ Ἀστρολ. = 90' 2
 εἰς τὴν ἀστρολόγησιν 5 (0' 404' 0" 181' 0" 288) Ἀστρολ. = 11' 2 Ἀστρολ. = 33' δ
 εἰς τὴν ἀστρολόγησιν 1 (-210' 0" 405' 0" 205) Ἀστρολ. = 10δ' 0 Ἀστρολ. = 13' 9
 Εἰς τὴν ἀστρολόγησιν: συνδυασμῶν 1=Η' 3=Ε' 2=Λ

Η21= 5' 26+51 Η25= 8' 96+51 Η22= -δ' 26+51
 Η51= -2' 26+51 Η55= δ' 56+51 Η52= 8' 96+51
 Η11= 1' 56+50 Η15= -2' 26+51 Η12= 5' 26+51

q lus-cw

ἡμερῶν 20
 εἰς τὴν ἀστρολόγησιν (0' 019' - 412' 0" 403) Ἀστρολ. = -8δ' 0 Ἀστρολ. = 54' 0
 ἡμερῶν 19= 1' 46+53 q lus-cw

DE BOOK ORIGINALLY PAGE 12

ἡμερῶν 19 βῆμα: εἰς τὴν 1' qib= 99' εἰς τὴν -114' qed lwee
 εἰς τὴν βῆμα: εἰς τὴν 320' qib= 24' εἰς τὴν -49' qed lwee
 εἰς τὴν βῆμα: εἰς τὴν 20

980921001

εἰς τὴν ἀστρολόγησιν 2 (-589° - 262' 0" ΒΔ) Ἀστρολ. = -159' δ Ἀστρολ. = 90' 2
 εἰς τὴν ἀστρολόγησιν 5 (0' 404' 0" 181' 0" 288) Ἀστρολ. = 11' 2 Ἀστρολ. = 33' δ
 εἰς τὴν ἀστρολόγησιν 1 (-210' 0" 405' 0" 205) Ἀστρολ. = 10δ' 0 Ἀστρολ. = 13' 9
 Εἰς τὴν ἀστρολόγησιν: συνδυασμῶν 1=Η' 3=Ε' 2=Λ

Η21= 9' 56+51 Η25= 5' 26+53 Η22= -5' 26+53
 Η51= -1' 26+53 Η55= 5' 26+53 Η52= 9' 26+53
 Η11= 2' 46+50 Η15= -1' 26+53 Η12= 9' 56+51

q lus-cw

ἡμερῶν 5δ
 εἰς τὴν ἀστρολόγησιν (0' 019' - 412' 0" 403) Ἀστρολ. = -8δ' 0 Ἀστρολ. = 54' 0
 ἡμερῶν 19= 2' 86+53 q lus-cw
 ἡμερῶν 19 βῆμα: εἰς τὴν 1' qib= 99' εἰς τὴν -114' qed lwee
 εἰς τὴν βῆμα: εἰς τὴν 320' qib= 24' εἰς τὴν -49' qed lwee
 εἰς τὴν βῆμα: εἰς τὴν 5δ

980920214

εἰς τὴν ἀστρολόγησιν 2 (-589° - 262' 0" ΒΔ) Ἀστρολ. = -159' δ Ἀστρολ. = 90' 2
 εἰς τὴν ἀστρολόγησιν 5 (0' 404' 0" 181' 0" 288) Ἀστρολ. = 11' 2 Ἀστρολ. = 33' δ
 εἰς τὴν ἀστρολόγησιν 1 (-210' 0" 405' 0" 205) Ἀστρολ. = 10δ' 0 Ἀστρολ. = 13' 9
 Εἰς τὴν ἀστρολόγησιν: συνδυασμῶν 1=Η' 3=Ε' 2=Λ

Η21= 1' 46+51 Η25= 2' 16+51 Η22= -2' 26+51
 Η51= -2' 26+51 Η55= 2' 26+51 Η52= 2' 16+51
 Η11= 3' 26+1δ Η15= -2' 26+51 Η12= 1' 46+51

q lus-cw

DE BOOK ORIGINALLY PAGE 12

C-5

εἰδουλευστρολ 5=(0°δ04'0"181'0"288) λσc95°= 11°2 λσcqtB= 35°δ
 εἰδουλευστρολ 1=(-°210'0"δ05'0"205) λσc95°= 10δ°0 λσcqtB= 13°9
 Εἰδουλευστρολ: cσmbουεuf 1=H' 5=E' 2=λ

M21= 1°19+51 M25= 4°08+51 M22= -4°26+51
 M51= -5°98+51 M55= 4°28+51 M52= 4°08+51 qλue-cw
 M11= 2°18+1δ M15= -5°98+51 M12= 1°19+51

wσueuf ρεueσλ 32:
 εἰτBλσcρολ=(0°019°-°δ12'0"403) λσc95= -8δ°0 λσcqtB= 34°0
 wσueuf wσ= 9°26+51 qλue-cw
 σπκ119λλ b19ue: ερ119ε= 1° q1B= 99° ε11B=-114° qεδ1εεε
 19119 b19ue: ερ119ε= 320° q1B= 24° ε11B=-49° qεδ1εεε
 19119 b19ue cσ11919ou σ119ερελ 22

300103030

εἰδουλευστρολ 2=(-°5δ9°-°2δ2'0"831) λσc95°= -159°δ λσcqtB= 90°2
 εἰδουλευστρολ 5=(0°δ04'0"181'0"288) λσc95°= 11°2 λσcqtB= 35°δ
 εἰδουλευστρολ 1=(-°210'0"δ05'0"205) λσc95°= 10δ°0 λσcqtB= 13°9
 Εἰδουλευστρολ: cσmbουεuf 1=H' 5=E' 2=λ

M21= 1°48+51 M25= 2°18+51 M22= -2°28+51
 M51= -2°28+51 M55= 2°28+51 M52= 2°18+51 qλue-cw
 M11= 3°28+1δ M15= -2°28+51 M12= 1°48+51

wσueuf ρεueσλ 24:
 εἰτBλσcρολ=(0°019°-°δ12'0"403) λσc95= -8δ°0 λσcqtB= 34°0
 wσueuf wσ= 8°28+51 qλue-cw
 σπκ119λλ b19ue: ερ119ε= 1° q1B= 99° ε11B=-114° qεδ1εεε
 19119 b19ue: ερ119ε= 320° q1B= 24° ε11B=-49° qεδ1εεε
 19119 b19ue cσ11919ou σ119ερελ 24

980934011

εἰδουλευστρολ 2=(-°5δ9°-°2δ2'0"831) λσc95°= -159°δ λσcqtB= 90°2
 εἰδουλευστρολ 5=(0°δ04'0"181'0"288) λσc95°= 11°2 λσcqtB= 35°δ
 εἰδουλευστρολ 1=(-°210'0"δ05'0"205) λσc95°= 10δ°0 λσcqtB= 13°9
 Εἰδουλευστρολ: cσmbουεuf 1=H' 5=E' 2=λ

M21= 1°48+51 M25= 2°18+51 M22= -2°28+51
 M51= -2°28+51 M55= 2°28+51 M52= 2°18+51 qλue-cw
 M11= 3°28+1δ M15= -2°28+51 M12= 1°48+51

wσueuf ρεueσλ 22:
 εἰτBλσcρολ=(0°019°-°δ12'0"403) λσc95= -8δ°0 λσcqtB= 34°0
 wσueuf wσ= 8°28+51 qλue-cw
 σπκ119λλ b19ue: ερ119ε= 1° q1B= 99° ε11B=-114° qεδ1εεε
 19119 b19ue: ερ119ε= 320° q1B= 24° ε11B=-49° qεδ1εεε
 19119 b19ue cσ11919ou σ119ερελ 22

98093300δ

εἰδουλευστρολ 2=(-°5δ9°-°2δ2'0"831) λσc95°= -159°δ λσcqtB= 90°2
 εἰδουλευστρολ 5=(0°δ04'0"181'0"288) λσc95°= 11°2 λσcqtB= 35°δ
 εἰδουλευστρολ 1=(-°210'0"δ05'0"205) λσc95°= 10δ°0 λσcqtB= 13°9
 Εἰδουλευστρολ: cσmbουεuf 1=H' 5=E' 2=λ

M21= 1°48+51 M25= 2°18+51 M22= -2°28+51
 M51= -2°28+51 M55= 2°28+51 M52= 2°18+51 qλue-cw
 M11= 3°28+1δ M15= -2°28+51 M12= 1°48+51

wσueuf ρεueσλ 23:
 εἰτBλσcρολ=(0°019°-°δ12'0"403) λσc95= -8δ°0 λσcqtB= 34°0
 wσueuf wσ= 8°28+51 qλue-cw
 σπκ119λλ b19ue: ερ119ε= 1° q1B= 99° ε11B=-114° qεδ1εεε
 19119 b19ue: ερ119ε= 320° q1B= 24° ε11B=-49° qεδ1εεε
 19119 b19ue cσ11919ou σ119ερελ 23

Ernif b'isue eojnifou unmpak 42
1203532015

ei d'euvaecfoa 2=(-.549°,-.242°0'8X11) aecq5° = -159° 6' aecqib = 60° 2'
ei d'euvaecfoa 3=(0° 404'0'181°0'288) aecq5° = 11° 2' aecqib = 55° 6'
ei d'euvaecfoa 1=(-.210°0'0' 0° 205°) aecq5° = 108° 0' aecqib = 15° 9'
Ei d'euvaecfoa ei combouanf 1=M° 3=E° 2=A°
wouanf feura 451 aecq5 = -86° 0' aecqib = 54° 0'
ei d'euvaecfoa 1=(0° 019°,-.412°0'403) aecq5 = -86° 0' aecqib = 54° 0'
wouanf feura 451 aecq5 = -86° 0' aecqib = 54° 0'
Ernif b'isue eojnifou unmpak 45

1203532009

ei d'euvaecfoa 2=(-.549°,-.242°0'8X11) aecq5° = -159° 6' aecqib = 60° 2'
ei d'euvaecfoa 3=(0° 404'0'181°0'288) aecq5° = 11° 2' aecqib = 55° 6'
ei d'euvaecfoa 1=(-.210°0'0'405°0'205) aecq5° = 108° 0' aecqib = 15° 9'
Ei d'euvaecfoa ei combouanf 1=M° 3=E° 2=A°
wouanf feura 451 aecq5 = -86° 0' aecqib = 54° 0'
ei d'euvaecfoa 1=(0° 019°,-.412°0'403) aecq5 = -86° 0' aecqib = 54° 0'
wouanf feura 451 aecq5 = -86° 0' aecqib = 54° 0'

wouanf feura 401 aecq5 = -86° 0' aecqib = 54° 0'
ei d'euvaecfoa 2=(-.549°,-.242°0'8X11) aecq5° = -159° 6' aecqib = 60° 2'
ei d'euvaecfoa 3=(0° 404'0'181°0'288) aecq5° = 11° 2' aecqib = 55° 6'
ei d'euvaecfoa 1=(-.210°0'0'405°0'205) aecq5° = 108° 0' aecqib = 15° 9'
Ei d'euvaecfoa ei combouanf 1=M° 3=E° 2=A°

1203532004

wouanf feura 401 aecq5 = -86° 0' aecqib = 54° 0'
ei d'euvaecfoa 2=(-.549°,-.242°0'8X11) aecq5° = -159° 6' aecqib = 60° 2'
ei d'euvaecfoa 3=(0° 404'0'181°0'288) aecq5° = 11° 2' aecqib = 55° 6'
ei d'euvaecfoa 1=(-.210°0'0'405°0'205) aecq5° = 108° 0' aecqib = 15° 9'
Ei d'euvaecfoa ei combouanf 1=M° 3=E° 2=A°
wouanf feura 401 aecq5 = -86° 0' aecqib = 54° 0'
ei d'euvaecfoa 2=(0° 019°,-.412°0'403) aecq5 = -86° 0' aecqib = 54° 0'
wouanf feura 401 aecq5 = -86° 0' aecqib = 54° 0'
Ernif b'isue eojnifou unmpak 40

1203532001

ei d'euvaecfoa 2=(-.549°,-.242°0'8X11) aecq5° = -159° 6' aecqib = 60° 2'
ei d'euvaecfoa 3=(0° 404'0'181°0'288) aecq5° = 11° 2' aecqib = 55° 6'
ei d'euvaecfoa 1=(-.210°0'0'405°0'205) aecq5° = 108° 0' aecqib = 15° 9'
Ei d'euvaecfoa ei combouanf 1=M° 3=E° 2=A°
wouanf feura 401 aecq5 = -86° 0' aecqib = 54° 0'
ei d'euvaecfoa 2=(0° 019°,-.412°0'403) aecq5 = -86° 0' aecqib = 54° 0'
wouanf feura 401 aecq5 = -86° 0' aecqib = 54° 0'

eiDauaeCfoA 2=(-.536P^-.362^0^B11) aecrs^=-15P^d aecqib= P0^2
 eiDauaeCfoA 5=(0^d04^0^1B1^0^2BB) aecrs^= 11^2 aecqib= 55^d
 eiDauaeCfoA 1=(-.210^0^d05^0^205) aecrs^= 108^0 aecqib= 15^P
 EiDauaeCfoA: comboneuf 1=M^ S=E^ 2=A

womeuf feuraA qA: aecrs^=-88^0 aecqib= 54^0
 Moeuf qA: B^2e+SI qAue-cw
 smiJkA biJno: efrIke= 1^ qib= P0^ eJib=-114^ qeAsee
 fmiJf biJno: efrIke= 520^ qib= 24^ eJib=-4P^ qeAsee
 fmiJf biJno: efrIke= 520^ qib= 24^ eJib=-4P^ qeAsee

Y30205015

eiDauaeCfoA 2=(-.536P^-.362^0^B11) aecrs^=-15P^d aecqib= P0^2
 eiDauaeCfoA 5=(0^d04^0^1B1^0^2BB) aecrs^= 11^2 aecqib= 55^d
 eiDauaeCfoA 1=(-.210^0^d05^0^205) aecrs^= 108^0 aecqib= 15^P
 EiDauaeCfoA: comboneuf 1=M^ S=E^ 2=A

womeuf feuraA qA: aecrs^=-88^0 aecqib= 54^0
 Moeuf qA: B^2e+SI qAue-cw
 smiJkA biJno: efrIke= 1^ qib= P0^ eJib=-114^ qeAsee
 fmiJf biJno: efrIke= 520^ qib= 24^ eJib=-4P^ qeAsee
 fmiJf biJno: efrIke= 520^ qib= 24^ eJib=-4P^ qeAsee

Y30205015

eiDauaeCfoA 2=(-.536P^-.362^0^B11) aecrs^=-15P^d aecqib= P0^2
 eiDauaeCfoA 5=(0^d04^0^1B1^0^2BB) aecrs^= 11^2 aecqib= 55^d
 eiDauaeCfoA 1=(-.210^0^d05^0^205) aecrs^= 108^0 aecqib= 15^P
 EiDauaeCfoA: comboneuf 1=M^ S=E^ 2=A

womeuf feuraA qA: aecrs^=-88^0 aecqib= 54^0
 Moeuf qA: B^2e+SI qAue-cw
 smiJkA biJno: efrIke= 1^ qib= P0^ eJib=-114^ qeAsee
 fmiJf biJno: efrIke= 520^ qib= 24^ eJib=-4P^ qeAsee
 fmiJf biJno: efrIke= 520^ qib= 24^ eJib=-4P^ qeAsee

eiDauaeCfoA 2=(-.536P^-.362^0^B11) aecrs^=-15P^d aecqib= P0^2
 eiDauaeCfoA 5=(0^d04^0^1B1^0^2BB) aecrs^= 11^2 aecqib= 55^d
 eiDauaeCfoA 1=(-.210^0^d05^0^205) aecrs^= 108^0 aecqib= 15^P
 EiDauaeCfoA: comboneuf 1=M^ S=E^ 2=A

womeuf feuraA qA: aecrs^=-88^0 aecqib= 54^0
 Moeuf qA: B^2e+SI qAue-cw
 smiJkA biJno: efrIke= 1^ qib= P0^ eJib=-114^ qeAsee
 fmiJf biJno: efrIke= 520^ qib= 24^ eJib=-4P^ qeAsee
 fmiJf biJno: efrIke= 520^ qib= 24^ eJib=-4P^ qeAsee

Y30205011

eiDauaeCfoA 2=(-.536P^-.362^0^B11) aecrs^=-15P^d aecqib= P0^2
 eiDauaeCfoA 5=(0^d04^0^1B1^0^2BB) aecrs^= 11^2 aecqib= 55^d
 eiDauaeCfoA 1=(-.210^0^d05^0^205) aecrs^= 108^0 aecqib= 15^P
 EiDauaeCfoA: comboneuf 1=M^ S=E^ 2=A

womeuf feuraA qA: aecrs^=-88^0 aecqib= 54^0
 Moeuf qA: B^2e+SI qAue-cw
 smiJkA biJno: efrIke= 1^ qib= P0^ eJib=-114^ qeAsee
 fmiJf biJno: efrIke= 520^ qib= 24^ eJib=-4P^ qeAsee
 fmiJf biJno: efrIke= 520^ qib= 24^ eJib=-4P^ qeAsee

M21= -1.2e+52 M25= 5.4e+52 M32= 5.2e+52 qAve-cw
 M11= 2.2e+51 M15= -1.2e+52 M13= 6.1e+52
 womeuf feuzca 201
 etibaecfoa=(0.01e⁴,-.912⁴0⁴403) vecs= -89⁴0 acqtb= 54⁴0
 Hoveuf Mo= B.1e+52 qAve-cw
 xoxijka biyues eflife= 1. qib= 60⁴ qib=-114⁴ qedleez
 tsnif biyues eflife= 520⁴ qib= 24⁴ qib=-46⁴ qedleez
 Lsnif biyue eojnifeu unmapa 20

130202002

etiduaecfoa 2=(-.59e⁴,-.292⁴0⁴831) vecs= -159⁴6 acqtb= 60⁴2
 etiduaecfoa 5=(0.404⁴0⁴181⁴0⁴288) vecs= 11⁴2 acqtb= 55⁴6
 etiduaecfoa 1=(-.210⁴0⁴405⁴0⁴205) vecs= 109⁴0 acqtb= 15⁴6
 Etiduaecfoa: combouef 1=M⁴ 3=E⁴ 2=A
 M21= 1.4e+51 M25= 2.1e+51 M23= -2.2e+51
 M31= -2.2e+51 M35= 2.2e+51 M32= 2.1e+51
 M11= 5.2e+49 M15= -2.2e+51 M13= 1.4e+51
 womeuf feuzca 491
 etibaecfoa=(0.01e⁴,-.912⁴0⁴403) vecs= -89⁴0 acqtb= 54⁴0
 Hoveuf Mo= B.2e+51 qAve-cw
 xoxijka biyues eflife= 1. qib= 60⁴ qib=-114⁴ qedleez
 tsnif biyues eflife= 520⁴ qib= 24⁴ qib=-46⁴ qedleez
 Lsnif biyue eojnifeu unmapa 49

130202002

etiduaecfoa 2=(-.59e⁴,-.292⁴0⁴831) vecs= -159⁴6 acqtb= 60⁴2
 etiduaecfoa 5=(0.404⁴0⁴181⁴0⁴288) vecs= 11⁴2 acqtb= 55⁴6
 etiduaecfoa 1=(-.210⁴0⁴405⁴0⁴205) vecs= 109⁴0 acqtb= 15⁴6
 Etiduaecfoa: combouef 1=M⁴ 3=E⁴ 2=A
 M21= 1.4e+51 M25= 2.1e+51 M23= -2.2e+51
 M31= -2.2e+51 M35= 2.2e+51 M32= 2.1e+51
 M11= 5.2e+49 M15= -2.2e+51 M13= 1.4e+51
 womeuf feuzca 481
 etibaecfoa=(0.01e⁴,-.912⁴0⁴403) vecs= -89⁴0 acqtb= 54⁴0
 Hoveuf Mo= B.2e+51 qAve-cw
 xoxijka biyues eflife= 1. qib= 60⁴ qib=-114⁴ qedleez
 tsnif biyues eflife= 520⁴ qib= 24⁴ qib=-46⁴ qedleez
 Lsnif biyue eojnifeu unmapa 48

130202002

etiduaecfoa 2=(-.59e⁴,-.292⁴0⁴831) vecs= -159⁴6 acqtb= 60⁴2
 etiduaecfoa 5=(0.404⁴0⁴181⁴0⁴288) vecs= 11⁴2 acqtb= 55⁴6
 etiduaecfoa 1=(-.210⁴0⁴405⁴0⁴205) vecs= 109⁴0 acqtb= 15⁴6
 Etiduaecfoa: combouef 1=M⁴ 3=E⁴ 2=A
 M21= 1.2e+52 M25= 2.0e+52 M23= -2.4e+52
 M31= -2.2e+52 M35= 2.2e+52 M32= 2.0e+52
 M11= 5.2e+50 M15= -2.2e+52 M13= 1.2e+52
 womeuf feuzca 451
 etibaecfoa=(0.01e⁴,-.912⁴0⁴403) vecs= -89⁴0 acqtb= 54⁴0
 Hoveuf Mo= B.1e+52 qAve-cw
 xoxijka biyues eflife= 1. qib= 60⁴ qib=-114⁴ qedleez
 tsnif biyues eflife= 520⁴ qib= 24⁴ qib=-46⁴ qedleez
 Lsnif biyue eojnifeu unmapa 45

130202002



εἰς βλῆστρον: (0° 01' 9" - 212° 0' 40") ἄβσγς = -8δ° 0 ἄβσqtβ = 54° 0
 ἡμῶν μσ = 1° 46' 55 qλυσ-cw
 ἀπὸ τῆς βλῆστρον: εἰς τῆς = 1° qtβ = 49° εἰς τῆς = -114° qεδλῶεε
 εἰς τῆς βλῆστρον: εἰς τῆς = 520° qtβ = 24° εἰς τῆς = -49° qεδλῶεε
 εἰς τῆς βλῆστρον ἀποτῆστρον ὑπερὸς 25

Δ20202008

εἰς βλῆστρον 2 = (-° 5δφ' - 2δ2° 0' 8Δ1) ἄβσγς = -159° δ ἄβσqtβ = 90° 2
 εἰς βλῆστρον 5 = (0° 80φ' 0' 181° 0' 288) ἄβσγς = 11° 2 ἄβσqtβ = 55° δ
 εἰς βλῆστρον 1 = (-° 210° 0' 805° 0' 205) ἄβσγς = 10δ° 0 ἄβσqtβ = 1Δ° φ
 εἰς βλῆστρον: κομβοῦσφ 1=H' 5=E' 2=Λ

W21 =	2° 86' 51	W25 =	1° 46' 55	W22 =	-1° 26' 55
W51 =	-δ° 16' 51	W55 =	1° 26' 55	W52 =	1° 46' 55
W11 =	5° 06' 50	W15 =	-δ° 16' 51	W12 =	2° 86' 51

qλυσ-cw

ἡμῶν μσ 21:
 εἰς βλῆστρον: (0° 01' 9" - 212° 0' 40") ἄβσγς = -8δ° 0 ἄβσqtβ = 54° 0
 ἡμῶν μσ = 5° 26' 55 qλυσ-cw
 ἀπὸ τῆς βλῆστρον: εἰς τῆς = 1° qtβ = 49° εἰς τῆς = -114° qεδλῶεε
 εἰς τῆς βλῆστρον: εἰς τῆς = 520° qtβ = 24° εἰς τῆς = -49° qεδλῶεε
 εἰς τῆς βλῆστρον ἀποτῆστρον ὑπερὸς 21

Δ20202002

εἰς βλῆστρον 2 = (-° 5δφ' - 2δ2° 0' 8Δ1) ἄβσγς = -159° δ ἄβσqtβ = 90° 2
 εἰς βλῆστρον 5 = (0° 80φ' 0' 181° 0' 288) ἄβσγς = 11° 2 ἄβσqtβ = 55° δ
 εἰς βλῆστρον 1 = (-° 210° 0' 805° 0' 205) ἄβσγς = 10δ° 0 ἄβσqtβ = 1Δ° φ
 εἰς βλῆστρον: κομβοῦσφ 1=H' 5=E' 2=Λ

W21 =	9° 16' 55	W25 =	5° 26' 55	W22 =	-5° 26' 55
-------	-----------	-------	-----------	-------	------------